

**DEVELOPMENT AND PERFORMANCE EVALUATION OF
SELF-LUBRICATING GRINDING WHEELS IN GRINDING
INCONEL 718**

A Dissertation work
Submitted in Partial Fulfilment of the Requirements
for the Award of the Degree of

DOCTOR OF PHILOSOPHY
in
MECHANICAL ENGINEERING
by
BHANU PAVAN RAVURI
(Roll No. 701138)
Under the Guidance of

Dr. M. Amrita
(External Supervisor)
Associate Professor, MED
GVP College of Engineering
Visakhapatnam

Dr. A. VENU GOPAL
(Supervisor)
Professor
MED
NIT WARANGAL



**DEPARTMENT OF MECHANICAL ENGINEERING
NATIONAL INSTITUTE OF TECHNOLOGY
WARANGAL-506004 (A.P), INDIA**

October, 2018

**DEPARTMENT OF MECHANICAL ENGINEERING
NATIONAL INSTITUTE OF TECHNOLOGY
WARANGAL - 506004 (TELANGANA), INDIA.**



CERTIFICATE

This is to certify that the work presented in the thesis entitled "**Development and performance evaluation of self-lubricating grinding wheels in grinding Inconel 718**" which is being submitted by **Mr. Bhanu Pavan Ravuri** (Roll No. 701138), is a bona-fide work submitted to National Institute of Technology, Warangal in partial fulfillment of the requirement for the award of the degree of **Doctor of Philosophy in Mechanical Engineering**. To the best of our knowledge, the work incorporated in the thesis has not been submitted to any other university or institute for the award of any other degree or diploma.

Dr. M. Amrita
(External Supervisor)
Associate Professor, MED
GVP College of Engineering
Visakhapatnam

Dr. A. VENU GOPAL
(Supervisor)
Professor
MED
NIT WARANGAL

DECLARATION

This is to certify that the work presented in the thesis titled **“Development and performance evaluation of self-lubricating grinding wheels in grinding Inconel 718”** is a bona-fide work done by me under the supervision of **Dr. A. Venu Gopal & Dr. M. Amrita** and was not submitted elsewhere for the award of any degree.

I declare that this written submission represents my ideas in my own words and where others' ideas or words have been included, I have adequately cited and referenced the original sources. I also declare that I have adhered to all principles of academic honesty and integrity and have not misrepresented or fabricated or falsified any idea/data/fact/source in my submission. I understand that any violation of the above will be a cause for disciplinary action by the institute and can also evoke penal action from the sources which have thus not been properly cited or from whom proper permission has not been taken when needed.

Bhanu Pavan Ravuri
Roll. No. 701138

Acknowledgments

I take this opportunity to express my sincere gratitude to **Dr. A. Venu Gopal**, Professor, MED, for his guidance, motivation, patience, and care, from the very first day I met him. I am truly fortunate to be associated with him during this course of the research.

I especially thank **Dr. R. R. Srikant**, Assistant Professor, Department of Technology, University of Northern Iowa, the U.S.A., who was my first external supervisor when he was in GITAM, for his helping hand and motivation.

I thank **Dr. M. Amrita**, Associate Professor, MED, GVP College of Engineering, Visakhapatnam, external supervisor, for taking time from her busy schedule and correcting journal papers and thesis time to time, and word by word.

I thank **Dr. P. Bangaru Babu**, Head (MED) & Chairman DSC, **Dr. L. Krishnanand**, Member DSC and **Dr. M. K. Mohan**, Member DSC for their wisdom, continuous suggestions and feedback.

I thank **Dr. P. Vamsi Krishna**, Associate Processor, MED for sparing his time to share valuable insights in presenting the concepts in the presentation and thesis. I thank all the faculty members of MED who helped me directly or indirectly.

I also extend my thanks to **Dr. G. Bhanu Kiran**, my best friend, for his selfless help and **Dr. H. Ravi Sankar** for introducing Dr. A. Venu Gopal.

I express my heartfelt thanks to **GITAM, Head of the Mechanical Engineering Department and Head of the Industrial Engineering Department**, for giving me permissions to use lab facilities, **Dr. V. Srinivas**, for giving us permission to use his project equipment and to all the lab technicians who helped me in conducting the experiments. I extend my heartfelt thanks to all the colleagues at GITAM who encouraged me to move forward.

I especially thank my close friends who stood beside me every moment. I thank my family friends who supported my family and me during my travel to NITW.

I am deeply indebted to my parents **Sri R. Nageswara Rao and Smt R. Lakshmi Tulasamma** for their immense support in every respect. I also thank my sister's family for constant support.

I thank my lovely family, for whom all these efforts are meant for. I thank my children **R. Sai Veda Vihari and R. Sai Kavya Sudha** for their little sacrifices and finally, I thank my wife **R. Jhansi Rani** for everything.

R. Bhanu Pavan

ABSTRACT

Surface grinding is an abrasive technique, in which each abrasive grain acts as a cutting tool. Due to rubbing and ploughing of the workpiece surface by the abrasive grits, intense heat and high cutting forces develop at the wheel–workpiece interface. These, in turn, cause poor surface finish, higher specific power requirements, higher wheel wear, microcracks, thermal burns, residual stresses and phase transformations. This phenomenon is more prominent in difficult-to-machine materials like Inconel 718 due to its high hot strength, poor thermal conductivity, high thermal expansion coefficient, etc., which in turn affects the surface and sub-surface quality of the ground components. The surface quality of the ground components is of prime concern especially in aerospace applications as they influence failures produced by fatigue, wear, creep and stress corrosion. Hence, in order to extend the life of the ground parts, surface quality has to be improved by reducing the excessive heat and cutting forces generated during grinding of Inconel 718.

The most commonly used technique for controlling the temperatures and cutting forces is flooding the contact zone with cutting fluids to aid lubrication and cooling. In spite of having numerous advantages, flood cooling has some serious disadvantages concerned with economic and ecological aspects. Minimum Quantity Lubrication of the grinding zone with cutting fluids seems to be a potential alternative to economic and ecological concerns of the flood grinding. However, performance wise MQL grinding stood between dry and flood grinding due to insufficient cooling and improper lubrication at grinding site. Hence, the development of new strategies and lubricants which can provide better cooling and lubrication at the grinding zone is very much essential for energy efficient and sustainable grinding.

Solid lubricants (graphite, molybdenum disulphide, calcium fluoride, boric acid, etc.) which can provide lubricity over a wide range of temperatures seem to be an effective alternative to the conventional cutting fluids. However, efficient delivery of the solid lubricants at the wheel–workpiece interface is a major hindrance in achieving the desired results. In addition, type and quantity of solid lubricant will also have profound influences on the process results. Among various solid lubricants, very limitedly explored graphene nanoplatelets (GNP) were selected in

this work due to their remarkable properties such as high thermal conductivity and self-lubricating behaviour. In view of these drawbacks, the present work focuses on exploring the effectiveness of GNP in reducing the friction and associated heat generation in the grinding process by developing efficient methods for proper application of GNP at the wheel-workpiece interface with an ultimate objective to improve the wheel life and surface quality of Inconel 718. For this purpose GNP based self-lubricating grinding wheel and GNP based nano-cutting fluids were developed and their performance in terms of surface finish, wheel wear, grinding temperatures, specific energy requirements, etc. are evaluated and presented in this work.

Self-lubricating resin bonded grinding wheels with varying GNP concentrations (0.25, 0.5, 1, 2 and 4 wt %), and surface areas (300, 500 and 750 m²/g) are manufactured, in order to have a proper application of solid lubricants at the wheel-workpiece interface. For this purpose, GNP is impregnated into the wheel structure during the moulding stage itself. In order to ensure the uniform dispersion of GNP without any entanglements, GNP is treated with a cationic surfactant. Different aspects of grinding performance (i.e. cutting forces, grinding temperatures, surface roughness, grinding coefficient, specific grinding energy and grinding wheel wear) are evaluated by grinding Inconel 718 in dry condition with these newly developed self-lubricating grinding wheels and compared the results with that of the standard grinding wheel. The experimental results show a considerable improvement in grinding process results with GNP as compared to standard grinding wheels. Grinding wheels having 2 wt% GNP has produced lower grinding forces and grinding temperatures, and better surface finish. Among various GNP surface areas considered, GNP with the larger surface area is found to be more effective in improving the quality of the ground surface.

Another approach adopted in this work for effective application of GNP at wheel workpiece interface is to deliver GNP into grinding zone in the form of aerosols by using conventional cutting fluid and air as a medium. For this purpose, nano-cutting fluids with varying concentrations (0.1, 0.2, 0.3, 0.4 and 0.5 wt%) and surface areas (300, 500 and 750 m²/g) of GNP are prepared. The basic properties like thermal conductivity and viscosity are evaluated at different temperatures. Since the effectiveness of the cutting fluid in providing effective cooling and proper lubrication at the grinding wheel-workpiece interface depends on the thermal

conductivity and viscosity, these properties are evaluated at different temperatures. It is observed that viscosity increased with increase in GNP concentration and surface area but decreased with increase in temperature. Thermal conductivity observed to be enhanced significantly with an increase in GNP weight fractions, surface area and temperature. Furthermore, to assess the performance of the developed nano-cutting fluids, Inconel 718 is ground using conventional grinding wheel while delivering minimum quantity nano-cutting fluid into grinding zone in the form of aerosols. The experimental results show that GNP significantly lowers the grinding force, grinding temperature, surface roughness, grinding coefficient and specific grinding energy. Nano-cutting fluid with 0.3 wt% and $750 \text{ m}^2/\text{g}$ GNP is found to be effective in improving the surface quality of the Inconel 718.

Further, Inconel 718 is ground in different grinding environments i.e. standard grinding wheel in dry, self-lubricating grinding wheels in the dry, standard grinding wheel in nanoMQL and self-lubricating grinding wheels in nanoMQL environments. Overall, the combination of self-lubricating grinding wheels and nanoMQL has led to decrease of various aspects of grinding performances (i.e. cutting forces, grinding temperatures, surface roughness, grinding coefficient and specific grinding energy) and yielded improved surface quality of Inconel 718 components.

Keywords: Inconel 718, Graphene nanoplatelets, Grinding, Self-lubricating grinding wheels, nano-cutting fluids, nanoMQL

Contents

	Page No
Acknowledgment.....	i
Abstract.....	iii
List of Figures.....	vi
List of Tables.....	x

Chapter I - Introduction

1.1 Introduction.....	1
1.2 Difficult to machine materials.....	1
1.2.1 Inconel 718.....	1
1.3 Grinding.....	2
1.4 Cutting fluids in grinding.....	4
1.5 Solid lubricants in grinding.....	4
1.5.1 Graphene nanoplatelets.....	5
1.5.2 Self-lubricating grinding wheels.....	6
1.5.3 NanoMQL.....	8
1.6 Present work.....	8
1.6.1 Outline of the thesis.....	8

Chapter II - Literature Review

2.1 Introduction.....	10
2.2 Machining of Inconel 718.....	10
2.3 MQL in machining.....	11
2.4 Solid Lubricants in Grinding.....	15

	Page No
2.4.1 Nanofluids.....	18
2.4.2 NanoMQL.....	22
2.4.3 Graphene nanoplatelets.....	24
2.5 Research gaps in the literature.....	27
2.6 Objectives and Scope of the present study.....	28
 Chapter III – Experimentation	
3.1 Introduction.....	29
3.2 Selection of the Materials.....	29
3.2.1 Inconel 718.....	29
3.2.2 Graphene nanoplatelets.....	30
3.3 Development of GNP impregnated grinding wheel.....	32
3.4 Preparation of GNP based nano-cutting fluids.....	34
3.4.1 Measurement of thermal conductivity.....	35
3.4.2 Measurement of Viscosity.....	36
3.5 Experimental set up.....	37
3.5.1 Grinding machine.....	37
3.5.2 MQL system.....	38
3.5.3 Measurement of cutting force.....	39
3.5.4 Measurement of cutting temperature.....	40
3.6 Measurement of surface roughness.....	41
3.7 Experimentation procedure.....	42

Chapter IV - Development and performance evaluation of self-lubricating grinding wheel in grinding Inconel 718

4.1 Introduction.....	46
4.2 Grinding experiments.....	46
4.2.1 Grinding forces.....	47
4.2.2 Grinding temperature.....	49
4.2.3 Surface roughness.....	50
4.3 Grinding Coefficient.....	51
4.4 Specific Grinding Energy.....	52
4.5 Grinding wheel wear ratio.....	53
4.6 Influence of GNP surface area on grinding.....	54
4.7 Summary.....	58

Chapter V - Development and performance evaluation of GNP based nanoMQL in grinding of Inconel 718

5.1 Introduction.....	60
5.2 Preparation of GNP based nano-cutting fluids.....	60
5.2.1 Thermal conductivity.....	61
5.2.2 Viscosity.....	62
5.3 Grinding Experiments.....	63
5.3.1 Grinding force.....	63
5.3.2 Grinding temperatures.....	65

	Page No
5.3.3 Surface roughness.....	66
5.4 Grinding coefficient.....	67
5.5 Specific grinding energy.....	68
5.6 Effect of GNP surface area.....	69
5.7 Summary.....	75
 Chapter VI – The Grinding performance of Self Lubricating Grinding Wheel with nanoMQL in grinding	
6.1 Introduction.....	77
6.2 Grinding experiments.....	77
6.2.1 Grinding forces.....	78
6.2.2 Grinding Temperature.....	79
6.2.3 Surface roughness.....	81
6.3 Grinding coefficient.....	82
6.4 Specific Grinding Energy.....	82
6.5 Summary.....	83
 Chapter VII - Conclusions and future scope of the work	
7.1 Conclusions.....	84
7.1.1 Performance evaluation of self-lubricating grinding Wheels.....	84
7.1.2 Performance evaluation of grinding with nanoMQL.....	85

	Page No
7.1.3 Performance evaluation of self-lubricating grinding wheels with nanoMQL.....	86
7.2 Future Scope of the work.....	86
References.....	88
List of publications from this research work.....	98
Bio-Data.....	99

List of Figures

Fig No.	Title	Page No.
Fig 1.1.	Variation in rake angle with grits of different shape	3
Fig 1.2.	Grinding wheel and workpiece interaction	3
Fig 1.3.	Hexagonal Boron Nitride Structure	5
Fig 1.4.	A TEM image of GNP	6
Fig 1.5.	Flow chart of the present work	7
Fig 2.1.	Affected layers for (a)Dry grinding (b)Wet grinding (c) Pure oil MQL (d) Oil water MQL	13
Fig 2.2.	(a) Abrasive grains wear mechanisms of vitrified bond corundum after grinding(magnification: 175 \times), (b) a schematic of oil mist spray in MQL grinding and (c) lubricant sources at the interface of the grain and workpiece surfaces	14
Fig 2.3	(a) wheel after the slots cut on it-20 slots, (b) lubricant sandwiched wheel ready for experimentation-10 slots	16
Fig 2.4	Appearance of (a) graphite and (b) aluminum oxide particles	17
Fig 2.5	Schematic illustration of a physical model for the structure of a graphite-impregnated grinding wheel	17
Fig 2.6.	The thermal conductivity of nanofluids	20
Fig 2.7.	Variation of viscosity with volume fraction	21
Fig 2.8.	Variation of viscosity with temperature for SiO_2 dispersion in water	21
Fig 2.9.	Schematic of nanoparticle jet MQL grinding	23
Fig 2.10.	Schematic of nanoparticles in grinding interface	23
Fig 3.1.	Inconel 718 component procured	30
Fig 3.2.	Ultrasonic probe sonicator	31

Fig No.	Title	Page No.
Fig 3.3.	Vacuum filtration setup	31
Fig 3.4.	Vacuum Oven	32
Fig 3.5.	Solid lumps obtained after drying	32
Fig 3.6.	Various stages in the manufacturing of GNP impregnated grinding wheel (a) preparing ingredients of the wheel (b) mixing (c) filling mixture in a mould (d) pressing with a hydraulic press (e) transferring pressed wheels to the furnace and (f) curing	33
Fig 3.7.	Grinding wheels (a) Standard Grinding Wheel (b) GNP impregnated grinding wheel	34
Fig 3.8.	Stability of nano-cutting fluids with (a) 0wt.% GNP, (b) 0.4wt.% raw GNP in a day and (c) 0.4wt.% functionalized GNP after 5 days	34
Fig 3.9.	KD2 Pro	36
Fig 3.10	DV-III Ultra Rheometer	37
Fig 3.11.	Sartaj surface grinding machine	38
Fig 3.12.	UnistCoolubricator system	38
Fig 3.13.	Kistler Dynamometer	39
Fig 3.14.	Experimental set up for surface grinding	40
Fig 3.15.	Measurement of grinding temperatures	41
Fig. 3.16.	Digital display of thermocouple	41
Fig 3.17.	Mitutoyo SJ 310 surface roughness testing equipment	42
Fig 3.18.	Schematic representation of MQL grinding of Inconel 718	43
Fig 4.1.	Effect of GNP concentration on Normal Force	48
Fig 4.2.	Effect of GNP concentration on Tangential force	49
Fig 4.3.	Effect of GNP concentration on grinding temperature	50
Fig 4.4.	Effect of GNP concentration on surface roughness	51
Fig 4.5.	Effect of GNP concentration on grinding coefficient	52
Fig 4.6.	Effect of GNP concentration on specific grinding energy	53

Fig No.	Title	Page No.
Fig 4.7.	Effect of GNP concentration on wheel wear	53
Fig 4.8.	Effect of GNP surface area on the normal force	55
Fig 4.9.	Effect of GNP surface area on the tangential force	56
Fig 4.10.	Effect of GNP surface area on grinding temperature	56
Fig 4.11.	Effect of GNP surface area on surface roughness	56
Fig 4.12.	Effect of GNP surface area on grinding coefficient	57
Fig 4.13.	Effect of GNP surface area on specific grinding energy	57
Fig 4.14.	Grinding wheel wear rate for different grinding wheels	58
Fig 5.1.	The thermal conductivity of cutting fluids with varying weight fractions of GNP	62
Fig 5.2.	Effect of weight fractions of GNP on the viscosity of nano-cutting fluids	62
Fig 5.3.	Effect of GNPs concentration on the normal force	65
Fig 5.4.	Effect of GNP concentration on the tangential force	65
Fig 5.5.	Effect of GNP based nano-cutting fluid on grinding temperature	66
Fig 5.6.	Effect of GNP based nano-cutting fluid on surface roughness	67
Fig 5.7.	Effect of GNP based nano-cutting fluid on grinding coefficient	68
Fig 5.8.	Variation of specific grinding energy with variation in GNP concentration and specific surface area	69
Fig 5.9.	The thermal conductivity of cutting fluids with a varying surface area of GNP	71
Fig 5.10.	The viscosity of cutting fluids with a varying surface area of GNP	71
Fig 5.11.	Effect of GNP surface area on the normal force	72
Fig 5.12.	Effect of GNP surface area on the tangential force	73
Fig 5.13.	Effect of GNP surface area on temperature	73
Fig 5.14.	Effect of GNP surface area on surface roughness	74

Fig No.	Title	Page No.
Fig 5.15.	Effect of GNP surface area on grinding coefficient	74
Fig 5.16.	Effect of GNP surface area on specific grinding energy	74
Fig. 6.1.	Normal force for various combinations of grinding	78
Fig. 6.2.	Tangential force for various combinations of grinding	79
Fig. 6.3.	Grinding temperatures for various combinations of grinding	80
Fig. 6.4.	Surface roughness for various combinations of grinding	81
Fig. 6.5.	Grinding coefficient for various combinations	82
Fig. 6.6.	Specific Grinding Energy for various combinations of grinding	83

List of Tables

Table No.	Title	Page No.
Table 2.1.	Comparison of graphene dispersed canola oil with pure canola oil	26
Table 3.1.	Grades of GNP	30
Table 3.2.	Experimental Conditions	43
Table 4.1	Nomenclature of GNP impregnated grinding wheels	46
Table 4.2.	Nomenclature of GNP impregnated grinding wheels with a varying surface area	54
Table 5.1.	Nomenclature of nano-cutting fluids with varying weight fractions of GNP	61
Table 5.2.	Nomenclature of nano-cutting fluids with 3 grades of GNP with 3 weight fractions	70
Table 5.3.	Nomenclature of nano-cutting fluids with a varying surface area of GNP	70
Table 6.1.	Various combinations of grinding	78

Chapter I

Introduction

1.1 Introduction

Titanium and nickel-based alloys are being widely used in military, aerospace, nuclear and gas turbine industries because of their very high strength and high-temperature resistance. Ti6Al4V and Inconel 718 are used in military projectile applications and jet engine fan containment applications [1]. Nickel-based superalloys are used in hot sections of gas turbine engines [2]. Because of their extraordinary mechanical and chemical properties, they are used widely in aerospace applications. Due to their poor thermal conductivity and sensitivity to strain hardening, they are named as "difficult to machine materials". In the present research, new strategies are tried to improve the machining of Inconel 718, one of the difficult to machine materials.

1.2 Difficult to machine materials

The materials, which produce very high cutting forces and/or heat, cause excessive tool wear and lead to difficulty in chip formation and/or low surface quality, are referred as difficult to machine materials. Titanium and nickel-based alloys are readily considered as difficult to machine materials or hard to cut materials. Generally, the materials categorized under difficult-to-machine materials are refractory and superalloys which contain chromium, niobium, tantalum, cobalt, tungsten, rhenium, molybdenum, steel, nickel, titanium etc. as alloying elements. However, difficult to machine materials are not just limited to this list of alloys, but also extended to composites, structural ceramics, polymers, magnesium alloys etc. Among these difficult to machine materials, Inconel 718 alloy, which is nickel-based, is selected in the present work.

1.2.1 Inconel 718

Inconel 718, a nickel-based alloy, has very good fatigue endurance up to 700° C. It exhibits extraordinary hot strength and hardness. Its mechanical and chemical properties are not much affected at higher temperatures. It is also corrosion and creep resistant. It has some

other special properties like high erosion and thermal fatigue resistivity, it offers resistance to thermal shock, and it has a high melting point. Due to these desirable properties, Inconel 718 is used in aerospace applications. Because of the high strength, Inconel 718 produce a high amount of temperatures and forces during grinding operations. And as Inconel 718 is not a good conductor of heat, the generated heat is not effectively dissipated through the workpiece.

The drastic rise in temperature leads to excessive tool wear and results in the poor surface quality of the workpiece. Below 650°C, the hardness of Inconel 718 increases with the rise in temperature [3]. This rise in temperature does not help in softening the material and improving the machinability. High temperature also alters the microstructure of the workpiece material, induces residual stresses, causes microcracks, and leads to variation in the micro-hardness through the formation of the white layer. All these problems affect the service life of the machined component, in particular, fatigue resistivity. Another specific problem while machining Inconel 718 is the metallurgical damage in subsurface because of the work hardening as a response to high cutting forces. Due to shortened tool life, low cutting speeds, and poor surface and subsurface quality, machining Inconel 718 is becoming a costlier process.

1.3 Grinding

Grinding is the most commonly chosen process where good surface finish and, high form and dimensional accuracy are primarily important. Grinding is preferred to machine hard materials which are difficult to machine using conventional machining processes. Sharpening and finishing cutting tools, contour and form grinding of hot and cold working dies, from grinding of gears and threads, finishing of cylindrical and flat surfaces and stock removal are the major applications of grinding. And hence, Grinding is an invertible machining process in all industries like machine tools manufacturing, automobile, and aerospace engineering.

In grinding, material removal occurs by shearing and ploughing in the form of microchips by abrasive grits. These grits are held on the wheel by metallic and non-metallic bonds. Almost, any material, soft or hard, ductile or brittle, can be cut by grinding operation. Mainly, the grinding process can be characterized by high specific energy which is required due to high cutting speed, huge negative rake angle (Fig 1.1), chip removal and undesirable interaction between wheel-workpiece.

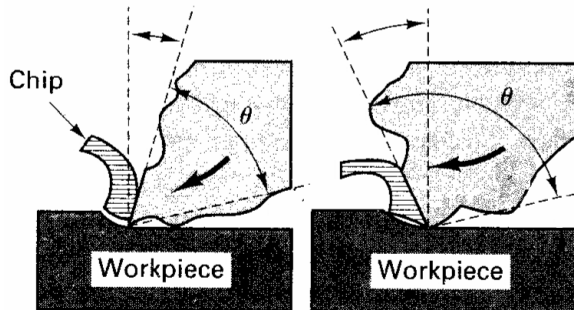


Fig 1.1 Variation in rake angle with grits of different shape [4]

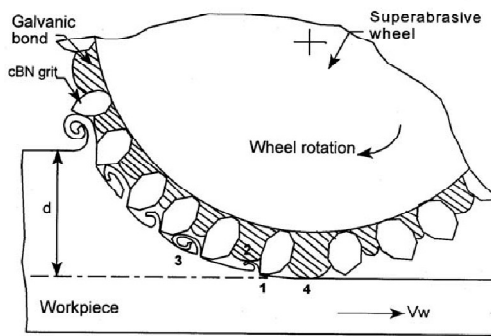


Fig 1.2 Grinding wheel and workpiece interaction [4]

Grinding wheel and workpiece interaction happens in four different ways as illustrated in Fig 1.2., and they are 1. grit-workpiece (chip forming), 2. chip-bond, 3. chip-workpiece and 4. Bond-workpiece. Among these, grit workpiece interaction alone is productive which produce chips, and the other ways are undesirably increasing force and energy requirements.

The generated heat because of the above reasons, causes many problems like, large heat affected zone (HAZ), change in microstructure and hardness of the workpiece, development of over-tempered and un-tempered martensitic layer while grinding ferrous alloys, burnings and the associated problems, and development of large tensile residual stresses and thus microcracks [5].

Another severe problem with grinding is the accumulation of chips in the inter grit spaces, i.e. wheel loading. To clear the chips, grinding wheels are to be redressed frequently to increase the grinding efficiency, which cuts down the useful wheel life. Besides, wheel loading leads to a rise in the temperature, grinding forces, and vibrations, which further leads to poor surface finish and surface integrity. All these problems associated with grinding are prominent in grinding 'difficult-to-machine materials'.

In this regard, to improve the quality of the ground surface and to reduce the heat produced cuttings fluids are being employed from decades.

1.4 Cutting fluids in grinding

Cutting fluids are used in grinding operations to reduce the friction and enhance the lubrication in the grinding zone and to remove the heat generated because of plastic deformation in the wheel-workpiece interface. Moreover, these cutting fluids will also flush the chips away.

The method of flooding cutting fluid in grinding zone to reduce the difficulties in grinding difficult to machine materials has few limitations:

1. Air barrier confines the accessibility of grinding fluid into the grinding zone [6].
2. Even a small quantity of cutting fluid enters the grinding zone, film boiling takes place which further increases the heat generated at the wheel-work interface [7].
3. After crossing a certain grinding temperature, the lubricity of cutting fluid is getting degraded [8].

Besides, the majority of the cutting fluids are harmful to the operator's health [8], not safe to the environment, and making machining costlier. The estimated cost spent on cutting fluids is around 20-30% of total manufacturing cost [6], in the case of machining difficult-to-machine materials. Further, cutting fluids need regular maintenance to preserve their optimum characteristics. Cutting fluids provide favorable conditions to grow bacteria and fungi. In the presence of bacteria, emulsion gets split up effecting both lubricity and pH of cutting fluid. As pH value changes, the risk of corrosion on both machine tool and workpiece increases. In view of these challenges associated with the use of cutting fluids, alternate strategies such as the use of solid lubricants are to be developed, either to minimize or to eliminate the use of cutting fluids.

1.5 Solid lubricants in grinding

Generally, solid lubricants are very attractive substitutes for cutting fluids as they are less toxic, environmentally friendly, biodegradable and have the capacity to lubricate over a

range of pressure and temperatures. Boric acid (H_3BO_3), molybdenum disulphide (MoS_2), calcium fluoride (CaF_2) and graphite are popular solid lubricants that are used in grinding by various researchers.

Solid lubricants are attractive because of their lamellar structure i.e. they exist in layer by layer structure which is held by week Vander Waal's forces. These layers can easily slip over another when applied shear loads. Fig 1.3 shows the Hexagonal Boron Nitride Structure [10]. This structure of solid lubricants provides lubrication in the contact zones.

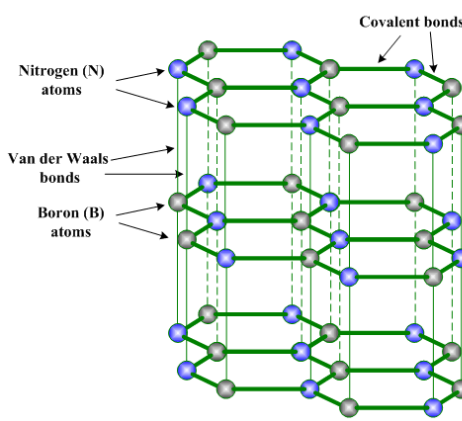


Fig 1.3. Hexagonal Boron Nitride structure [10]

Recently, graphene nanoplatelets have attracted researchers because of their unique structure and remarkable properties. Hence, graphene nanoplatelets are chosen as a solid lubricant in this work.

1.5.1 Graphene nanoplatelets (GNP)

Graphene, an interesting allotrope of carbon, has been drawing the attention of researchers because of its extraordinary properties like high modulus of elasticity, good electrical and thermal conductivity, and self-lubricating behavior [11]. Being two-dimensional matter, graphene offers unique wear and friction properties which are not commonly seen in conventional materials. Besides its renowned optical, electrical, thermal and mechanical properties, it can also act as a solid lubricant or colloidal liquid lubricant. Graphene consists of a stack of graphene sheets represented by vertical lines as shown in Fig 1.4. These sheets are kept close together by Vander Waals forces and they can easily slip relative to each other

under the application of shear loads [12]. Since graphene exists as sheets or platelets in nano-thickness, it is renowned as graphene nanoplatelets (GNP).

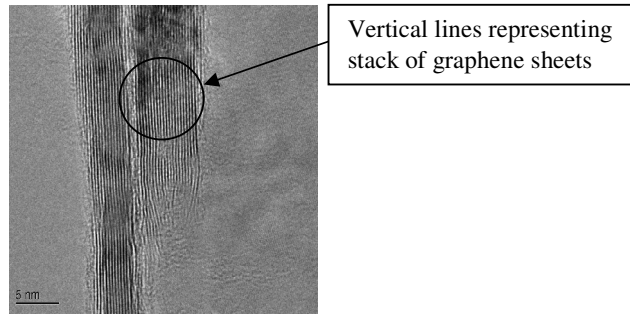


Fig 1.4 TEM image of GNP [13]

The extreme mechanical strength of GNP is a very important property for wear protection. As GNP is shown to be impermeable for gases and liquids, such as oxygen and water, it slows down the corrosive and oxidation phenomena while grinding is done. GNP is also able to replace solid films usually provided for reducing adhesion cum friction of different surfaces with its two dimensional, low surface energy, smooth and slippery atomic layers [14, 15]. All the above-mentioned properties make GNP very attractive for challenging tribological applications to obtain low friction and low wear conditions.

Since GNP have all the essential properties that a solid lubricant should possess, researchers are paying attention and making efforts in using it in machining to minimize friction. In this research work, GNP is impregnated in the grinding wheels to make self-lubricating grinding wheels and dispersed in cutting fluids to use in nanoMQL, to study their performance in grinding Inconel 718.

1.5.2 Self-lubricating grinding wheels

Solid lubricants are supplied to machining zone to reduce friction, and hence temperature generated, in many methods. Popularly, solid lubricants are fed in powder form, paste form. Graphite is sandwiched in the grooves made in grinding wheel [16]. Few solid lubricants are directly moulded in the grinding wheels to provide effective lubrication in the grinding zone [17]. These grinding wheels are called as self-lubricating grinding wheels. In the present study, GNP impregnated grinding wheels are developed.

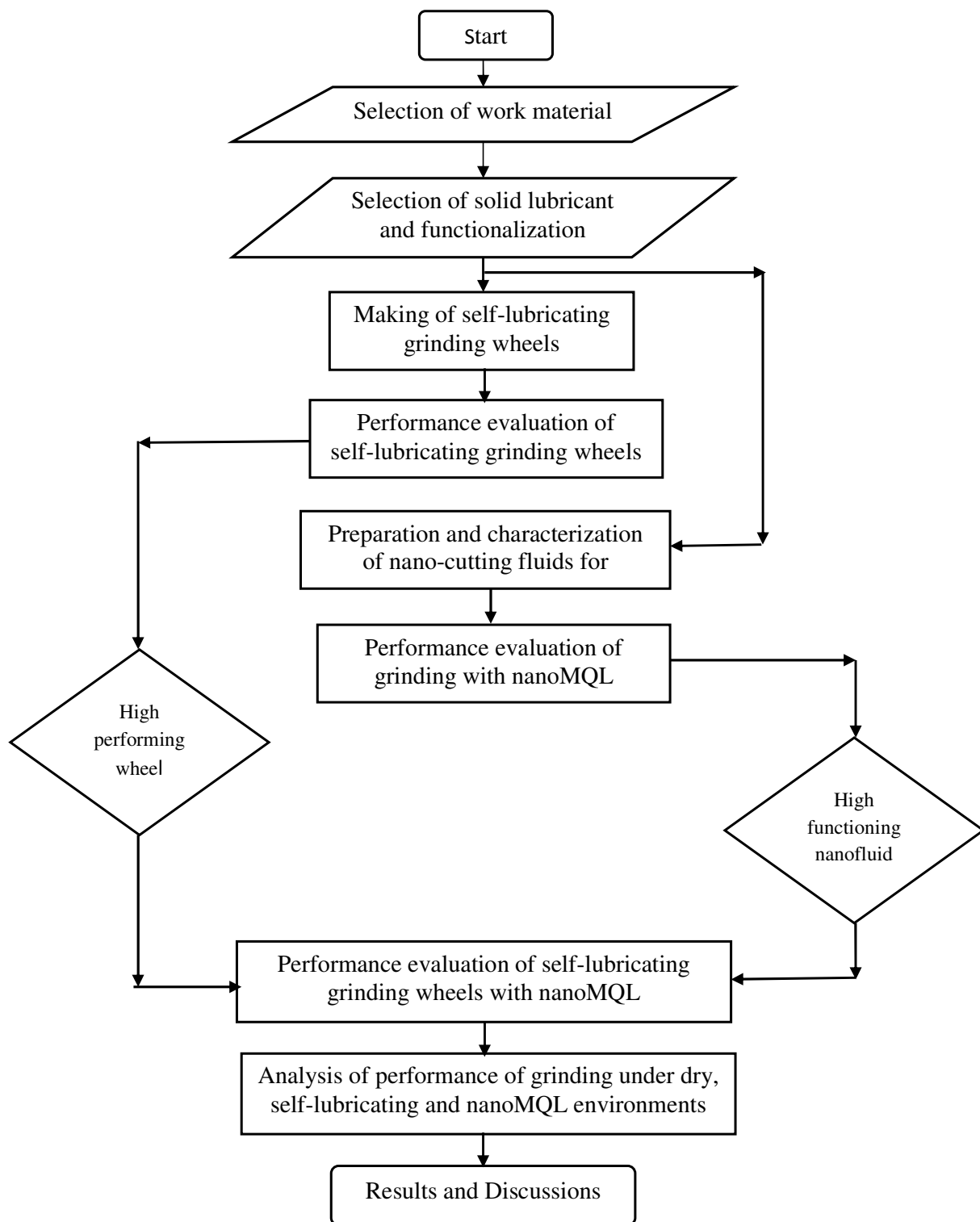


Fig 1.5. Flow chart of the present work

1.5.3 NanoMQL

Health and environmental concern on the use of cutting fluids during manufacturing has led to the development of minimum quantity lubrication (MQL) [18]. Minimum quantity lubrication (MQL) became another alternative to use the cutting fluids to minimize their drawbacks. In MQL, a very small quantity of cutting fluid is sent forcefully (E.g. by means of compressed air) into the machining zone. MQL becomes more efficient in adding nanoparticles to cutting fluids [19]. Nanoparticles dispersed in the cutting fluids are called as nano-cutting fluids. When nano-cutting fluids are used in MQL, it is popularly called as nanoMQL. In this work, GNP based nano-cutting fluids are prepared and used in nanoMQL to grind Inconel 718 components.

1.6 Present work

In general, quality of the grinding assessed by measuring the surface roughness of the ground surface, grinding temperatures, and grinding forces etc. In the present work grinding forces, grinding temperatures, surface roughness, grinding coefficient, specific grinding energy and grinding wheel wear are considered as performance parameters to assess new strategies adopted.

This work focuses on improving the surface quality and reducing the energy requirements for grinding of difficult to machine materials with an ultimate objective of enhancing the life of the components made with difficult to machine materials. The intended objective of improving the surface quality ground Inconel 718 component is achieved in the different stages. The present work is represented in the following flow chart Fig 1.5.

1.6.1 Outline of the thesis

The thesis has been divided into VIII chapters.

Chapter I introduces various challenges in grinding difficult to machine materials, drawbacks associated with the use of cutting fluids, and the use of solid lubricants to overcome these challenges and drawbacks. In addition, a brief summary of the work carried out in the present study is reported.

Chapter II presents a comprehensive study of literature, leading to the current work. This chapter contains a discussion on the work reported by many researchers regarding various methods of improving the surface quality of difficult to machine materials. Gaps in the literature and objectives of the present works are presented.

Chapter III gives the details of the selection of the materials, specifications of the equipment used, measurement procedures used to measure input parameters and output parameters and experimental procedure followed.

Chapter IV reports the effect of self-lubricating grinding wheels developed with varying weight fractions and surface areas of GNP in grinding Inconel 718 components on various grinding performance measures.

Chapter V presents the variation in basic properties of nano-cutting fluids with respect to concentration and surface area of GNP, the experimental investigations on nanoMQL grinding of Inconel 718 component with the prepared GNP based nano-cutting fluids.

Chapter VI reports the effect of grinding Inconel 718 with various combinations of the grinding wheel and grinding conditions on various grinding performance measures.

Chapter VII presents the major conclusions drawn from the present work and various other aspects, which are worthy for further investigation are suggested.

Chapter II

Literature Review

2.1 Introduction

In this chapter, the motivation for the current research has been discussed in detail. The attempts that are made by different researchers in the areas of machining of difficult to machine materials, solid lubricants, nano-MQL and grinding are discussed elaborately. The need for the current work has been established at the end of the chapter.

2.2 Machining of Inconel 718:

Nowadays, aircraft engines are featured by greater fuel efficiency and reliability. Engines can perform longer and fly over oceans for several years. In addition to commercial use, the military sector is also mainly based on the greatest performance of jet engines [1]. To receive the highest value of the performance and cost, the aero engines are manufactured from the high performing materials like Inconel 718. Inconel 718 is perfect for applications in a high-temperature environment where creep, heat resistance and corrosion are needed [20]. It is a key solution of hot structural applications, therefore, it is widely used in the various industrial applications such as hot sections of gas turbine engines [2], nuclear reactors [21], components for liquid-fueled rockets, sheet metal parts for cryogenic tanks [22].

Aeronautic structures are exposed to severe temperature, stress and hostile environmental conditions. Surface integrity is utmost important for the workpiece undergoing higher mechanical and thermal loads [23]. Surface condition is an ever-increasing and influencing parameter on the component performance. The origin of component failures depends on the quality of the machined surface. Utmost attention and importance should be given to characteristics of the machined component surface [24, 25]. Many researchers have investigated on machining of Inconel718, and it's surface integrity [24-29].

Precision grinding is one of the key processes which guarantee the accuracy and high surface quality for Inconel718 component parts. However, when Inconel718 component is being ground, there is difficulty in conducting the heat generated in the grinding zone to the

base metal as it is having poor thermal conductivity. Moreover, because of the high grinding energy ratio during grinding of hard-to-cut materials, a major portion of the grinding energy is converted into grinding heat and accumulated in the grinding zone. If this heat is not removed from the grinding zone, the temperature would be increasing sharply, which has a severe influence on quality, thereby service life of the component [30]. In this regard, finding an effective method either to reduce the temperature generated with the help of the lubricants or to remove the heat with the help of coolant or combining both. Reduction and removal of the heat have a great significance in improving the quality of the workpiece. Usually, the techniques adapted for cooling and lubrication are traditional flood cooling, cryogenic cooling, cold air cooling, use of solid lubricants and Minimum Quantity Lubrication (MQL). From the cooling effect and environment point of view, MQL and solid lubricants are regarded as more effective green manufacturing techniques [31-35].

2.3 MQL in machining

There are two major functions of cutting fluids, one is to lubricate and another is to cool the machining zone. They affect machining conditions by lowering the temperatures, heat affected zone, by improving the surface finish, tool life etc. Proper maintenance is required when cutting fluids are used in the form of a flood. And also cutting fluids are to be properly disposed of. EPA (Environmental Protection Agency) put cutting fluids into hazardous wastes list. Properly disposing of the cutting fluids is also a costly affair; including grinding fluid cost along with filtering, waste disposal etc., which takes a great part of total cost [35]. Triethanolamine, an essential ingredient of cutting fluids, causes cancer and asthma [36]. Long term exposure to cutting fluids causes dermatitis and inhaling its mist causes respiratory problems [37]. According to NIOSH (The National Institute for Occupational Safety and Health) recommendations, a worker should not be exposed to aerosols of cutting fluids for more than 10hr/day during a 40-hr work week, limited to a rate 0.4 mg of cutting fluid per m^3 of air [38].

Researchers started thinking of alternative methods like the use of solid lubricants, MQL, etc. Solid lubricants like graphite, MoS_2 , etc., are supplied into machining zone in different forms like powder, paste, etc. But, there was no effective method of application of these lubricants. MQL (Minimum Quantity Lubrication) is another alternative to cutting fluids

where a small amount of liquid is being injected into the machining zone directly with the help of compressed air.

Unlike flood cooling (in which large quantity of fluid is poured and reused), in MQL technique small amount of fluid is supplied to the machining zone. When cooling and lubrication required at a time, then MQCL is used, where straight oils or emulsion are applied to provide localized cooling and lubrication [39]. As just sufficient quantity of cutting fluid is used in these MQL techniques, disposal and maintenance are not required.

MQL systems are of three types [40]. 1. Cutting fluid is drawn into the machining zone with the help of the air by creating low pressure. 2. With the help of a dosing pump, cutting fluid is supplied without using air. 3. Through the pressure system, lubricant and compressed air are mixed and sprayed in the cutting zone where both compressed air and lubricant can be varied independently.

Many researchers have been investigating the application of MQL in different machining processes. Yasir et al. [41] observed the effect of MQL in machining Ti-6Al-4V with PVD coated cemented carbide tool with supplying water-immiscible oil at 50 ml/hr and 100 ml/hr and three speeds, 120, 135 and 150 m/min. Among these, 135 m/min gave a longer life at 100 ml/hr mist cooling. MQL was found to be better when the tool begins to wear, because of better lubrication.

Alves et al. [42] did an internal grinding of quenched and tempered SAE 52100 steel by applying both MQL and conventional techniques. Flow rates of 40 ml/hr, 60 ml/hr and 80 ml/hr are applied in their study. Better surface roughness values were observed with the flood cooling technique as the proposed MQL was unable to flush the chips away. Tai et al. [43] took nine varieties of cutting fluids and compared each other by considering properties like lubricity, wettability, mist characteristics, extreme pressures etc., and correlated for machinability. High mist concentration, low viscosity, large mist droplet diameter and high wettability were recorded to give good machinability. This machinability performance evaluation is also done on drilling and reaming, applying the above nine fluids as MQL. Optimum machining was observed with low viscous cutting fluid. Cong Moa et al. [44] used pure mineral oil and water-oil mix in MQL to grind AISI52100 with aluminium oxide (mesh size 100) grinding wheel and their performance was compared with that of dry grinding and

conventional cutting fluid (water based) applied at 6 l/min. MQL reduced the temperatures generated and cutting forces and enhanced the surface quality of the ground workpiece. The thickness of heat affected layer and the grinding temperature were reduced when the oil-water mix is used in MQL, while surface roughness and tangential forces were reduced when pure oil is used. Affected layers are shown in Fig 2.1. Thaker et al. [45] investigated the influence of various MQL parameters like delivery pressure, lubricant quality, nozzle direction, pulse frequency, cutting speed and feed on cutting Inconel718. It was recommended that the low cutting speed and feed, high delivery pressure (13MPa), the quantity of lubrication and pulse frequency, and inclined nozzle direction would result in low cutting force, temperature and tool wear. It was also concluded that the operator's health is protected and detrimental effects on the environment were reduced with the pulsed jet mode in MQL.

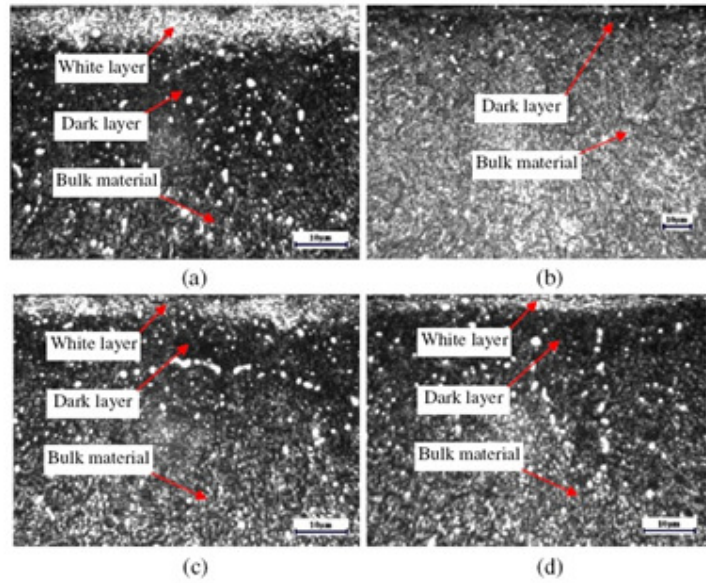


Fig 2.1 Affected layers for (a) Dry grinding (b) Wet grinding (c) Pure oil MQL (d) Oil water MQL [44]

Sadeghi et al. [46] used different grinding fluids: Synthetic oil, vegetable oil, Behran cutting oil 34 and Behran cutting oil 53 in MQL grinding to grind low alloy steel AISI4140 using Al_2O_3 grinding wheel. All the above lubricants were applied to the grinding zone at different flow rates and at different air pressures. It was observed that both normal and tangential forces were reduced on using the MQL technique when compared to flood cooling as MQL provided better slipping of abrasives at the interface. Among the oils used, synthetic oil gave the lowest tangential force, Behran cutting oil 53 and vegetable oil gave better

cooling effects. From this study, it was also reported that during MQL, metal cutting happened due to shear and fracture, while it was due to plastic deformation and ploughing during flood cooling.

Tawakoli et al. [47] explained the mechanism of MQL as follows. Oil droplets temporarily store in the fractured grains and pores of the grinding wheel and reach the contact zone to cool and lubricate. Wheel pores and grain fractured grooves (formed during dressing) which are acting as a source of lubricant are shown in Fig 2.2.

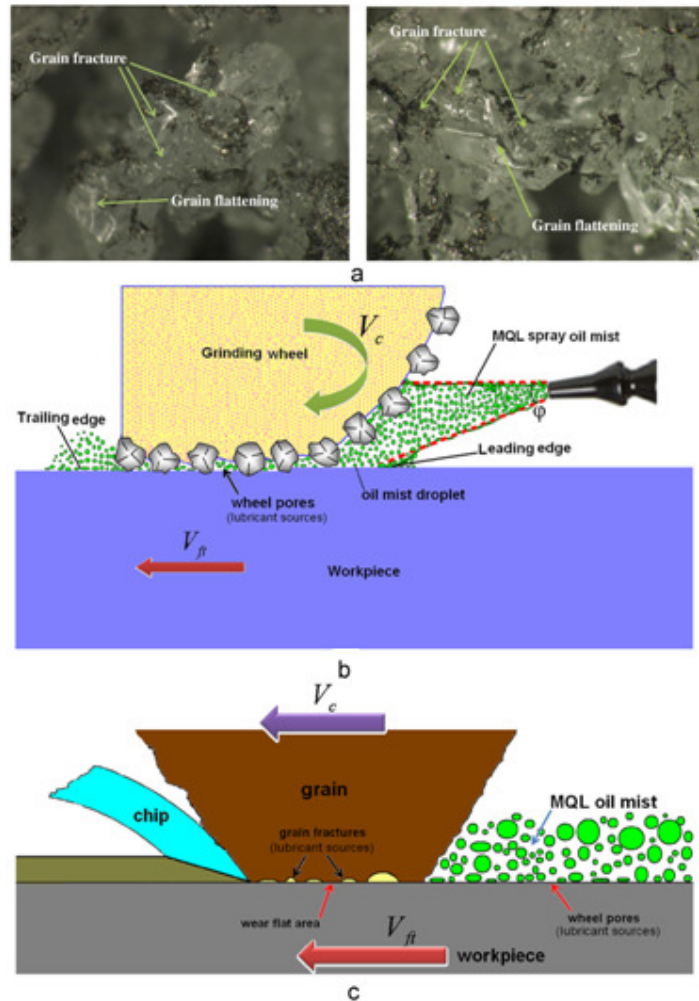


Fig 2.2 (a) Abrasive grains wear mechanisms of vitrified bond corundum after grinding (magnification: 175 \times), (b) schematic of oil mist spray in MQL grinding, and (c) lubricant sources at the interface of the grain and workpiece surfaces [47].

Silva et al. [48] analysed the behaviour of MQL and compared it with conventional cooling with an intention to produce high-quality mechanical components, not only in the point of functionality but also in the point of safety. The material used was ABNT 4340 steel, grinding wheel used was 38A60KV. LB1000 lubricant was supplied as MQL along with air and lubricants with adjustable flow rates. They observed that MQL had produced higher compressive residual stresses than the conventional cooling, which were beneficiary for mechanical properties like fatigue strength and service life of components.

From the above discussions and available literature MQL with either neat oils or water-soluble oil has several advantages over conventional flood cooling in terms of machining parameters like tool wear, cutting forces, temperature and specific energy. As the MQL system uses a small amount of cutting fluid, MQL would definitely be a superior process when a fluid with special cooling and lubricating properties is used in it. This led to exploring properties and utility of nanofluids in machining operations as they have high lubricating and heat carrying abilities.

2.4 Solid Lubricants in Grinding

The friction between wheel and workpiece can be minimized, by means of effective lubrication, and further intensity of the heat responsible for the thermal damage could be reduced. There are many solid lubricants identified in modern tribology which can sustain over a wide range of temperatures and provide lubricity [49, 50].

Venu et al. [51] used graphite as a solid lubricant in ceramic grinding. Graphite with an average particle size of $1\mu\text{m}$ was kept in the hopper and sent to the grinding zone by gravity, and then it was vibrated by the cover plate of the grinding wheel. At $3\text{ mm}^3/\text{sec}$ solid lubricant supply, it was observed that there was a reduction in grinding forces, specific grinding energy and surface roughness.

Shaji and Radhakrishnan [16] developed graphite sandwiched grinding wheels. The concept of solid lubricant sandwiched wheels was to get two benefits of interrupted grinding and benefits of the solid lubricant in grinding. This technique was adapted by making slots across the width of the wheel radially inwards by abrasive water jet cutting as shown in Fig 2.3. These slots were made radial inwards. The width of slot inside was more, and the slot was convergent towards the periphery of the grinding wheel so that solid lubricant filler

would not come out. Solid lubricant filler is composed of phenolic liquid resin, powder resin, fine AA grit and 50% graphite by weight. After mixing these ingredients thoroughly, the filler was filled in the slots made in the grinding wheel. The stuffed grinding wheels were cooled after curing was done. And the newly made wheels withstood the standard tests performed on the grinding wheels. As the number of slots increases, an increase of normal forces and a decrease of tangential forces was observed. In the case of an increased number of slots, because of the increased supply of solid lubricant, wheel clogging was more and hence normal forces were also more. At the same time, because of the increased number of slots, interruptions for grinding were more and thus resulting in lesser tangential forces. Grinding force ratio and specific energy were observed to be lowered for sandwiched wheels compared to standard wheels.

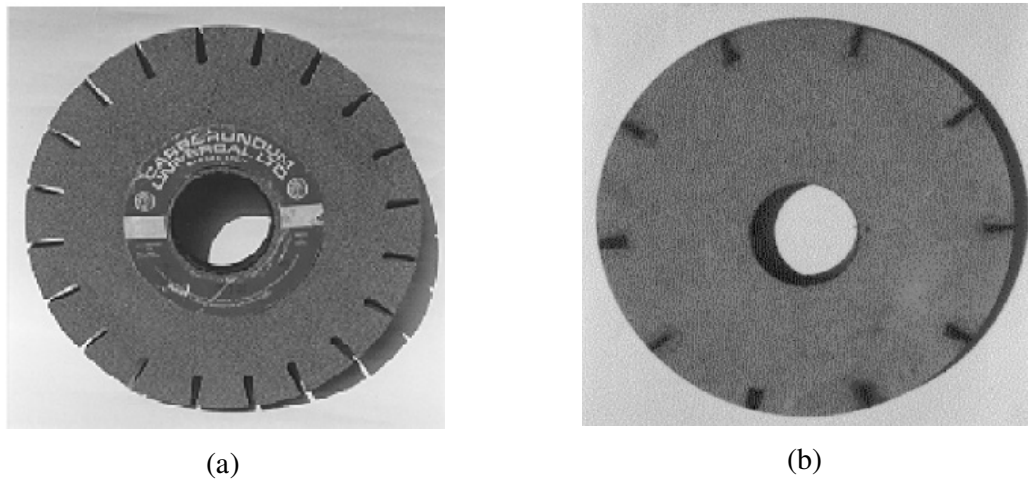


Fig 2.3. (a) wheel after the slots cut on it—20 slots, (b) lubricant sandwiched wheel ready for experimentation—10 slots [16].

Ming Yi Tsai et al. [52] developed micro graphite impregnated grinding wheel. The newly designed grinding wheels were made of aluminium oxide grit in which micro graphite had been impregnated to lubricate the grinding zone. Particles of micro graphite were heat treated with hydrogen which was flown at 500°C for minimum 30 minutes at a rate of 2 L/min to disperse the graphite particles uniformly in the graphite wheel. Because of hydrogenation, the surface of the graphite particles was covered with layers of hydrogen ion (H⁺) so that they repel each other. Images of the micro graphite and alumina were shown in Fig 2.4. Their particle sizes were 50 and 150 μm respectively. Graphite was taken to mix in

Al_2O_3 in five weight fractions of 0.1, 0.5, 1, 3 and 5%. Schematic illustration of a physical model for the structure of graphite-impregnated grinding wheel is seen in Fig 2.5. Then, there was no much difference in the surface roughness, but thermal damages were reduced. When the amount of graphite was being increased (3 and 5 wt%), wheel wear ratio was observed to be more. Graphite below 0.5 wt% was suggested for extended wheel life.

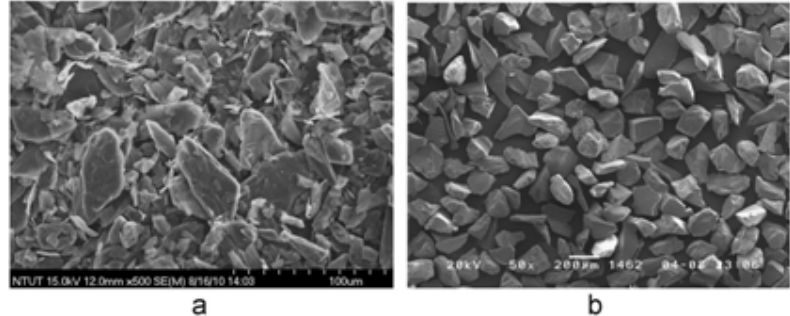


Fig 2.4. Appearance of (a) graphite and (b) aluminium oxide particles [52].

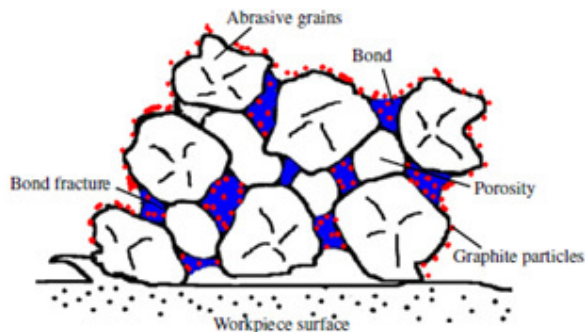


Fig 2.5. Schematic illustration of a physical model for the structure of graphite-impregnated grinding wheel [52]

Shaji and Radhakrishnan [17] tried to make graphite and calcium fluoride (CaF_2) moulded grinding wheels with vitrified bonded A60K5 wheel composition. But, both the wheels failed for the following reason. Vitrified temperature generally would be of the order of 1400°C , while at 550°C , graphite gets oxidized. The resulting products of oxidation affected bond strength and failed to take the speed test. Similarly, CaF_2 moulded wheels also failed speed test because CaF_2 was reacting with silicate present in the grinding wheel and weakening the bond strength. Thus they chose an alternate solution, resin bond, to mould solid lubricants into grinding wheels. The baking temperature was only $150\text{--}200^\circ\text{C}$, both graphite and calcium fluoride can withstand this temperature. Resin bonded grinding wheels

were structured and could be used in high-speed machining. Wheels moulded of graphite were made on adding graphite at 3%, 6% and 9% weight fractions. While making CaF_2 moulded wheels, CaF_2 was added at 5%, 10% and 15% weight fractions. Graphite was added relatively in lower weight fractions than that of CaF_2 because CaF_2 increases its adhesiveness causing greater bond strength with the rise in the temperature [53]. Compared to vitrified bonded wheels, wheel wear was observed to be higher for resin bonded wheels of their soft structure and thermal softening nature. Resin bonded wheels were failed by thermal softening than by grain fracture, in turn, causing bond fracture as in vitrified wheels due to mechanical stress [54-56]. Grinding forces, specific energy and surface roughness that solid lubricants were effective in improving the grinding quality with solid lubricants. Saturation in the effectiveness of their lubricity was observed with increasing the amount of solid lubricant.

From the above literature, solid lubricants are effective in grinding in reducing the friction and temperature generated. MQL with nanofluids is also proven to be effective in taking off the heat generated. In the current investigation, for better grinding performance, attempts are made to combine these two, reducing the heat and removing the heat at the grinding zone. And graphene nanoplatelets (GNP) are newer solid lubricants which are used rarely in machining. Here in this study, GNP is impregnated in the grinding wheels to reduce friction and used as nanoparticles in nanoMQL to remove the heat generated from the contact zone.

2.4.1 Nanofluids

Nanofluids are fluids in which solid particles at nano-size are suspended. These nano-sized particles are expected to increase the heat carrying capacity of the fluid and also make the fluid a better lubricant. Hence, thermal conductivity and viscosity of nanofluids are studied by many researchers to find how these two properties are affected by the addition of the nanoparticles.

Thermal conductivity is a key property of nanofluid which denotes the ability to take the heat away from the machining zone. Viscosity is the resistance offered by a fluid to its own flow, is another property of nanofluid which decides the lubricity, in turn, reduces the heat generated. An ample number of research papers is available to study these two important properties of Nanofluids.

Eastman et al. [57] took ethylene glycol fluid as a base fluid and suspended copper nanoparticles and found that the dispersion was having higher thermal conductivity with respect to the base fluid. From their study, three points are noticed: Thermal conductivity was enhanced up to 40% with small volume fraction (<1%), suspension stability with thioglycolic acid as a stabilizer is improved. Suspensions used in two days of preparation exhibited greater thermal conductivity than the liquid stored up to two months. A report presented by Buongiomo et al. [58] on International Nanofluid Property Benchmark Exercise or INPBE, in which, 30 organizations measured the thermal conductivity of similar nanofluid samples, using optical, steady state, transient hot wire methods etc. They observed that when the aspect ratio and concentration of nanoparticles are increased, thermal conductivity increased, and thermal conductivity decreased when the thermal conductivity of the base fluid is decreased. For all the methods, a maximum deviation from the average of the thermal conductivities measured is 5% for water-based samples and 10% for polyalphaolefins lubricant based samples.

Xie et al. [59] prepared many nanofluids, measured thermal conductivities for those to know the influence of various factors: size of nanoparticles, volume fraction, tested temperature, pre-treatment process, the thermal conductivity of the base fluid and additives added. Non-oxide and oxide nanofluids exhibited higher thermal conductivity than the base fluid and thermal conductivity further increases with an increase in the volume fractions. Graphene dispersions showed higher thermal conductivity than oxide nanofluids. But CNT suspension showed better thermal conductivity than those of Graphene for same particle loading. For most of the nanofluids, thermal conductivity enhancement is independent of temperature, but for Cu nanofluids, thermal conductivity was increasing with temperature because of the Brownian motion. When 5% nanoparticles of Al_2O_3 were suspended in water and pump oil, thermal conductivity increased by 22% and 38% respectively when 1% CNT dispersed in distilled water, ethylene glycol and decene, the thermal conductivity increased by 7%, 12.7% and 19.6% respectively. And enhancement of thermal conductivity was more with CNT than Al_2O_3 , independent of the base fluid type. Considering the influence of the size of nanoparticles, an optimal value for Al_2O_3 was existed, while for CNT, thermal conductivity was found to increase with the decrease in the nanoparticle average diameter.

Ding et al. [60] gave a detailed report on conduction and convection under both natural and forced environments, and also at the boiling condition. He found that thermal conductivity increased due to networking of nanoparticles with an increase in the concentration, but in convection, it decreased due to an increase in the viscosity. Boiling heat transfer increased for both Al_2O_3 and TiO_2 and this increment was sensitive to variation in the concentration of TiO_2 . Fig 2.6 depicts the thermal conductivity data collected at room temperature from their own work as well as the data reported in the literature. They had analysed the data points, splitting into two groups, and each group was separated by a band. Left side points were for CNT and metal particles based nanofluids and right side ones were for metal oxides and carbide based nanofluids. Two groups exhibited an increase in thermal conductivity with concentration.

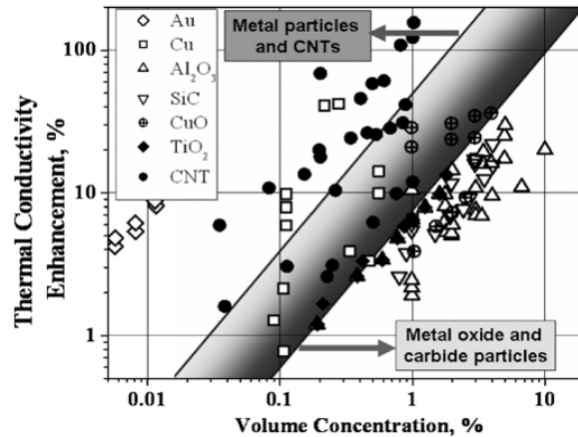


Fig 2.6. The thermal conductivity of nanofluids [60]

The viscosity of a fluid is the resistance to its own flow. The variation in the viscosity of the base fluid with respect to the type of nanoparticle inclusion has been reported by many researchers. Garg et al. [61] suspended copper nanoparticles varied from 0.4% to 2% by volume fraction in ethylene glycol. The viscosity of the suspensions was also measured by rheometer and observed that it was enhanced by four times that estimated by Einstein's viscosity law. Fig 2.7 shows the change in viscosity with the corresponding change in volume fraction of the nanoparticles.

Tavman et al. [62] dispersed nanoparticles of SiO_2 and Al_2O_3 in water. SiO_2 particles of 12 nm in three vol% (0.45, 1.85 and 4 vol%), and Al_2O_3 particles of 30 nm in two vol%

(0.5 and 1.5 vol%) were dispersed in water and measured viscosity by vibro-viscometer. Viscosity was observed to increase rapidly with an increase in concentration and a decrease in temperature, but the trend couldn't be assessed with Einstein model. Viscosity variation with temperature for SiO₂ dispersion in water is shown in Fig 2.8.

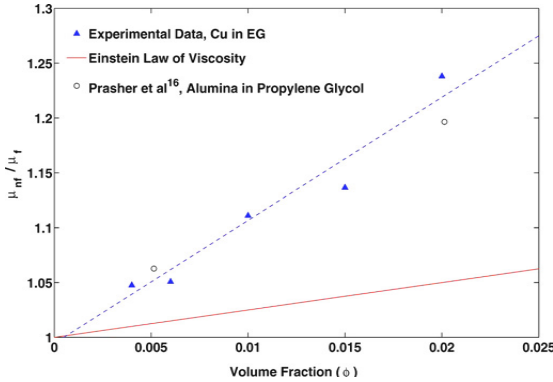


Fig. 2.7. Variation of viscosity with volume fraction [61]

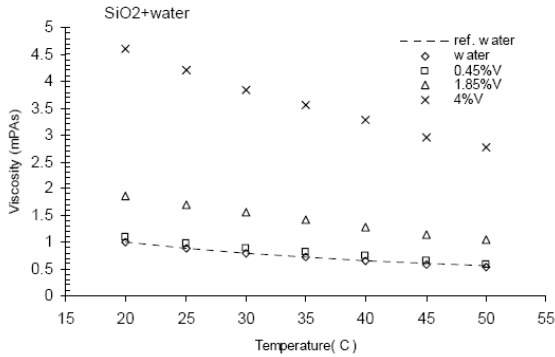


Fig. 2.8. Variation of viscosity with temperature for SiO₂ dispersion in water [62]

Zhu et al. [63] prepared Cu-H₂O nanofluids and measured viscosity using capillary viscometers, varying the weight fractions of nanoparticles (Cu) and Surfactant (SDBS). The concentration of surfactant and temperature were found to be major influential factors in affecting viscosity and concentration of Cu found to be less influential.

In another investigation, Mirmohammadi et al. [64] studied the effect of size, shape and quantity of nanoparticles, alcohol addition, temperature and sonication time on thermal conductivity, viscosity and shelf stability of nanofluids. Thermal conductivity increased with increase in particle concentration, temperature and sonication time, and with a decrease in alcohol quantity. Viscosity decreased with increase in the quantity of alcohol, temperature and sonication time, a decrease in particle concentration. Increase in the size of particles up to 250

nm, led to a decrease in both viscosity and thermal conductivity, and bigger particles ≈ 800 nm increased both viscosity and thermal conductivity drastically.

Nanofluids are having all the properties that ideal grinding fluid should and many researchers used these nanofluids in MQL form in grinding to reduce heat and to reduce the heat generated.

2.4.2 NanoMQL

Zhang Dong et al. [65] experimented to evaluate nano MQL grinding. They used Molybdenum Disulphide, Carbon Nanotubes and Zirconium Dioxide as nanoparticles in MQL fluid (5% of Syntilo9930 is mixed in 95% water). They used a grinding wheel WA80MV12P in which abrasives were alumina, bond was vitrified. The workpiece was hardened steel. The authors found that specific grinding energy was lowest for MoS_2 [32.7 J/mm^3], 8.22% and 10.39% lower than CNT and ZrO_2 . MoS_2 volume concentrations are varied, 1%, 2% and 3%. Better lubrication effects were observed at 2%. Frictional coefficient, specific grinding energy and surface roughness decreased as MoS_2 content increased from 1% to 2%. These output parameters increased when MoS_2 increased from 2% to 3% due to clustering of nanoparticles at higher volumes. Nanoparticle droplets which were dropped in the grinding zone helped the grinding zone to cool (Fig 2.9) and lubricate (Fig 2.10). Nanoparticles, additives in grinding fluid, increased the thermal conductivity of the grinding fluid and convective heat transfer capacity of nanoparticle jet flow according to the theory of heat transfer enhancement by solids. Nanoparticles present in the droplets act as balls in ball bearings and turn the sliding friction to rolling friction, offering lesser resistance thereby generating lower temperatures. The specific energy in grinding for MQL (45.5 J/mm^3) was higher than that of flood grinding (29.85 J/mm^3), but specific grinding energy for nanoparticles MQL (32.7 J/mm^3) was very close to that of flood grinding. Hence, the authors proved that nano-MQL would be the best alternative for flood cooling with respect to grinding performance.

In a study, a grinding wheel with silicon carbide as abrasive (GC60K5V) and Ti-6Al-4V material were taken by Setti et al. [66]. Grinding speed 17 m/s, table speed 9m/min, depth of cut 5 μm . Dressing parameters were: Dressing depth:10 μm , dressing lead:250mm/min, no. of dressing passes: 4. Water was the base fluid; Al_2O_3 and CuO were the nanoparticles for the

nanofluids. Surfactant Sodium Dodecyl Benzene Sulfonate (SDBS) was added to the base fluid at a 1/10th weight fraction of nanoparticle weight. Nanoparticles were added in different volume fractions, 0.05%, 0.1% and 1%. Significant reduction in the coefficient of friction was observed with nano-MQL with Al_2O_3 when compared with nano-MQL with CuO , MQL with soluble oil, flood and dry. Nano-MQL grinding is efficient because of tribofilm formation on the surface to be ground. This tribofilm formation was observed more for Al_2O_3 than CuO as Al_2O_3 had a high melting point ($\approx 2200^\circ\text{C}$) than that of CuO ($\approx 1100^\circ\text{C}$)

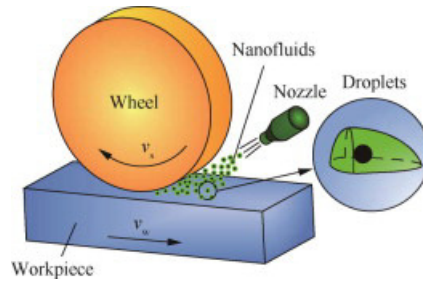


Fig 2.9. Schematic of nanoparticle jet MQL grinding [65].

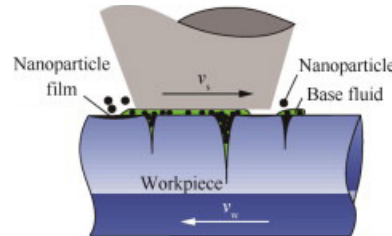


Fig 2.10. Schematic of nanoparticles in grinding interface [65].

In an investigation, Zhang et al. [67] found that the coefficient of friction between the grinding wheel and the workpiece, and the specific grinding energy were decreasing with the addition of nanoparticles in the nanofluids. But, they observed that after the addition of a certain quantity of nanoparticles, both, the coefficient of friction and the specific grinding energy started increasing. In this study, researchers used nanoparticles jet MQL containing MoS_2 nanoparticles at different concentrations 2%, 4%, 6% and 8%. Compared with 2% mass fraction, coefficient of friction values for 4%, 6% and 8% mass fractions of MoS_2 were lower by 2.9%, 7.4% and 5.8%, specific grinding energy values were lower by 3.5%, 5.8% and 3.9% respectively. From the above data, it can be concluded that the coefficient of friction and specific grinding energy lowered from 2% to 6% mass fractions, and started increasing between 6% and 8%. In the liquid suspension, while nanoparticles are moving, they crash and

gather to form clusters; hence more concentration of nanoparticles results in agglomeration. Finally, nanoparticles lose dynamic stability and lower the lubrication property of nanofluids, causing the coefficient of friction to increase.

Kalita et al. [68] used surface grinders using vitreous bonded grinding wheels with Aluminum Oxide (Al_2O_3) and Norton abrasives along with nanofluids (paraffin oil as a base fluid and MoS_2 as nanoparticles) to machine ASTM AS36 grade 100-70-30 ductile cast iron. The surface quality of the ground components is analyzed with SEM. The grinding performance was evaluated on finding out grinding forces, G – Ratio, specific grinding energy, and temperature, under different grinding environments, Dry grinding, MQL, MQL with microparticles and MQL with nanoparticles. MoS_2 nanoparticles suspended in paraffin in 2% and 8% weight fractions. Nano-MQL with 8% gave the best performance in all output parameters grinding forces, G – Ratio, specific grinding energy except temperature. Flood cooling gave minimum temperature and the next best was recorded with 8% nano-MQL. Between 2% and 8% nano-MQL, there was no much difference in thermal conductivity, but 8% nano-MQL had exhibited minimum temperature because of the good lubrication and minimum friction. From SEM-EDS microanalysis of both ground surface and grinding wheel after grinding showed that nanoparticles presented in the nano-lubricants were forming tribofilms and the pores in grinding wheel acted as micro-reservoirs for nano-lubricants and gave lubricity during grinding. Both tribofilms and micro-reservoirs proved nano-MQL a better process.

2.4.3 Graphene nanoplatelets

As discussed above, solid lubricants are effective in reducing the heat and are also effective in removing the heat when suspended in coolants. But, some of the solid lubricants are sensitive to the test environment. Example, MoS_2 will not lubricate in the presence of water or oxygen molecules, similarly, graphite or boric acid will not act as a lubricant in the absence of moisture in the surrounding air [49]. The solid lubricant, which is the most durable, environmentally insensitive (chemically inert) and easy to be sent to the grinding zone/ contact interfaces, is most desirable. Graphene provided extreme wear resistance in all tested environments without posing any adverse effects on the environment [69]. Graphene is a solid lubricant as well as is environment-friendly. So, it is selected as a solid lubricant in the present study.

Graphene is one of the allotropes of carbon which consists of carbon atoms arranged in a single layer, and in a hexagonal lattice [70]. This thinnest material is a basic structural element in many allotropes of carbon like graphite, charcoal, diamond and etc. Unintentionally, it has been used for centuries in the form of graphite and pencils, but there was no standard and controlled method to extract it. In 2004, Andre Geim and Konstantin Novoselov (University of Manchester) have rediscovered, isolated and characterized Graphene [68]. They isolated it using mechanical exfoliation or ‘Scotch-tape’ method [69], in which highly ordered pyrolytic graphite (HOPG) is peeled into multiple layers by commercially available adhesive tape and transferred those layers on to the substrate by pressing against it. Later many easy methods to produce graphene has been discovered like Dry mechanical exfoliation [69, 70]; chemical exfoliation [71, 72]; unzipping of CNTs through chemical, electrochemical or physical methods [73]; Chemical vapour deposition [74, 75] and etc. Both of them, Andre Geim and Konstantin Novoselov (University of Manchester), jointly won the Nobel Prize in Physics for ground-breaking experiments regarding 2D material graphene, in 2010 [79].

Being two-dimensional material, Graphene offers unique wear and friction properties which are not generally observed in conventional materials. Graphene’s mechanical properties were tested by Lee et al. [80] and confirmed that it is one of the strongest materials ever tested. This extraordinary mechanical strength is very much important in tribological point of view, as it protects the substrate from the wear or rubbing. Graphene is impermeable to liquids and gases, and thus protects the rubbed layers from water or oxygen molecules, to get oxidized [81]. This wonderful material can also be used as a pure solid lubricant, and also as a suspension in liquid lubricant [82]. Balandin et al. [83] measured the thermal conductivity of graphene, compared it with CNT and revealed that graphene can serve better than CNT as a thermal conductor. Its extreme strength, chemical inertness, the easy shear capability to slide over one layer on the layer, and the heat transfer capability because of its high thermal conductivity made this material novel and attractive to use it in the present research.

Chu et al. [84] aimed at creating enhanced environmentally benign graphene platelet-based cutting fluids to improve high-performance micro-machining. They used plant-based canola oil as base oil in which functionalized graphene was dispersed at three different weight fractions, 0.05%, 0.10% and 0.15%. Higher weight fractions over 0.15% were not considered

as it was difficult to get homogeneous graphene dispersions. After functionalization with carboxyl surfactants, mixer of graphene and canola oil were sonicated, and tested for the thermal conductivity, coefficient of friction and kinematic viscosity. In Table 2.1, all values are compared with the case where pure canola oil is used. Thermal conductivity and kinematic viscosity were observed to be increased, the coefficient of friction was observed to be lowered, with an increase in weight fractions of graphene.

Table 2.1. Comparison of graphene dispersed canola oil with pure canola oil [84]

Graphene (Wt %)	Thermal Conductivity (% of increment)	Coefficient of Friction (% of decrement)	Kinematic viscosity (% of increment)	Temperature (% of decrement)	Cutting Force (% of decrement)	Surface roughness (% of decrement)
0.05	0.66	45.45	2.27	24	6.9	10.3
0.10	1.9	36.36	3.69	31	11.3	8.6
0.15	2	21.21	4.44	58	8.9	5.9

Similarly, Temperature, cutting force and surface roughness were also observed to be decreased with increase in the graphene wt %. But, the rate of decrement in the cutting force was decreased between 0.10% and 0.15% wt % graphene, due to the undispersed clumps of graphene at that high graphene concentration (0.15%). Finally, Chu et al. [84] concluded that graphene was effective in improving the micro-machining.

Ranjbarzadeh et al. [85] prepared graphene oxide based nanofluids to use in machining for cooling purpose and also tested for their stability and thermal conductivity. They varied pH of base fluid and duration of the ultrasonic waves and measured Zeta potential. It is observed that high Zeta potential gave more stability. 0.1, 0.2, 0.3 and 0.4% mass fractions of graphene oxide nanoparticles were used in the suspensions. Thermal conductivity was increasing with the addition of graphene oxide. It is increased by 71% for 0.4% mass fraction compared to pure base fluid. And hence, they concluded that the addition

of graphene oxide nanoparticles increases the heat carrying capability of base fluid drastically and helps to cool in the machining process.

Singh et. al [86] developed hybrid nano-cutting fluid and evaluated its performance in hard turning. In this investigation, graphene nanoplatelets (GNP) along with alumina were mixed to develop hybrid cutting fluid. GNP was added in 0.25, 0.75 and 1.25% volumetric concentrations. Hybrid cutting fluid exhibited higher thermal conductivity and higher viscosity with the addition of nanoparticles, but lower than individual constituents. Hybrid nanofluids had also generated the least wear. Addition of GNP increased the wettability compared to both alumina-based cutting fluid and base cutting fluid. This study revealed that turning of AISI 304 has improved in MQL environment with newly developed hybrid nanofluid when compared to alumina-based cutting fluid. It shows that GNP enhanced the performance of hybrid nanofluids.

Uysal [87] used nano graphene reinforced vegetable oil in machining AISI 430 stainless steel. As stainless steel having lower thermal conductivity and work hardening nature, milling of stainless steel may result in failure of milling tool such as flank wear, crater wear, cracks, chipping, etc. He applied nano graphene reinforced vegetable oil through MQL in 1% and 2% weight percentages, at two MQL flow rates of 20 and 40 ml/h. It was observed that nano graphene reinforced vegetable oil had advantages over dry milling and pure vegetable oil milling in terms of initial flank wear.

2.5 Research gaps in the literature

The increasing use of Inconel 718 in the various critical applications is demanding novel and improved methods of machining strategies to improve the surface quality of Inconel 718 components. Grinding is one of the most used machining processes to finish the Inconel 718 components. GNP is a relatively new solid lubricant which is not being used regularly and commercially.

Very few studies reported using graphene as a solid lubricant in machining as a colloidal substance but no literature was found using it in self-lubricating tool in grinding. GNP was used in nanoMQL, but it is not explored in combination with the grinding process. No literature is found in the combination of GNP, nanoMQL, grinding and Inconel 718. To

fill this research gap, efforts are put combining all these to improve the surface quality and service life of Inconel 718 components.

2.6 Specific objectives of the present research

The specific objectives of the present research are

- To develop and evaluate GNP impregnated self-lubricating grinding wheels in grinding Inconel 718
- To study the influence of GNP concentration and surface area on the performance of self-lubricating grinding wheels in grinding Inconel 718
- To study the influence of GNP concentration and surface area on basic properties of GNP based nanofluids
- To evaluate the performance of GNP based nanofluids in grinding Inconel 718 in the nanoMQL environment
- To evaluate the performance of GNP impregnated self-lubricating grinding wheels in grinding Inconel 718 in the nanoMQL environment

Chapter III

Experimentation

3.1 Introduction

Aiming to improve the surface quality of Inconel 718 workpiece, resin bonded grinding wheels are developed by impregnating GNP into the wheel structure during wheel molding stage itself and also GNP based nano-cutting fluids with different weight fractions and specific surface areas of GNP are developed in order to have proper application of solid lubricants at the wheel-workpiece interface. Different aspects of the grinding performance such as grinding forces, grinding temperature, surface roughness, grinding coefficient, specific grinding energy and grinding wheel wear are evaluated and compared with the conventional grinding wheel performance.

In this chapter, selection of materials, development of self-lubricating grinding wheels, preparation of nano-fluids, measurement of thermal conductivity and viscosity, experimental setup, details of equipment used and procedure followed for measuring the process performance are discussed in detail.

3.2 Selection of Materials

Among difficult to machine materials, Inconel 718 is chosen as workpiece material and similarly, GNP is chosen as a solid lubricant.

3.2.1 Inconel 718

Inconel 718 plates of 80 mm x 70 mm x 5 mm are directly procured from M/s Mosam Impex Pvt. Ltd., Mumbai, whose chemical composition is (in weight %): 52.46 Nickel, 19.15 Chromium, 10.40 Aluminium, 4.94 Niobium, 3.04 Molybdenum, 1.08 Titanium, 0.15 Silicon, 0.05 Manganese, 0.04 Carbon, 0.006 Phosphorus, 0.002 Sulfur, 0.002 Boron, 0.002 Magnesium. Mechanical properties of this superalloy are tensile strength - 1489 MPa; yield strength 1319

MPa; elongation - 20 %; shrinkage - 46 %; and hardness of material - 468HV. The two holes of diameter 8 mm are meant to hold the workpiece on the dynamometer firmly with the help screw fasteners as shown Fig 3.1



Fig 3.1. Inconel 718 component procured

3.2.2 Graphene nanoplatelets

Graphene nanoplatelets with a trade name of xGnP, procured from xG sciences, USA, are used for development of self-lubricating grinding wheel. They are made from synthetic, acid-intercalated graphite based on a microwave exfoliation method [12]. GNP with three average surface areas 300, 500 and 750 m^2/g , with an average thickness of 2 nm, the average width of 1-2 μm (Table 3.1) are used in this work.

Table 3.1. Grades of GNP

Grade	Average Surface area (m^2/g)
Grade I	300
Grade II	500
Grade III	750

Surface treatment of GNP

In order to disentangle the nanoplatelets that tend to cling together and to ensure uniform dispersion of GNP in grinding wheel, nanoplatelets are treated with a cationic surfactant. Cetyl Trimethyl Ammonium Bromide (CTAB) is selected for this purpose as it will not cause any damage to morphology and GNP during processing, and is economical [13]. A pre-measured amount of GNP is added to acetone consisting of 15mg of CTAB and then sonicated for 1 hour using ultrasonic probe sonicator (Fig 3.2). After sonicating for a specified time, treated GNP is obtained by vacuum filtering the suspension as shown in Fig 3.3 using Millipore PVDF membrane filter paper with a pore diameter of 0.22 μm . The sample is then dried in a vacuum oven (Fig 3.4) at 60°C for 12 hours. The solid lumps (Fig 3.5) obtained after drying are pounded into a fine powder using mortar and pestle.



Fig 3.2. Ultrasonic probe sonicator



Fig 3.3. Vacuum filtration setup

Ultrasonic probe sonicator:

Make	: M/s Electrosonic Industries, Mumbai
Maximum power output	: 600 watts
Operating frequency	: 20 kHz
Input	: 110 V AC @ 10 A
Programmable timer	: 1s- 1h



Fig 3.4. Vacuum Oven



Fig 3.5. Solid lumps obtained after drying

Vacuum Filtration:

Borosilicate glass membrane Filter Holder Assembly with membrane support

Membrane diameter: 47mm

Funnel Cap: 300

Flask cap: 1000ml

Aluminium duck clamp

Membrane filters:

Make: Millipore GVWP04700 Durapore® PVDF Membrane Filter,

Hydrophilic Plain White

Diameter: 47mm; Pore Size: 0.22 μ m; Thickness: 125 μ m; Porosity: 70%; Gravimetric Extractables: 0.5%

3.3 Development of GNP impregnated grinding wheel

Resin bonded grinding wheels are softer when compared to Vitrified wheels. It is usual practice to choose soft grinding wheels to machine hard materials, and hence resin bonded grinding wheels are chosen to machine Inconel 718 workpiece. The GNP impregnated resin bonded grinding wheels are manufactured as shown in Fig 3.6. Excluding GNP, grinding wheel consists of 80% aluminum oxide abrasives, 12% liquid bonding material, 5% powder resin, 3% additives by weight. An A80K6B grinding wheel with 200 mm x 25 mm x 31.75 mm size is

taken as a standard wheel. Fig 3.6 depicts the various stages of the manufacturing process of the GNP impregnated grinding wheel. Initially, measured amounts of abrasives, resin, additives, and GNP are thoroughly mixed by a mixer as shown in Figure 3.6 (b). After thorough mixing, wheel mould is filled with the mixture and then pressed at 147 MPa for a minute in the hydraulic press as shown in Figure 3.6 (d). Then the pressed wheels as shown in figure 3.6 (e) are transferred to furnace for curing. Finally, the wheels are cured in the furnace at a temperature of 180°C.

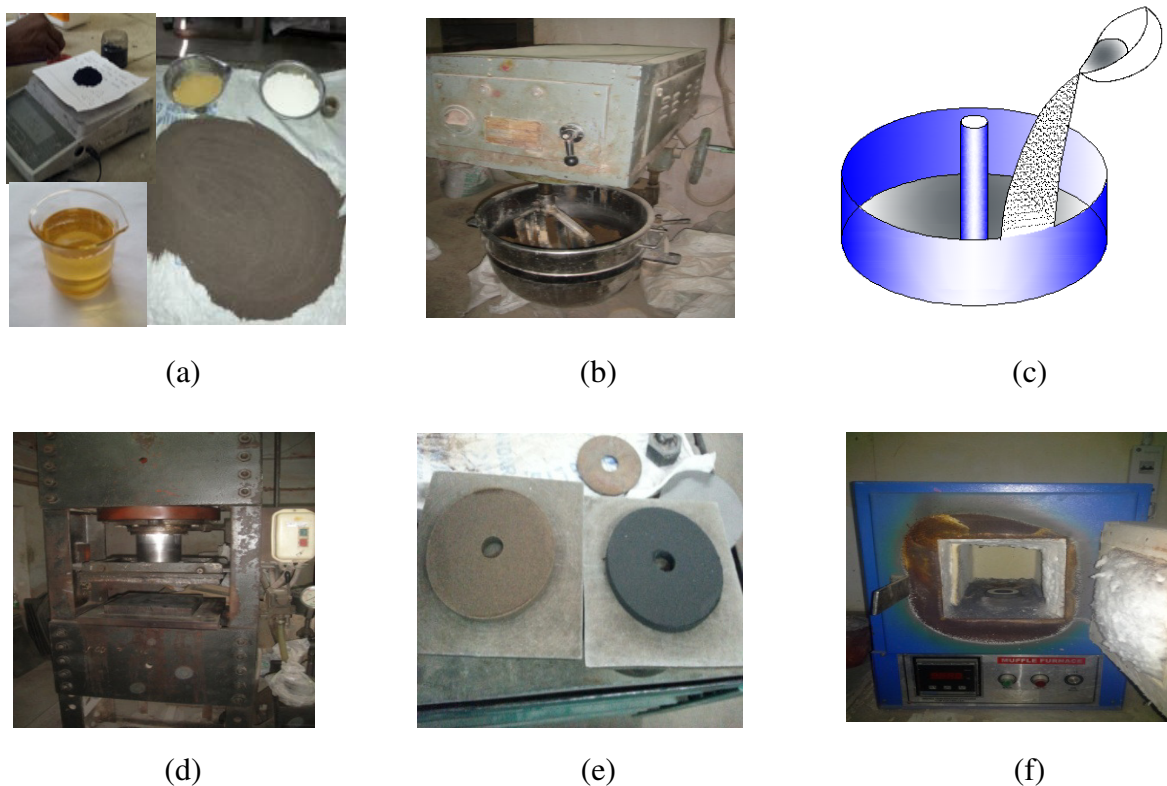


Fig 3.6. Various stages in the manufacturing of GNP impregnated grinding wheel (a) preparing ingredients of the wheel (b) mixing (c) filling mixture in the mould (d) pressing with a hydraulic press (e) transferring pressed wheels to the furnace and (f) curing

From the Fig 3.6 (e) and, Fig 3.7 (a) & (b), it is observed that GNP added wheels are darker compared normal grinding wheel, and visually, it is assessed that GNP is spread across all the grinding wheels.

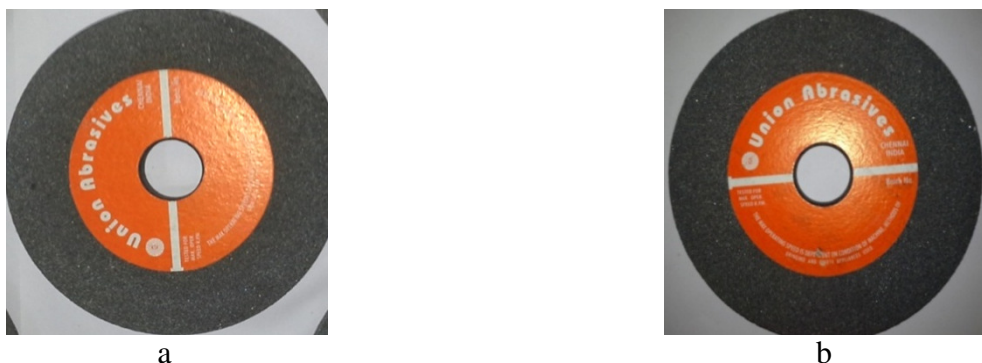


Fig 3.7.D (a) Standard Grinding Wheel (b) GNP impregnated grinding wheel

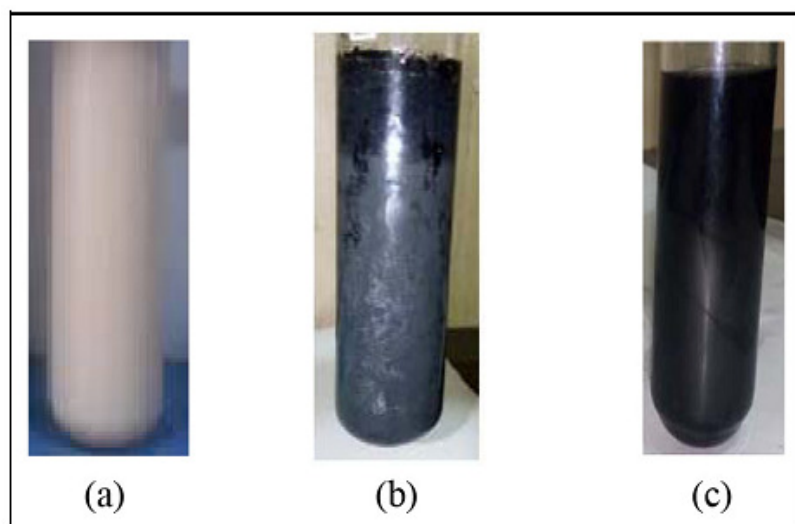


Fig 3.8. Stability of nano-cutting fluids with (a) 0wt.% GNP, (b) 0.4wt.% raw GNP in a day and (c) 0.4wt.% functionalized GNP after 5 days

3.4 Preparation of GNP based nano-cutting fluids

Water soluble oil, a mixture of water and concentrated soluble oil (95:5 by volume), is used as base cutting fluid for preparation of nano-cutting fluids. Nano-cutting fluids are prepared by adding CTAB surfactant wrapped GNP to base cutting fluid. The mixture is sonicated for 30 minutes using a probe sonicator at 35% amplitude. When raw GNP is used for the preparation of nanofluids, GNP started segregating especially in nanofluids consisting higher concentration within a day, whereas for nanofluids with surfactant wrapped GNP, dispersion remained stable even after five days. Fig 3.8 shows the stability of nano-cutting fluids. Fig 3.8 (a) shows the base

cutting fluid which is white in color. Fig 3.8 (b) shows the stability of 0.4wt% raw GNP after 1 day. It can be seen that graphene platelets agglomerated at the top, separating themselves from the base cutting fluid. Separation of graphene platelets from the sample (b) has caused a difference in color at top and bottom. Top dark layer is of agglomerated graphene. Movement of GNP from the bottom region to the top has made the color of bottom cutting fluid lighter. Fig 3.8 (c) shows stability of 0.4wt% functionalized GNP after 5 days. No agglomeration is formed. Uniform dispersion of GNP has given black color to the sample. Therefore, nanofluids, that are developed with surfactant wrapped GNP, are used for further study.

3.4.1 Measurement of thermal conductivity

Thermal conductivity is an important property of the cutting fluids which decides the heat carrying capacity it from the machining zone. The thermal conductivity of the nano-cutting fluids is measured using KD2 Pro (a transient heated needle, Fig 3.9) as per ASTM D5334-08 [88] within the temperature range of 30°C to 70°C. The thermal conductivity of each sample is measured for 5 times and mean values are reported. Before measuring, the equipment is calibrated by evaluating the thermal conductivity of water.

Specifications:

Operating Environment:

Controller : 0 to 50 °C

Sensors : -50 to +150 °C

Power : 4 AA cells

Case Size : 15.5 cm x 9.5 cm x 3.5 cm

Display : 3 cm x 6 cm, 128 x 64 pixel graphics LCD

Keypad : 6 key, sealed membrane

Data Storage: 4095 measurements in flash memory (both raw and processed data are stored for download)

Interface : 9-pin serial

Read Modes : Manual and Auto Read

Sensors:

Size	: 1.3 mm diameter x 60 mm long
Range	: 0.02 to 2.00 W/(m· K) (thermal conductivity) 50 to 5000 °Coca/W (thermal resistivity)
Accuracy (Conductivity): $\pm 5\%$ from 0.2 - 2 W/(m· K)	
	± 0.01 W/(m· K) from 0.02 - 0.2 W/(m· K)
Cable length	: 0.8 m



Fig 3.9. KD2 Pro

3.4.2 Measurement of Viscosity

The viscosity of a cutting fluid affects the lubricating environment in the cutting zone. The viscosity of the GNP based cutting fluid is measured using Brookfield viscometer (Fig 3.10). Initially, to ensure the accuracy of the instrument, the viscosity of the distilled water is measured at room temperature and error is found to be within $\pm 2\%$. After confirming the accuracy, the viscosity of each prepared nano-cutting fluid is measured as per ASTM D2983- 03 [89] within the temperature range of 25 °C to 60 °C. Each sample is measured five times and average values are reported.

Specifications:

Equipment: M/s DV-III Ultra Rheometer

Make: M/s. Brookfield Engineering Laboratories Inc., USA.

Built-in RTD temperature probe.

Accuracy: $\pm 1.0\%$ of range.

Repeatability: $\pm 0.2\%$.

USB connectivity.

Temperature range: 1°C to 100 °C.

Viscosity Range: 0.1 cP to 3k cP with no of increments 2.6 k.

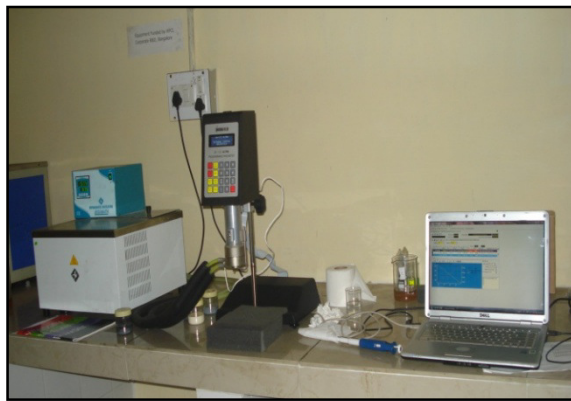


Fig. 3.10. DV-III Ultra Rheometer

3.5 Experimental set up

While grinding Inconel 718 components, forces and temperature are to be noted in parallel. MQL system is also to be set along with grinding machine only. In this section, specifications and working procedure of these grinding associated equipment are discussed.

3.5.1 Grinding Machine

In order to carry the grinding experiments, Sartaj surface grinding machine (Fig 3.11) is used. The dressing conditions are kept constant while a single-point diamond dresser is being used so that it would not influence the output variables of the processes. As the wear rate is higher in case of resin bonded wheels when compared to vitrified wheels, mode of dressing will not influence process results [90] and hence single point dressing mode is selected.

Make: M/s Sartaj Engineering works

Motor capacity: 1.5 HP

Bed Length: 450 mm

Cross Feed: 225 mm (maximum)

Vertical feed graduation: 0.01 mm

Crossfeed graduation: 0.05 mm

Table vertical movement with MICRO FEED: 0.005 mm (5 μm)



Fig 3.11. Sartaj surface grinding machine

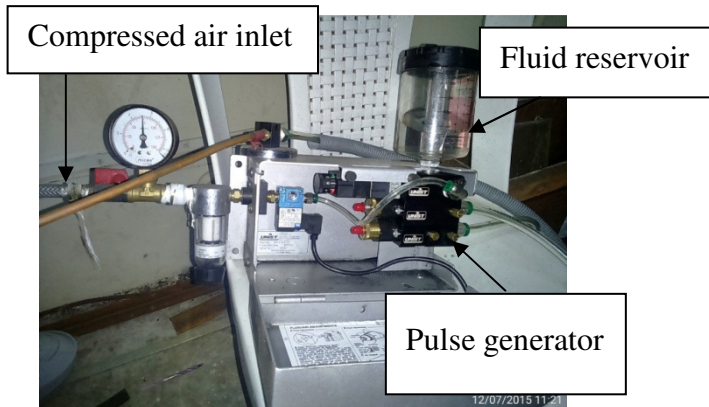


Fig 3.12. UnistCoolubricator system

3.5.2 MQL System

UnistCoolubricator System (Fig.3.12) has separate fluid and air output adjustment arrangement, which uses high-pressure air and can supply cutting fluid at a minimum flow rate of

1 mL/min. The pressure in the airline from the compressor is maintained constant at 75 psi using a pressure regulator. Required cutting fluid rate is attained by setting a pulse generator, brass adjustment knob to full stroke and air metering screw to $\frac{3}{4}$ revolutions.

3.5.3 Measurement of cutting force

Cutting forces are the key output parameters in evaluating the grinding performance, and further, those are useful to calculate specific grinding energy and grinding ratio. By using Kistler 4 - component piezoelectric dynamometer (Model: 9272) (Fig 3.16), forces are measured online sensibly and accurately and analyzed with Dyno software provided by M/s Kistler. Force plate is held firmly on the magnetic chuck. As shown in Fig 3.1., Inconel 718 plate is fastened to the force plate through the provisions with screws. For each cut made, forces are recorded and analyzed.

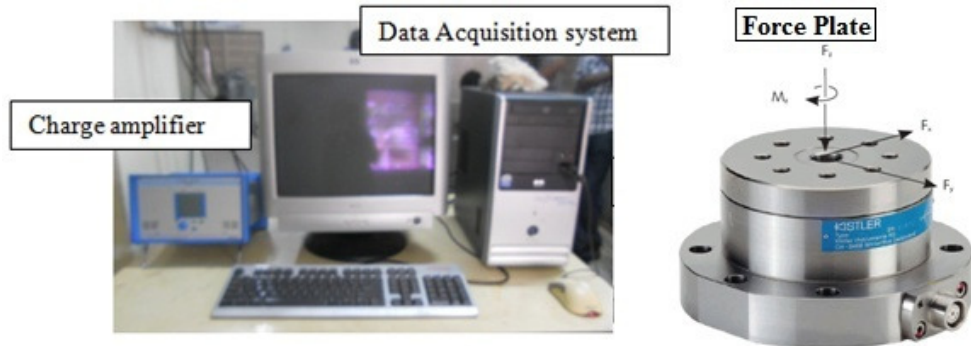


Fig 3.13. Kistler Dynamometer

Specifications

Measuring range	F _x , F _y	kN	- 5 to 5
	F _z	kN	- 5 to 20
	M _z	N-m	- 200 to 200
Calibrated measuring range 100%	F _x , F _y	kN	0 to 5
	F _z	kN	0 to 20
	M _z	Nm	0 to 200
			0 to - 200
Calibrated measuring range 10%	F _x , F _y	kN	0 to 0.5
	F _z	kN	0 to 2
	M _z	N-m	0 to 20
			0 to - 20

3.5.4 Measurement of cutting temperature

K-type thermocouple with digital temperature indicator is used for measuring the temperature. Temperatures are measured by placing thermocouple 2 mm below the surface of the workpiece as shown in Fig 3.14. The thermocouple is placed in a slot made for this purpose in the bottom of Inconel plate. After placing the thermocouple in the slot, a bottom plate is glued to the top plate. Fig. 3.15 shows the pictorial view for measurement of grinding temperature and Fig 3.16 shows the digital display of the thermocouple.

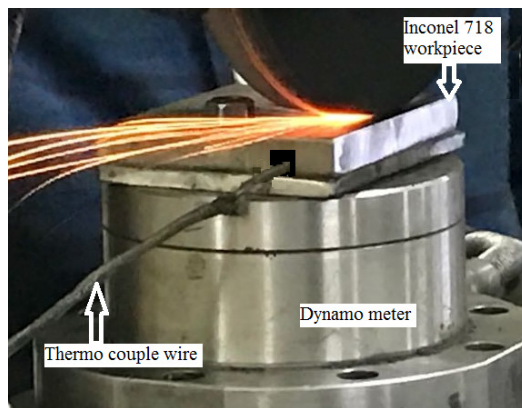


Fig 3.14. Experimental set up for surface grinding

Temperature indicator

Range : 0-1200 $^{\circ}\text{C}$.

Supply Voltage : 230 V, AC 50 Hz.

Input : Cr-Al (K-type)

Specifications:

Designation : K type, Shielded Thermocouple

Element outside diameter: 2 mm

Element Length : 120 mm

Element Type : Duplex

Sheath material : Recrystallised Alumina.

Temperature Range : -250 $^{\circ}\text{C}$ to 1260 $^{\circ}\text{C}$.

Tolerance : ± 2.2 $^{\circ}\text{C}$ or $\pm 0.75\%$ (whichever is greater between 0 $^{\circ}\text{C}$ to 1250 $^{\circ}\text{C}$).

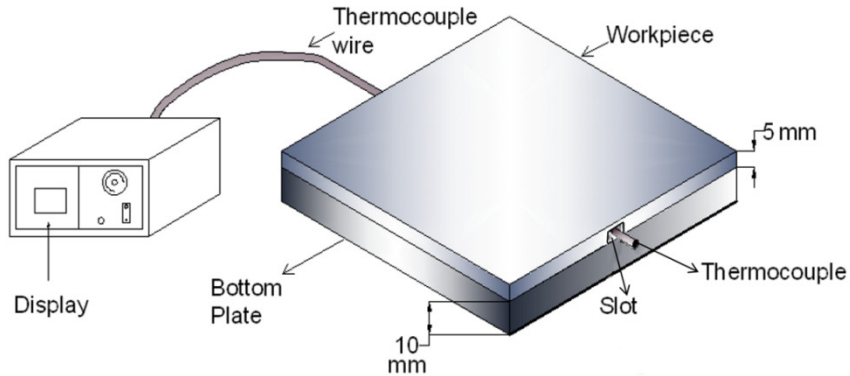


Fig 3.15. Measurement of grinding temperatures



Fig 3.16. Digital display of Thermocouple

3.6 Measurement of surface roughness

Surface finish has a profound influence on the fatigue life, stress corrosion etc. of the component. The life of the machined components and its performance is largely affected by the surface finish. A rougher surface will lead to premature failures of the components. And hence, the surface roughness is to be measured to evaluate the grinding performance. To measure the surface roughness of ground part on Inconel 718 workpiece, Mitutoyo SJ 310 (Fig 3.17) is used. The diamond tip of the stylus is reciprocated on the surface whose surface is to be measured. Irregularities on the surface are sensed by the detector and are converted into microns. The readings are measured through the digital display.

Equipment : Surftest SJ-301

Make : M/s Mitutoyo

Specifications:

Drive speed	Measuring:0.25mm/s Returning: 1mm/s
Detector retraction function	Stylus U P
Measuring force	4mN
Material of stylus	Diamond
Stylus tip radius	5 μ m
Radius of skid curvature	40mm
Measuring Range	Z-axis: 350 μ m (12000 μ in), X-axis: 12.5mm (.5")
Operating temperature	5°C – 40°C
Relative humidity	85% max



Fig 3.17. Mitutoyo SJ 310 surface roughness testing equipment

3.7 Experimentation procedure:

Inconel 718 workpiece of $80 \times 70 \times 5$ mm is directly procured along with two holes meant to mount it on a dynamometer force plate. Three grades of GNP (Table 3.1) are procured from xG sciences, USA. Surface treatment of GNP is done as mentioned in Section 3.2.2 to minimize the phenomena of agglomeration while making self-lubricating grinding wheels and nanofluids. GNP impregnated grinding wheels are made following the procedure mentioned in Section 3.3 with varying weight fractions (0.25, 0.5, 1, 2 and 4wt.%) of surface treated Grade II GNP. GNP based nanofluids are prepared according to Section 3.4 various weight fractions (0.1, 0.2, 0.3, 0.4 and 0.5wt.%) of surface treated Grade II GNP. Thermal conductivity and Viscosity

of prepared nanofluids are measured using KD2 Pro (Section 3.4.1) and Brookfield viscometer (Section 3.4.2) respectively to understand the effect of GNP concentration on grinding performance. The thermocouple is placed in a slot made for this purpose in the bottom of the Inconel plate. After placing the thermocouple in the slot, a bottom plate is glued to the top plate. Thermocouple sandwiched Inconel 718 plate is fastened to Kistler piezoelectric dynamometer (Model: 9272) force plate by means of screws. Inconel 718 plate, thermocouple wire, and dynamometer force plate assembly are set on grinding machine's magnetic table by means of magnetic force.

Table 3.2. Experimental Conditions

Machine:	Horizontal spindle surface grinding machine
Motor capacity:	1.5 HP
Wheel dimensions:	200×25×31.75 (mm)
Workpiece material:	Inconel 718
Wheel speed:	25 m/sec
Feed:	15 m/min
Infeed:	25 μ m
Method of grinding:	Dry grinding and MQL with a flow rate of 2.5 ml/min
Dressing conditions:	Single point diamond dresser; dressing speed: 2400 RPM; dressing depth: 30 μ m.

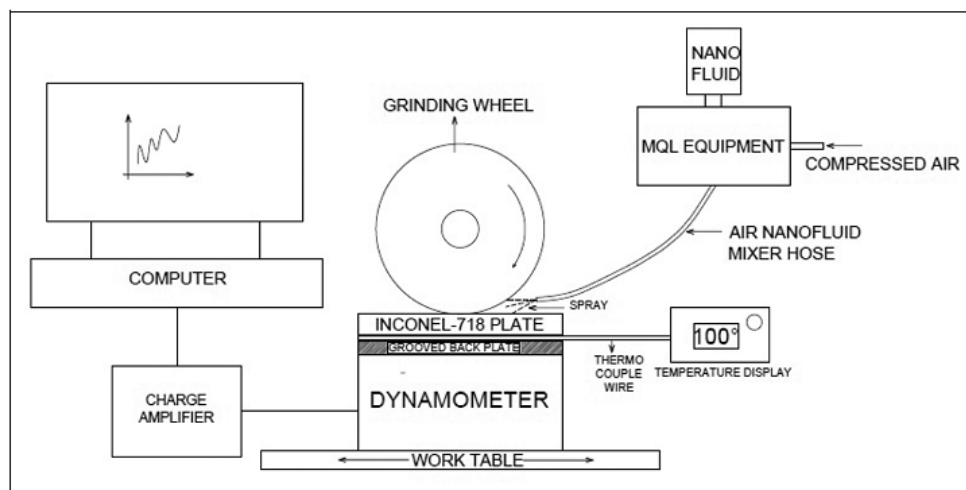


Fig 3.18. Schematic representation of MQL grinding of Inconel 718

Grinding is performed on Inconel 718 plate as per machining conditions listed in Table 3.2. Schematic diagram of the experimental set up is presented in Fig. 3.21. To account for uncertainties, all the experiments are carried out in triplicate, and their mean values are reported along with the standard deviation. The dressing conditions are kept constant while a single-point diamond dresser is being used so that it would not influence the output variables of the processes. Experiments are done in a dry environment using the standard grinding wheel (without GNP) and self-lubricated grinding wheels to evaluate the effect of GNP concentration on grinding performance.

Forces and Temperature are measured online while the grinding is being done. Grinding forces, F_z - Normal Force, F_y - Tangential Force, are recorded and analyzed with the dyno software. Temperature is measured using digital embedded K - type thermocouple at a small distance from the grinding zone. After grinding, the surface roughness is measured for all the ground surfaces using Mitutoyo SJ 310. Stylus diamond tip is reciprocated at three different places on the same ground surface, and the average value is considered as surface roughness.

Grinding coefficient and specific grinding energy are derived by using simple formulae from the measured force values and grinding input parameters. Grinding wheel wear ratio is calculated by calculating the weight of Inconel 718 removed during the cut and knowing the loss of grinding wheel before and after grinding with an electronic balance.

After analyzing the results, self-lubricating wheels with 2% GNP concentration are giving better performance. Next set of experiments are carried to know the influence of the surface area of GNP. In this, grinding wheels are made impregnating all three grades of GNP (Table 3.1) at three different GNP weight fractions, 1%, 2%, and 4%. These wheels are also tested for their performances similar to the procedure discussed above. Self-lubricating grinding wheels with GNP having a surface area $750 \text{ m}^2/\text{g}$ and 2 wt% are observed to be yielding the best performance.

Moving to the next stage of experimentation, grinding is done with a standard grinding wheel in the nanoMQL environment. In this, nano-cutting fluids with (0.1, 0.2, 0.3, 0.4 and 0.5wt.%) are applied using UnistCoolubricator System. Nano-cutting fluids sent at a flow rate of 2.5 mL/min by setting pulse generator to 40, brass adjustment knob to full stroke and air metering

screw to $\frac{3}{4}$ revolutions. Grinding performance in nanoMQL is tested for its performance in terms of grinding forces, grinding temperature, surface roughness, grinding coefficient and specific grinding energy as per the procedures discussed in the previous sections.

NanoMQL with nanofluid having 0.3 wt% GNP is giving better results. Further, experiments are carried to know the influence of the surface area of GNP. In this, nanofluids are prepared to disperse all three grades of GNP (Table 3.1) at three different GNP weight fractions, 0.2%, 0.3%, and 0.4%. These nanofluids are also tested for their performances similar to the procedure discussed above. Nanofluids with GNP having a surface area $750 \text{ m}^2/\text{g}$ and 0.3 wt% are observed to be yielding the best performance.

In the last stage of experiments, the best self-lubricating grinding wheel and the best nanofluid are used in combination to understand the synergetic effect of GNP on grinding and performance is evaluated in terms of grinding forces, grinding temperature, surface roughness, grinding coefficient and specific grinding energy as per the procedures discussed in the previous sections.

After analyzing the results, grinding Inconel 718 components with self-lubricating grinding wheel with GNP having a surface area $750 \text{ m}^2/\text{g}$ and 2 wt% in nanoMQL environment applying nanofluid GNP having a surface area $750 \text{ m}^2/\text{g}$ and 0.3 wt% is giving the best quality of the ground surface.

Chapter IV

Development and performance evaluation of self-lubricating grinding wheels in grinding Inconel 718

4.1 Introduction

It is understood that the efficiency of solid lubricants would be enhanced if those are effectively introduced into the grinding zone, by impregnating solid lubricants in grinding wheels [52]. To take advantage of this in the present work, resin bonded grinding wheels impregnated with varying GNP concentration and surface area are developed in order to evaluate their effect on various grinding performance measures. Performance of these developed grinding wheels is compared with a standard grinding wheel and presented in the following sections.

4.2 Grinding experiments

Table 4.1. Nomenclature of GNP impregnated grinding wheels

Wheel Designation	Weight fraction (wt %)	GNP
Wheel A (A80K6B)	0	Nil
Wheel B	0.25	Grade II
Wheel C	0.5	Grade II
Wheel D	1	Grade II
Wheel E	2	Grade II
Wheel F	4	Grade II

Initially, to evaluate the influence of GNP and its concentration in grinding wheels, GNP of Grade II (surface area $500 \text{ m}^2/\text{g}$) was impregnated in grinding wheels at different weight fractions, as discussed under Section 3.3. The newly developed grinding wheels were designated as given in Table 4.1. In order to compare the performance of GNP impregnated self-lubricating

grinding wheels, a standard wheel (A80K6B), without adding any GNP, has been considered and it is Wheel A in Table 4.1. Experimental setup and conditions are presented in Section 3.5. The grinding forces, grinding temperature, surface roughness, grinding coefficient, specific grinding energy and grinding wheel wear are measured and calculated as discussed in Section 3.7 in order to assess and compare the performance of the developed self-lubricating grinding wheels against the standard wheel. Results are discussed in the following sections.

4.2.1 Grinding forces

Grinding forces are measured online by using Kistler 4 - component piezoelectric dynamometer (Model: 9272) and analyzed with Dynoware software. The experimental set-up is shown in Section 3.5.3.

Grinding forces viz. normal forces and tangential forces are important parameters by which performance of any grinding process can be evaluated. Various components contribute to these grinding forces are primary ploughing, secondary ploughing, micro-fracturing, wheel loading, shearing, friction, bonding material, re-deposited debris, etc. [16]. The relative contributions of these components depend on workpiece material, process parameters, wheel surface contribution, abrasive characteristics and presence of cutting fluids etc. Fig 4.3 shows the variations in normal and tangential forces generated during grinding Inconel 718.

Normal forces press the abrasives into the workpiece and lead to the removal of material. This force component influences wheel wear, surface roughness, geometrical and dimensional accuracy. It is evident from Fig 4.1, substantial reduction in normal force is observed with graphene impregnated grinding wheels as compared to the standard wheel (Wheel A). Among various components that contribute to normal forces, productive components (shearing, secondary ploughing, micro-fracturing, etc.) are non-frictional in nature and non-productive components are frictional in nature. Productive components of grinding forces primarily depend on infeed whereas non-productive components are independent of infeed [91]. As infeed is kept constant at $15\mu\text{m}$, a decrease in normal force with graphene impregnated grinding wheels may be attributed to a reduction in non-productive components which in turn might be due to effective lubrication of GNP that is applied directly at the wheel-workpiece interface. That effective

lubrication is because of the arrangement of platelets. Platelets of graphene are kept close by van der Waals forces [12]. In the presence of shear loads, the platelets will slide over each other and thereby reduces the frictional force between wheel and workpiece interface [92], leading to lowering the coefficient of friction. All the non-productive components which are frictional in nature reduce their magnitude due to the low coefficient of friction, leading to a reduction in normal force.

In addition, direct application of solid lubricant at wheel-workpiece interface might have minimized wheel clogging by swarf, which in turn reduces the normal forces to some extent [16]. As the quantity of GNP inclusions in the wheel increases, reduction in normal force is observed up to 2 wt% content. Further with a higher quantity of GNP (i.e. 4 wt.%), an increase in normal force is observed which may be due to possible saturation of lubricant effectiveness [17].

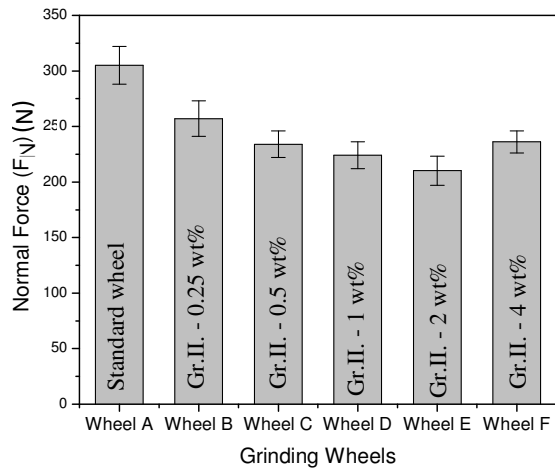


Fig 4.1. Effect of GNP concentration on Normal Force

Tangential grinding force influences the power requirements in the grinding process. The intensity of heat generation, interface temperature and surface integrity depends primarily on this component of the grinding force. It can be observed from Fig 4.2, GNP impregnated grinding wheels exhibited lower tangential forces as compared to the standard wheel. The effectiveness of the GNP in reducing the frictional effect at grinding zone is evident from the reduction of tangential forces. GNP presented in the grinding wheels slides on their own platelets and helps the grinding wheel to move smoothly on the work surface, which causes low tangential force.

Higher is the quantity of GNP in the wheel lower is the tangential force. At a higher quantity of GNP (i.e. for Wheel F), a slight increase in tangential force is observed which might also be attributed to a reduction in bond strength beyond saturation limit. The weakening of bond strength might lead to higher wheel wear and re-deposition of debris on the work surface [52].

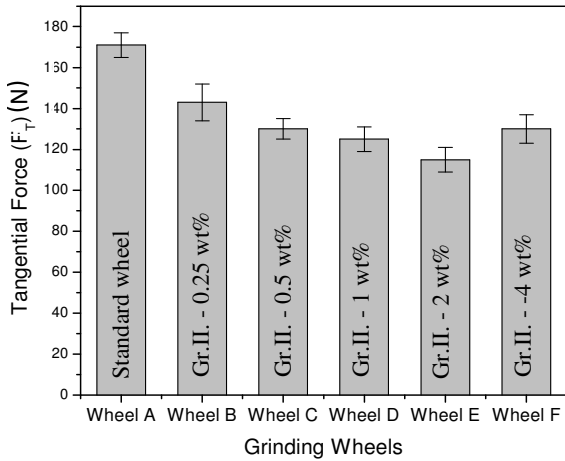


Fig 4.2. Effect of GNP concentration Tangential force

4.2.2 Grinding temperature

Temperature developed due to heat generated in grinding Inconel 718 is measured using K-type thermocouple as discussed under Section 3.5.4. These measurements show insight into thermal performance and lubrication effect of graphene impregnated grinding wheels at grinding zone. Fig 4.3 shows the temperatures of the Inconel 718 workpiece when ground with different grinding wheels. Graphene impregnated grinding wheels exhibited 4-19% reduction in cutting temperature as compared to a standard grinding wheel (Wheel A).

This reduction might be due to the high thermal conductivity characteristic [83] and lubricating property of GNP [69]. Direct availability of GNP at the grinding zone might have conducted the heat that is generated at the wheel-work interface and dissipated to the surroundings. Apart from conducting heat from the grinding zone, GNP present in grinding wheels acts in the chip-bond and bond-workpiece interactions (Fig 1.2) and reduces the friction between grinding wheel and workpiece. Less friction may also be because of the presence of

solid lubricants, as they soften at elevated temperatures [52]. The reduced grinding temperature will lead to less adhesion of work material to grinding wheel and better surface finish [93].

Grinding temperatures decreased with increasing in graphene concentration and 2wt.% graphene was found to be optimum in reducing the temperature. This may be because of the high number of GNP to carry the heat away and to lubricate wheel-work interface. However, an increase in grinding temperature is observed beyond 2 wt.% concentration, which might be due to the saturation of lubricant effectiveness and possible agglomerations at higher weight content of graphene.

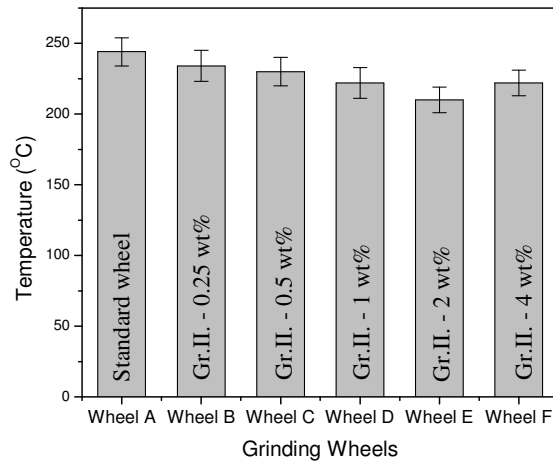


Fig 4.3. Effect of GNP concentration on grinding temperature

4.2.3 Surface roughness

It is a well-established fact that the surface roughness significantly affects the fatigue life, corrosion resistance, stress cracking, etc. of the products/components. Poor surface finish may lead to failure of the product/component well before the estimated life span. To extend the quality and life span of the ground components, surface finish has to be improved by lowering the grinding force and grinding temperatures [26]. The surface roughness of the ground surface is measured using surface roughness tester (Mitutoyo SJ 310) as discussed in Section 3.6. Effect of GNP concentration on mean surface roughness (Ra) of ground Inconel 718 components is depicted in Fig 4.4.

It is observed that the mean surface roughness values for graphene impregnated grinding wheels (Wheel B-F) were markedly lower than that of the standard wheel (Wheel A). It may be attributed to the reduced friction, cutting forces and grinding temperatures. Reduced friction leads to reduced temperatures. Reduced temperature results in less adhesion between wheel and work, which in turn reduces surface roughness [93].

Surface roughness also depends upon the geometry of the cutting tool [4]. GNP present in the grinding wheel leads to less adhesion between the wheel and work which reduces wheel clogging. This reduced wheel clogging keeps abrasive particles clean and sharp, leading better surface finish [52]. The mean surface roughness decreased with an increase in GNP content up to 2wt%. An increase in surface roughness is observed beyond 2wt% of graphene concentration because of the increased cutting forces and grinding temperature with higher graphene concentration.

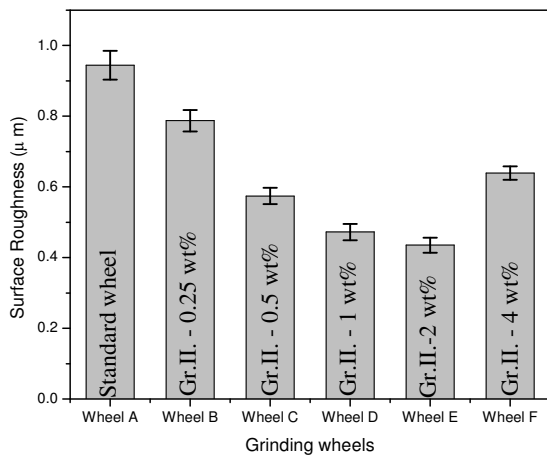


Fig 4.4. Effect of GNP concentration on surface roughness

4.3 Grinding Coefficient

Grinding coefficient is the ratio of tangential force to normal force. Unlike turning and milling processes, tangential forces will be nearly half of the normal forces in the case of grinding forces. This is due to very large negative rake angles of the grit, excessive rubbing action and adverse chip accommodation space which lead to wheel loading. The grinding coefficient also is known as grinding force ratio gives an indication of frictional effects in the grinding zone. Fig 4.5

depicts the variation of grinding coefficient with respect to various grinding wheels. This coefficient is lower for graphene impregnated grinding wheels when compared to the standard wheel. This indicates low friction at wheel workpiece interface due to the effective application of solid lubricants in the grinding zone.

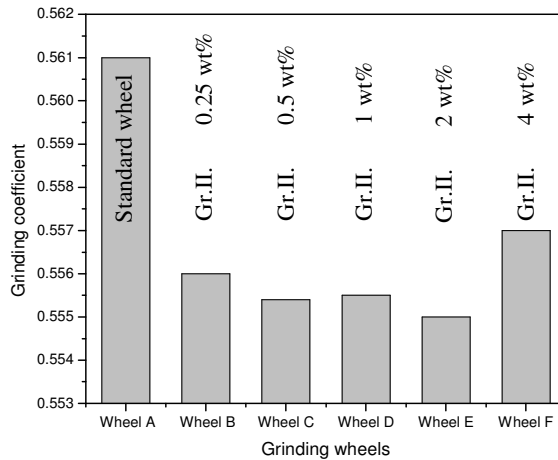


Fig 4.5. Effect of GNP concentration on grinding coefficient

4.4 Specific Grinding Energy

It is the energy required for removal of a unit volume of material, which can be evaluated by using equation 4.1.

$$u = \frac{F_t \times V}{v \times b \times d} \dots \dots \dots (4.1)$$

u: Specific grinding energy

F_t: Tangential grinding force (from Dynamometer)

V: Grinding wheel peripheral velocity

v: Work velocity

b: Width of cut

d: Depth of cut

Fig 4.6 shows the specific grinding energy for different grinding wheels. GNP impregnated grinding wheels exhibited lower specific energy as compared to the standard wheel (Wheel A). Significant reduction in energy requirements, nearly about 32% is observed for Wheel E as compared to the standard wheel. Primary components that contribute to the total

specific energy required for grinding process are sliding and ploughing. Sliding between abrasive grit, grain flat, bonding material and debris with workpiece contributes to the energy required for sliding. Displacement of metal around the grain to sideways contribute to the energy required for ploughing. These two non-productive energy components depend on friction at the wheel-workpiece interface. The decrease in energy requirements with graphene impregnated wheels may be due to effective lubrication provided by graphene at the grinding zone, which in turn reduces the energy required for ploughing and sliding.

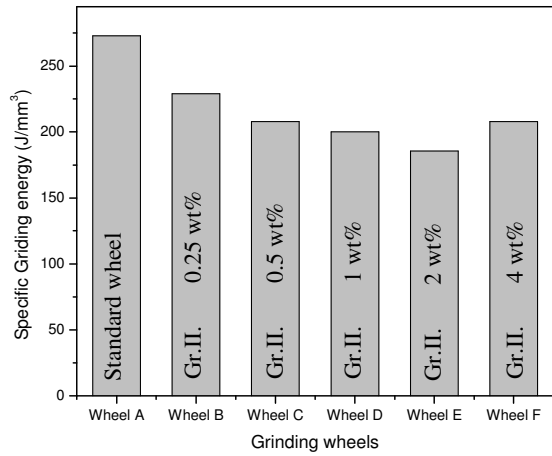


Fig 4.6. Effect of GNP concentration on specific grinding energy

4.5 Grinding wheel wear ratio

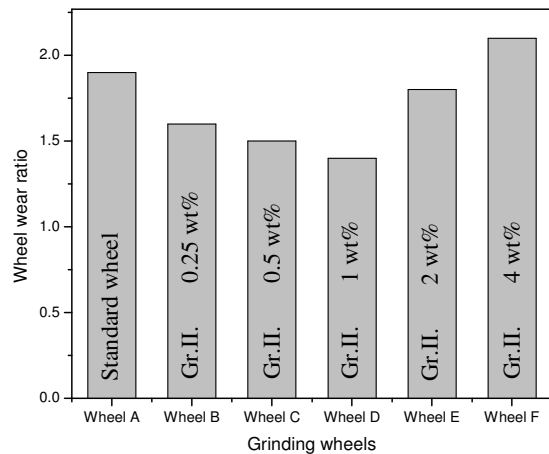


Fig 4.7. Effect of GNP concentration on wheel wear

Grinding wheel wear ratio is an important performance measure which gives an estimate on the life of the grinding wheel. Wheel wear ratio is defined as the ratio between the mass of the wheel wear to the mass of the material removed. Variations of the grinding wheel wear ratio with various GNP impregnated grinding wheels are shown in Fig 4.7. Incorporation of GNP has profoundly influenced the wear ratio. When compared to the standard wheel, grinding wheel wear ratio is lower when graphene concentration is 1 wt.%. Beyond 1wt.% graphene content, wear rate increased with an increase in GNP content. This might be due to the saturation of bond strength at 1wt.% graphene content and a further increase in graphene content might weaken the bond strength. One interesting observation was that the lubricant effectiveness saturated at 2 wt.% graphene content, whereas bond strength saturated at 1 wt.% GNP content.

From figures 4.1 to 4.7, it is clear that Wheel E i.e. GNP with surface area $500 \text{ m}^2/\text{g}$ with 2 wt% concentration is yielding better results in terms of reduced grinding forces and temperature, increased surface finish.

4.6 Influence of GNP surface area on grinding

Table 4.2. Nomenclature of GNP impregnated grinding wheels with a varying surface area

Wheel Designation	Weight fraction (wt %)	Graphene
Wheel G	1	Grade I
Wheel H	2	Grade I
Wheel I	4	Grade I
Wheel D	1	Grade II
Wheel E	2	Grade II
Wheel F	4	Grade II
Wheel J	1	Grade III
Wheel K	2	Grade III
Wheel L	4	Grade III

From Sections 4.1, 4.2 and 4.3, it is clear that GNP concentration in the grinding wheel is influencing grinding forces, grinding temperature and surface roughness. In this section, to observe the influence of GNP surface area on grinding Inconel 718 components, the other two

grades of GNP procured from xG sciences, USA, Grade I (surface area $300\text{ m}^2/\text{g}$) and Grade III (surface area $750\text{ m}^2/\text{g}$) are also used to develop self-lubricating grinding wheels. In order to investigate the effect of GNP surface area, the wheels with 1 wt% and 4 wt% of GNP, one level on each side of the 2 wt% which was proved to be yielding better results with a surface area of $500\text{ m}^2/\text{g}$, are developed. The nomenclature of these grinding wheels is presented in Table 4.2.

From the figures 4.8 to 4.13 for Grade I GNP (surface area $300\text{ m}^2/\text{g}$), among the Wheels G, H and I, Wheel H giving minimum surface roughness, grinding temperature, grinding forces, specific grinding energy and grinding coefficient i.e. grinding wheel with GNP 2 wt% was giving better performance. For Grade III GNP (surface area $750\text{ m}^2/\text{g}$), among the Wheels J, K and L, Wheel K giving minimum surface roughness, grinding temperature, grinding forces, specific grinding energy and grinding coefficient i.e. grinding wheel with GNP 2 wt% was giving better performance.

Fig 4.8 and 4.9 shows the effect of GNP surface area on normal and tangential grinding forces respectively. Both normal and tangential forces decreased with an increase in surface area. Platelets with a surface area of $750\text{ m}^2/\text{g}$ resulted in a reduction of normal and tangential forces by approximately 35% when compared to the standard wheel.

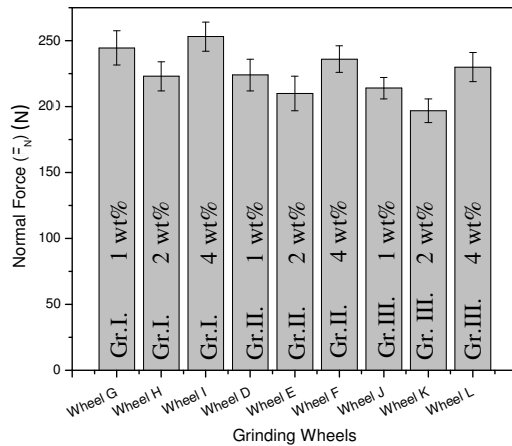


Fig 4.8. Effect of GNP surface area on the normal force

Fig 4.10 shows the effect of the GNP surface area on grinding temperature. In addition to graphene concentration, the surface area is found to be influential in reducing the grinding temperature. Temperature found to be decreased with an increase in surface area. Graphene

platelets with surface area $750 \text{ m}^2/\text{g}$ resulted in a decrease of temperature by 19% when compared to the standard grinding wheel.

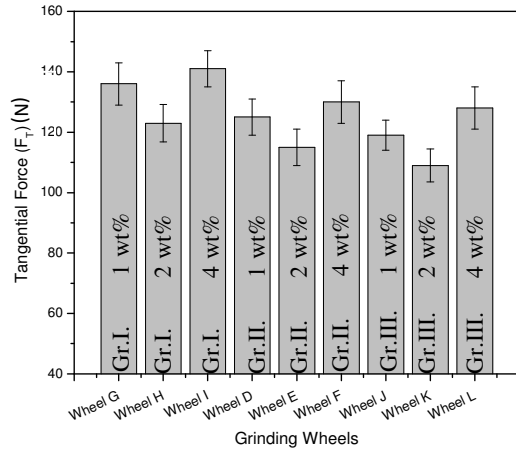


Fig 4.9. Effect of GNP surface area on the tangential force

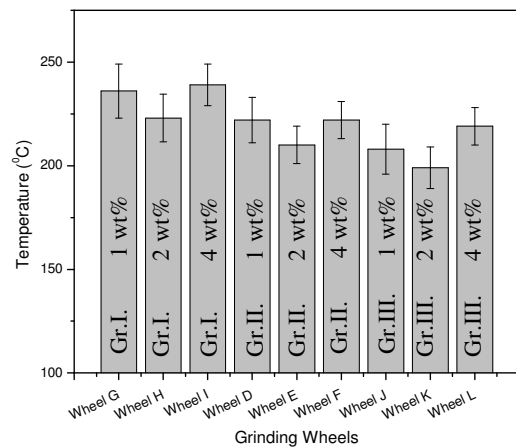


Fig 4.10. Effect of GNP surface area on grinding temperature

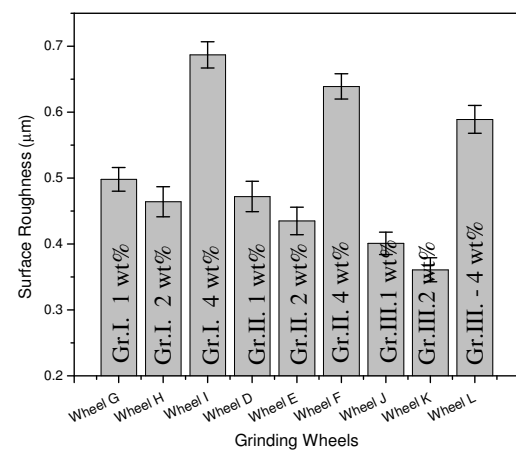


Fig 4.11. Effect of GNP surface area on surface roughness

It is apparent from Fig 4.11, GNP surface area has a noticeable influence on the surface roughness of the Inconel 718 component. Overall, surface roughness for the wheels H, E and K reduced by approximately 51%, 53%, and 61% respectively.

Figures 4.12 and 4.13 show the effect of the GNP surface area on grinding coefficient and specific grinding energy. As GNP surface area increases specific grinding energy and grinding coefficient decrease which indicates that surface area of GNP has a great influence.

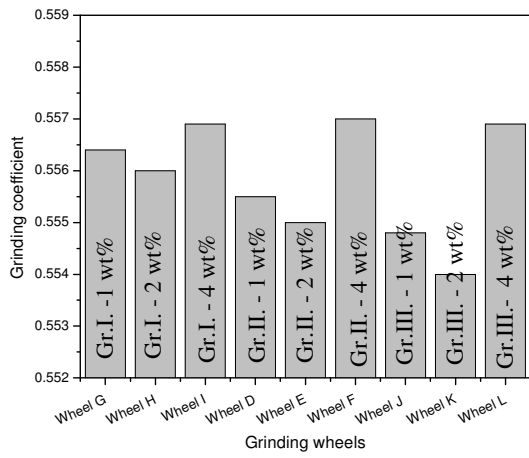


Fig 4.12. Effect of GNP surface area on grinding coefficient

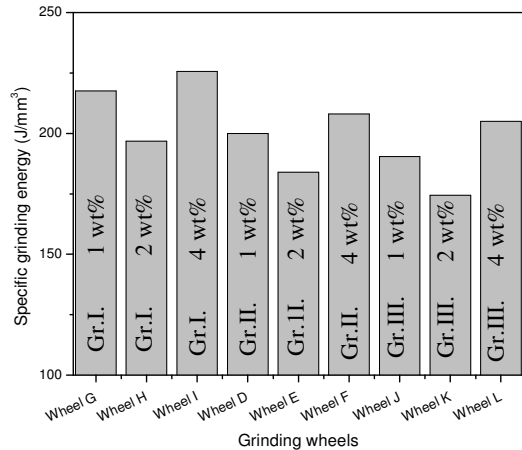


Fig 4.13. Effect of GNP surface area on specific grinding energy

From figures 4.7 and 4.14, an interesting observation is that the lubricant effectiveness saturated at 2 wt.% graphene content, whereas bond strength saturated at 1 wt.% GNP content. More amount of the GNP presented in the resin may be weakening its capacity in holding the abrasive particles. A similar trend was observed in another study [16] in developing graphite

moulded grinding wheels. Thus, if wheel life is of prime concern along with the surface quality then wheels with 1 wt.% graphene content are recommended. Another interesting observation is that wheel wear remains almost unaffected with an increase in platelet surface area; this implies that the influence of surface area on bond strength is almost negligible.

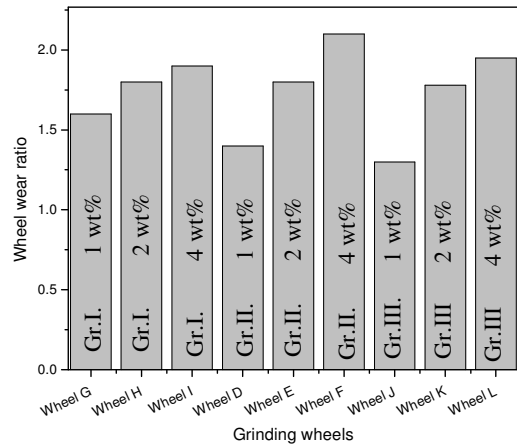


Fig 4.14. Grinding wheel wear rate for different grinding wheels

4.7 Summary

In this work, novel self-lubricating grinding wheels are developed by impregnating GNP into resin bonded grinding wheels for effective application of solid lubricant in the grinding zone. Grinding wheels with varying weight fractions and surface areas of GNP are developed. Investigations on grinding of Inconel 718 using self-lubricating grinding wheels are presented. Grinding responses such as grinding forces, grinding temperatures, surface roughness, grinding coefficient, specific grinding energy and grinding wheel wear are selected for performance evaluation of newly developed wheels and compared with the performance of standard grinding wheel (Wheel A)

GNP present in the self-lubricating grinding wheels acted as effective lubricant leading to the low coefficient of friction between wheel and work. This, in turn, led to reduced cutting forces, specific grinding energy and grinding. Lower grinding temperatures are reported because of GNP's high thermal conductivity characteristic in carrying heat away from the grinding zone and lubricating nature in generating less heat at the grinding zone. Low grinding forces and

temperatures resulted in low surface roughness. Grinding wheels having 2 wt% GNP concentration are recommended because this produces better surface finish and lower grinding forces and grinding temperatures. When wheel life is of concern, wheels with 1wt% GNP can be considered. Addition of GNP is weakening the bond strength. GNP with surface area ($750\text{ m}^2/\text{g}$) are more effective in improving the quality of the ground surface as it covers a larger area in the grinding zone.

Impregnating GNP in the grinding wheels, being an internal lubricating agent, played a vital role in reducing friction, and thereby reducing the heat generated in grinding Inconel 718. But, it could not play the role of external coolant in minimizing the heat produced. In order to investigate GNP's cooling behaviour, GNP based nano-cutting fluids are developed and its performance in grinding Inconel 718 in the next chapter.

Chapter V

Development and performance evaluation of GNP based nanoMQL in grinding Inconel 718

5.1 Introduction

Improving the surface quality of Inconel 718 components during grinding is one of the objectives of current research. It can be attained by reducing the heat generated and cooling work during the grinding. Using self-lubricated grinding wheels, the heat generated at the grinding zone is reduced significantly. However, a better cooling method is to be chosen in order to further enhance the grinding performance. Usage of cutting fluids is a better solution, but keeping health and environmental concerns into considerations, the next better alternative MQL is chosen [18]. Further, MQL becomes more efficient with the addition of nanoparticles to cutting fluids [19], GNP is used in making nano-cutting fluids in the present study.

Grinding of Inconel 718 with the prepared GNP based nano-cutting fluids in MQL is explored in this chapter. Nano-cutting fluids with different weight fractions and specific surface areas of GNP are developed. Since the effectiveness of the cutting fluid in providing effective cooling and proper lubrication at cutting tool-workpiece interface depends on the thermal conductivity and viscosity, these properties are evaluated. Further, the performance of GNP based cutting fluid in MQL grinding of Inconel 718 is investigated in terms of the surface roughness, grinding temperature, components of the grinding force (normal and tangential), specific grinding energy and grinding coefficient.

5.2 Preparation of GNP based nano-cutting fluids

GNP based nano-cutting fluids are prepared as discussed in Section 3.4. Initially, Grade II (surface area $500 \text{ m}^2/\text{g}$) GNP is taken to prepare the nano-cutting fluids to

understand how GNP concentration affects the thermal conductivity and viscosity. The fluids prepared are designated in Table 5.1.

Table 5.1 Nomenclature of nano-cutting fluids with varying weight fractions of GNP

Cutting fluid designation	Graphene nanoplatelets	
	Weight fraction (wt.%)	Surface Area m^2/g
CF1	0	--
CF2	0.1	500
CF3	0.2	500
CF4	0.3	500
CF5	0.4	500
CF6	0.5	500

5.2.1 Thermal conductivity

Thermal conductivity is an important property that should be possessed by a cutting fluid for providing effective cooling at the grinding zone. Enhanced thermal conductivity with the dispersion of nano-sized particles into the conventional cutting fluids results in an increase of the heat extraction capability which in turn decreases the temperature at the grinding zone. The thermal conductivity of nano-cutting fluids with varied weight fractions and specific surface areas of GNP are measured within the temperature range of 30°C to 70°C in the intervals of 10°C and results are presented in Fig 5.1. It is observed from these results that, the thermal conductivity depends on weight fractions of GNP in the cutting fluid and as well as on the temperatures. For all the weight fractions considered in this work, thermal conductivity increased linearly with increase in temperature. Increase in random motion of molecules and the rate of collisions with a rise in temperature might be responsible for the variation of the thermal conductivity with respect to temperature. Further, thermal conductivity also enhanced with an increase in the concentration of GNP in the base fluid. Nano-cutting fluids with 0.5 wt.% GNP exhibited the highest improvement of thermal conductivity. Enhancement

of thermal conductivity with the addition of GNP may be ascribed to the Brownian motion of the GNP in the fluid which in turn results in better heat transfer [59]. Besides this, the observed enhancement of thermal conductivity may also be ascribed to the formation of nano-layer at solid-liquid interface and nano-clustering.

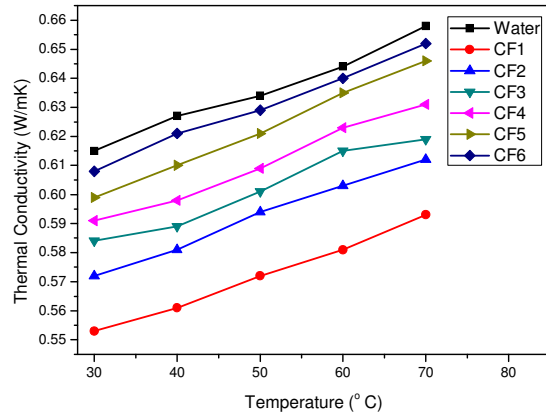


Fig 5.1. The thermal conductivity of cutting fluids with varying weight fractions of GNP

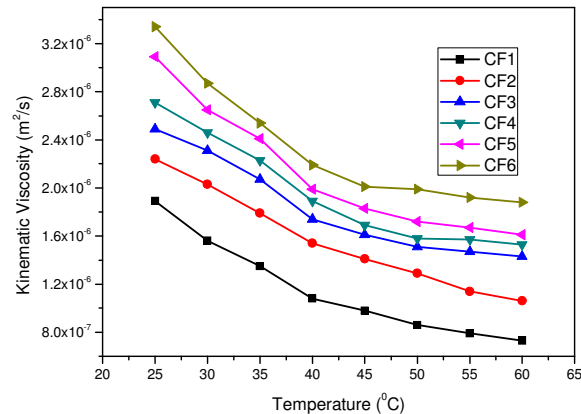


Fig 5.2. Effect of weight fractions of GNP on the viscosity of nano-cutting fluids

5.2.2 Viscosity

The effectiveness of the cutting fluid in providing proper lubrication at the machining zone largely depends on the viscosity of the cutting fluid. Variation of viscosities of the base fluid and nano-cutting fluids with respect to temperature is presented in Fig 5.2. The viscosity is observed to decrease with an increase in the temperature. With the increase in temperature of the fluid, intermolecular attractions

between the molecules of the base fluid and nanoparticles become weak, in turn, this increases the molecular mobility and result in a decrease of viscosity. Further, at all the temperatures considered, the viscosity is found to be increased with the increase in GNP concentration. A similar trend is reported by many studies [94-96]. Enhanced viscosity may be attributed to an increased hindrance to the flow of the fluid with the increase in concentrations of GNP. Moreover, as the concentration increases, nanoparticles agglomerate within the suspension. This, in turn, might lead to the enhancement of internal shear stress of the nanofluid because of the higher shear resistance offered by solid particles. In the study reported by Hussien et al. [97], the friction factor is found to be increased with the increase in nanoparticles concentration. This observation is attributed to the reduced mobility of the fluid due to the enhanced viscosity at higher concentrations of nanoparticles.

5.3 Grinding Experiments

Effect of MQL application of the developed nano-cutting fluids at the grinding zone on surface roughness, grinding temperature, grinding forces, grinding coefficient, and specific grinding energy are evaluated for the nanofluids mentioned in Table 5.1 and presented in the following sections. All the nano-cutting fluids prepared are presented in the grinding zone as mentioned in Section 3.5.2 as per grinding conditions mentioned in Section 3.7

5.3.1 Grinding force

Grinding forces are measured online by using Kistler 4 - component piezoelectric dynamometer (Model: 9272) and analyzed with Dynoware software. The experimental set-up is shown in Section 3.5.3.

Performance of any cutting fluid can be evaluated by measuring the normal and tangential components of grinding force. However, the relative contributions of these components on the final grinding force depends on a variety of factors like workpiece

material, process parameters, the efficiency of the cutting fluid, application of the cutting fluid at the grinding zone, etc. Components of the grinding force generated (normal and tangential) during the MQL grinding of Inconel 718 using GNP based nano-cutting fluids with varying weight fractions are presented in Figs 5.3 and 5.4 respectively.

The wheel wear, surface roughness, geometrical and dimensional accuracy of the workpiece are largely influenced by the normal force generated during the grinding process. As seen in Fig 5.3, MQL with soluble oil shows a significant reduction of normal force as compared to dry grinding. This reduction can be attributed to effective delivery of the cutting fluid by the pressurized air at the grinding zone, which in turn might have led to better cooling and lubrication of the grinding zone [18]. Addition of GNP to soluble oil results in a further decrease of surface roughness, which might be ascribed to extraordinary wetting ability of GNP when suspended in fluids [92]. GNP having layered structure is unstable and fold themselves into a fullerene-like structure when dispersed in fluids [98]. The suspended GNP spreads on the surface on which it is sprayed and forms a thick film adhering to surface. When GNP based nano-cutting fluids are sprayed along with compressed air, GNP forms a thick film on the workpiece. This thick film reduces the coefficient of friction between the grinding wheel and workpiece, resulting in lowered cutting forces. Further, the application of the pressurized fluid at the grinding zone might have reduced the wheel clogging [99], which in turn might have led to the reduction of normal force [16].

As the weight fraction of GNP in the cutting fluid increases, the normal force is found to be decreased up to 0.3wt.% GNP content. The normal force is found to be increased beyond this weight fraction, which may be due to the formation of aggregation of GNP nanoparticles at higher concentrations [84].

Variation of tangential force with GNP concentration is shown in Fig 5.4. Better penetration of cutting fluid into the grinding zone with the MQL technique has resulted in a decrease of tangential force as compared to dry grinding [18]. The film formed by GNP on the surface of Inconel 718 provides a good amount of lubrication [92] and helps the

grinding wheel to slide easily on the work. Tangential force reduces with increase in the concentration of GNP. In comparison with dry grinding, the maximum reduction of tangential force (from 171 N to 129 N) is achieved at 0.3wt.% GNP concentration.

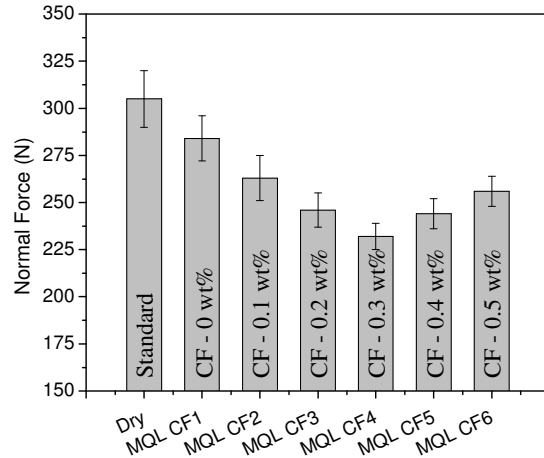


Fig 5.3. Effect of GNP concentration on the normal force

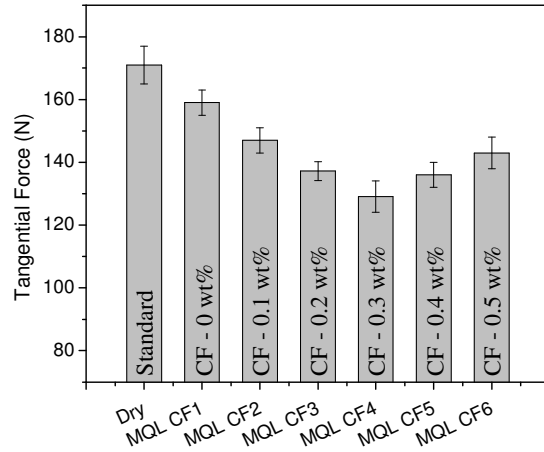


Fig 5.4. Effect of GNP concentration on the tangential force

5.3.2 Grinding temperature

In order to have an insight on the role of GNP inclusions in the cutting fluids, in providing cooling and lubrication of the grinding zone, temperatures are measured as per the section 3.5.4 and presented in Fig 5.5. MQL grinding has resulted in the reduction of the temperature generated at the grinding zone as compared with dry grinding. This decline in grinding temperature may be attributed to better cooling and lubrication

offered at the grinding zone by pressurized air and soluble oil respectively [18]. Further reduction in grinding temperature can be attributed to the high thermal conductivity of suspended GNP. GNP act as heat sinks when suspended in fluids and also shunt the heat away from the grinding zone [92], when supplied. This is also evident from the increased thermal conductivity of cutting fluids with the addition of GNP, as shown in Fig 5.1.

Grinding temperatures are found to be decreased with increase in GNP concentration. However, beyond 0.3wt.% GNP concentration, only a marginal decrease in temperature is observed. Unlike the grinding force, the grinding temperature is found to be decreased for cutting fluids with higher concentrations of GNP i.e. 0.4wt.% and 0.5wt.%. Marginal reduction in grinding temperature may be attributed to enhanced thermal conductivity at these higher concentrations.

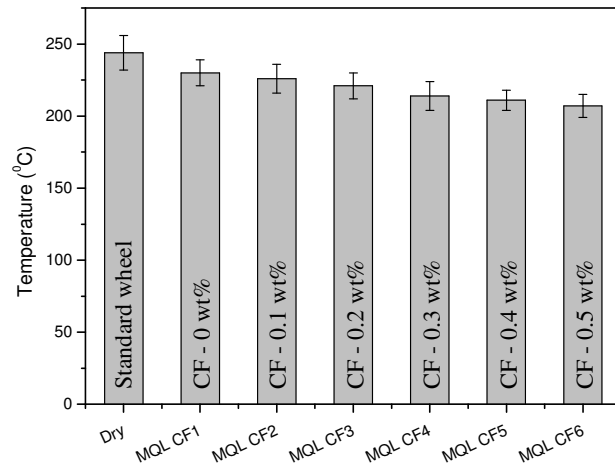


Fig 5.5 Effect of GNP based nano-cutting fluid on grinding temperature

5.3.3 Surface roughness

The surface roughness of all Inconel 718 components which are ground applying the nanofluids prepared is measured as mentioned in Section 3.6. Effect of minimum quantity lubrication in grinding Inconel 718 with nano-cutting fluids with varying concentrations of GNP on the surface roughness is presented in Fig 5.6. Dry grinding resulted in maximum surface roughness, which might be due to the absence of cutting

fluid to lubricate and cool the grinding zone. As compared to dry grinding, nanoMQL led to a significant reduction of surface roughness.

GNP supplied at the grinding zone in the form of aerosols reduced cutting forces and decreased rubbing, leading to a lowered surface roughness. Further, the improved thermal conductivity of the developed nano-cutting fluids with respect to the base fluid might also result in the decrease of surface roughness in pursuant to the better heat extraction from the grinding zone.

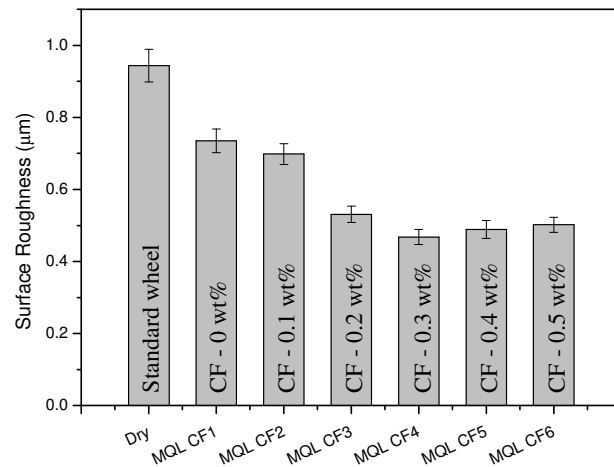


Fig 5.6. Effect of GNP based nano-cutting fluid on surface roughness

As seen in Fig 5.6, up to 0.3wt.% of GNP, surface roughness decreased with increase in concentration. Jia et al. [100] also reported a similar trend with nano MoS_2 based cutting fluid. At further higher concentrations of GNP, the surface roughness is found to be increased, which might be attributed to the aggregation of GNP at higher concentrations. Because of these aggregates, the effective number of platelets that contribute to the reduction of friction at the grinding zone gets reduced, which in turn might result in the enhancement of surface roughness.

5.4 Grinding coefficient

Fig 5.7 depicts the effect of the surface area of the GNP on the grinding coefficient. When compared to dry grinding, MQL grinding has exhibited lower grinding coefficient. Initially, up to certain GNP concentration, grinding coefficient decreased

with an increase in GNP weight fraction, and thereafter an increasing trend is observed. A similar trend was also reported by Zhang et al. [101]. Among the different GNP concentrations considered in this section, nano-cutting fluids consisting of GNP with 0.3 wt.% and specific surface area $500\text{m}^2/\text{g}$ exhibited the lowest grinding coefficient. In comparison with dry grinding, nano-cutting fluid (CF4) has resulted in a reduction of grinding coefficient from 0.561 to 0.557. This indicates the lower friction at the grinding zone due to the efficient lubrication provided by the nano-cutting fluid.

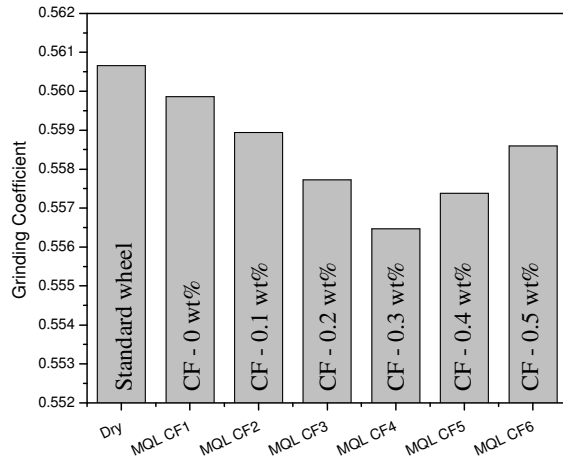


Fig 5.7. Effect of GNP based nano-cutting fluid on grinding coefficient

5.5 Specific grinding energy

Fig 5.8. shows the variation of the specific grinding energy with GNP concentration and specific surface area. MQL grinding resulted in lower specific grinding energy as compared to dry grinding. As the specific grinding energy majorly depends on the interface friction, lower energy requirement in MQL grinding may be attributed to lower friction at the interface, which is also apparent from the results of surface roughness and grinding coefficient. Incorporation of GNP in a soluble-oil has resulted in a reduction in energy requirements. Nano-cutting fluids have resulted in further reduction of energy requirements in the grinding process. This reduction might be because of the efficient lubrication provided by the GNP at the grinding zone. This, in turn, might have reduced the energy required for ploughing and sliding (non-productive energy

components). Nano-cutting fluid with 0.3wt.% GNP concentration with $500 \text{ m}^2/\text{g}$ has exhibited a considerable reduction in specific grinding energy by about 18% (from 273.6 J/mm^3 to 218.4 J/mm^3) as compared to dry grinding. A similar trend was observed in the work reported by Kalita et al. [68], where nano-lubricant has resulted in 43% decrement in specific grinding energy.

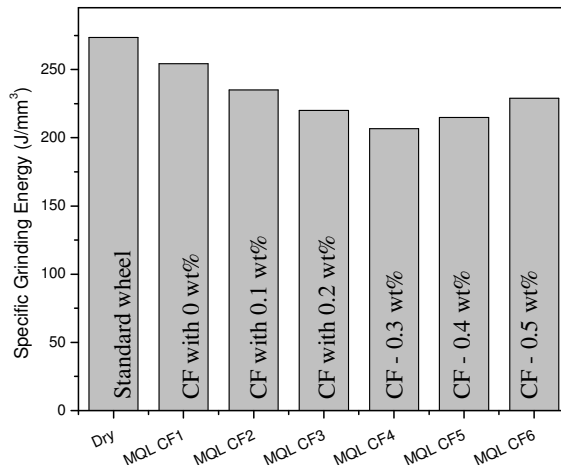


Fig 5.8. Variation of specific grinding energy with variation in GNP concentration and specific surface area

5.6 Effect of GNP surface area

GNP concentration in the cutting fluids shows positive results on grinding Inconel 718 components up to 0.3 wt%. Further, aggregation of GNP occurs with the increase in the quantity of the GNP [102]. To investigate this phenomenon, nanofluids are prepared at higher concentrations with other two grades, Grade I and Grade III GNP. In order to investigate the effect of GNP surface area, nano-cutting fluids are prepared with 0.2 and 0.4 wt%, one level on each side of 0.3 wt%, which proved to be yielding better results. The fluids prepared are designated in Table 5.2 and used in the grinding experiments.

It is observed that both thermal conductivity and viscosity continued to increase with an increase in concentration, even at the highest concentration, i.e. 0.5 wt%. Therefore, in order to evaluate the effect of the GNP surface area on thermal conductivity

and viscosity, only one concentration of GNP is taken and tested for three grades of GNP. The fluids prepared are designated as shown in Table 5.3.

Table 5.2. Nomenclature of nano-cutting fluids with 3 grades of GNP with 3 weight fractions

Cutting fluid designation	Graphene nanoplatelets	
	Weight fraction (wt.%)	Surface are (m ² /g)
CF 7	0.2	300
CF 8	0.3	300
CF 9	0.4	300
CF 3	0.2	500
CF 4	0.3	500
CF 5	0.4	500
CF 10	0.2	750
CF 11	0.3	750
CF 12	0.4	750

Table 5.3. Nomenclature of nano-cutting fluids with a varying surface area of GNP

Cutting fluid designation	Graphene nanoplatelets	
	Weight fraction (wt.%)	Surface are (m ² /g)
CF4	0.3	500
CF 8	0.3	300
CF 11	0.3	750

Apart from the temperature and the concentration of GNP, the surface area of GNP also profoundly influenced the thermal conductivity of the nano-cutting fluid. The effect of the GNP surface area on thermal conductivity is shown in Fig 5.9. Thermal conductivity is observed to be increased with an increase in the specific surface area of GNP. Cutting fluids with GNP having a specific surface area 750 m²/g exhibited the

highest improvement at all the temperatures considered as compared to GNP having specific surface areas 300 and 500 m^2/g .

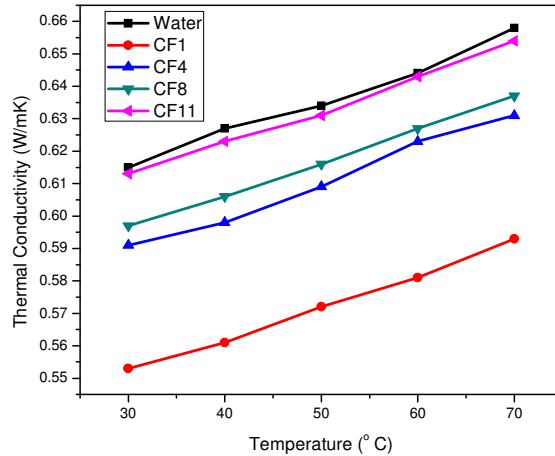


Fig 5.9. The thermal conductivity of cutting fluids with a varying surface area of GNP

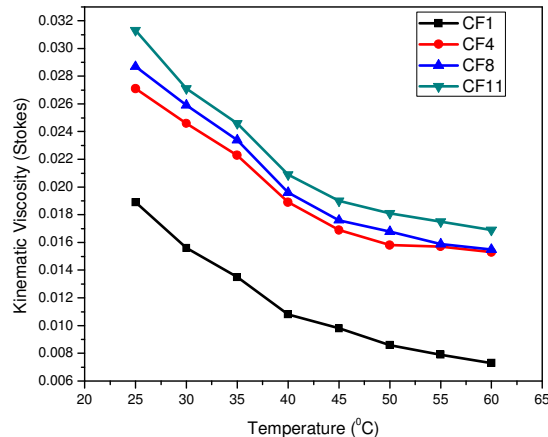


Fig 5.10. The viscosity of cutting fluids with a varying surface area of GNP

The surface area of the GNP also influenced the viscous behavior of the nano-cutting fluids. The effect of the GNP surface area on viscosity is depicted in Fig 5.10. As seen from this figure, an increase in viscosity is observed with an increase in the surface area of the GNP. Nano-cutting fluid with GNP surface area 750 m^2/g exhibited the highest viscosity at all the temperatures considered. Mehrali et al. [103] also observed a similar trend, wherein, the viscosity of the GNP based nanofluid increased with an increase in the specific surface area of nanoplatelets.

From the Figs 5.11 and 5.12., Grinding force (both Normal and Tangential forces) is minimum for MQL CF 8 among MQL CF 7, 8 and 9 which are prepared out of Grade I ($300 \text{ m}^2/\text{g}$) GNP with concentrations of 0.2, 0.3 and 0.4% respectively. Grinding force is minimum for MQL CF 11 among MQL CF 10, 11 and 12 which are prepared out of Grade III ($750 \text{ m}^2/\text{g}$) GNP with concentrations of 0.2, 0.3 and 0.4% respectively. And among MQL CF 4, 8 and 11, which gave minimum values of grinding force for Grade I, Grade II and Grade III GNP at 0.3 wt%, MQL CF 11 gave minimum value.

From the Fig 5.13, the temperature is minimum for MQL CF 8 among MQL CF 7, 8 and 9 which are prepared out of Grade I ($300 \text{ m}^2/\text{g}$) GNP with concentrations of 0.2, 0.3 and 0.4% respectively. Temperature is minimum for MQL CF 11 among MQL CF 10, 11 and 12 which are prepared out of Grade III ($750 \text{ m}^2/\text{g}$) GNP with concentrations of 0.2, 0.3 and 0.4% respectively. And among MQL CF 4, 8 and 11, which gave minimum values of temperature for Grade I, Grade II and Grade III GNP at 0.3 wt%, MQL CF 11 gave minimum value. From this, nano-cutting fluid with $750 \text{ m}^2/\text{g}$ at 0.3 wt% is giving the least temperature of all cutting fluids prepared.

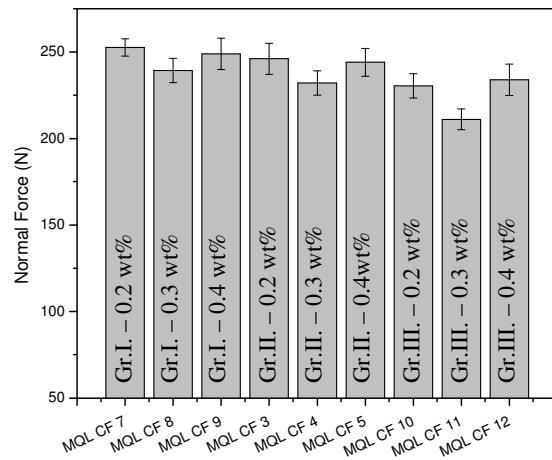


Fig 5.11. Effect of GNP surface area on the normal force

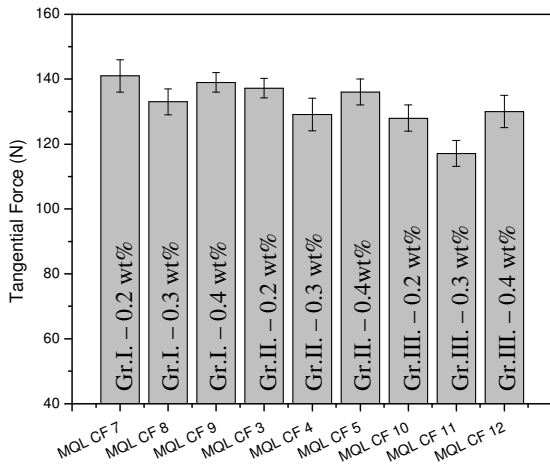


Fig 5.12. Effect of GNP surface area on the tangential force

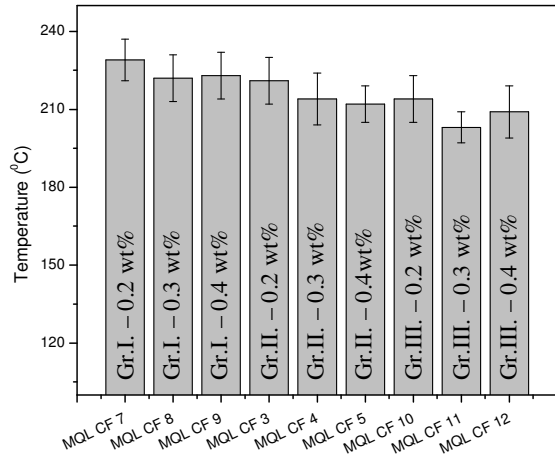


Fig 5.13. Effect of GNP surface area on temperature

From the Fig 5.14, Surface roughness is minimum for MQL CF 8 among MQL CF 7, 8 and 9 which are prepared out of Grade I ($300 \text{ m}^2/\text{g}$) GNP with concentrations of 0.2, 0.3 and 0.4% respectively. Surface roughness is minimum for MQL CF 11 among MQL CF 10, 11 and 12 which are prepared out of Grade III ($750 \text{ m}^2/\text{g}$) GNP with concentrations of 0.2, 0.3 and 0.4% respectively. And among MQL CF 4, 8 and 11, which gave minimum values of surface roughness for Grade I, Grade II and Grade III respectively, GNP at 0.3 wt%, MQL CF 11 resulted in minimum value. From this, nano-cutting fluid with $750 \text{ m}^2/\text{g}$ at 0.3 wt% is resulting in the least surface roughness of all cutting fluids prepared.

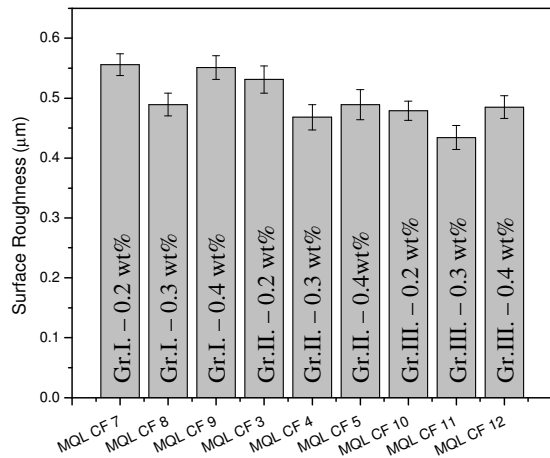


Fig 5.14 Effect of GNP surface area on surface roughness

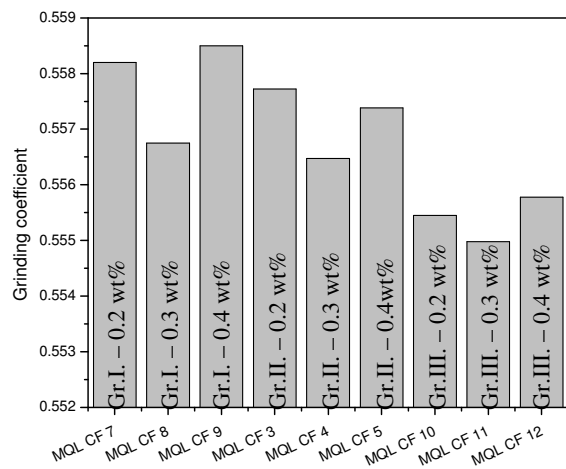


Fig 5.15. Effect of GNP surface area on grinding coefficient

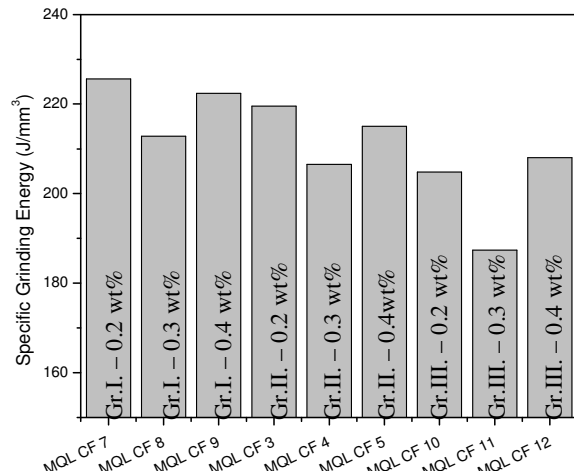


Fig 5.16. Effect of GNP surface area on specific grinding energy

From Figs. 5.15 and 5.16, it is observed that grinding coefficient and specific grinding energy are minimum for MQL CF 11. From this, nano-cutting fluid with 750 m²/g at 0.3 wt% is giving the least grinding force, grinding coefficient and specific grinding energy of all cutting fluids prepared.

From the above discussions, it is understood that the GNP surface area is influential when used in nanoMQL in reducing forces, temperature and surface roughness, and thereby grinding coefficient and specific grinding energy. When GNP surface area increases, the effective platelet surface area available per unit wt% of GNP increases. Thereby, the lubricity at the grinding zone increases and heat transfer ability of nano-cutting fluids also increases. All these lead to better performance and increases the surface quality of Inconel 718.

5.7 Summary

Nano-cutting fluids with varying concentrations and specific surface areas of GNP are developed and their performance in MQL grinding of Inconel 718 is investigated. Viscosity and thermal conductivity are found to be varied with varying concentrations and specific surface areas of GNP. Viscosity increased with increase in GNP concentration and specific surface area but decreased with increase in temperature. Thermal conductivity enhanced significantly with increase in GNP weight fractions, specific surface area, and temperature. As compared to dry and MQL grinding with soluble oil, MQL grinding with nano-cutting fluids has exhibited improved grinding performance due to the diminution of frictional effects at the grinding zone in pursuant to better lubrication and cooling provided by the GNP, which in turn attributed to the enhanced viscosity and thermal conductivity with addition of GNP to soluble oil apart from inherent ability of GNP to provide lubrication and effective penetration of GNP into grinding zone with MQL technique. Among various concentrations considered, nano-cutting fluid with 0.3wt.% GNP has resulted in a significant decline in grinding force, grinding coefficient, roughness, specific grinding energy, and temperature. Further, GNP

with surface area $750 \text{ m}^2/\text{g}$ is more effective in enhancing the surface quality of Inconel 718.

GNP based nano-cutting fluids resulted in reduced cutting forces by forming a lubricating film at the grinding zone. Improved thermal conductivity acted as heat sinks and conducted the heat generated from the grinding zone, leading to lower grinding temperatures. Reduced cutting forces and lower grinding temperatures affected positively on grinding Inconel 718, yielding to reduced surface roughness.

From the results of the investigations conducted in the earlier chapter and the current chapter, impregnated GNP in grinding wheels is proved to be an effective lubricant in reducing the amount of the heat generated, and also when it is present in nano-cutting fluids acted as a better coolant in reducing the heat generated. To avail these benefits together, grinding experiments are carried out with self-lubricating grinding wheels in a nanoMQL environment in the next chapter.

Chapter VI

The grinding performance of Self Lubricating Grinding Wheel with nanoMQL in grinding Inconel 718

6.1 Introduction

From the studies carried out on the developed self-lubricating grinding wheels, it is evident that the dry grinding of the Inconel 718 with the grinding wheel impregnated with 2wt.% GNP having a surface area of $750 \text{ m}^2/\text{g}$ has resulted in better surface quality, lower energy requirements and longer wheel life as compared to dry grinding with a conventional grinding wheel. Similarly, from the studies carried out on the MQL grinding of Inconel 718 with a conventional grinding wheel, it was observed that MQL grinding with nano-cutting fluid (0.3wt.% and $750 \text{ m}^2/\text{g}$ surface area GNP) yielded superior results. Hence, in order to verify the combined effect, i.e. a combination of self-lubricating grinding wheel and nanoMQL, experiments are carried out and results are compared with various other combinations.

6.2 Grinding experiments

In this chapter, Grinding is carried in 4 different combinations of grinding wheels and grinding conditions as shown in Table 6.1, and compared with each other. For comparison purpose, the first combination is taken as, Dry-Wheel A, in which grinding is done with the standard grinding wheel (A80K6B) in a dry environment without using any cutting fluid. The second combination is, Wheel K, in which the best-performed self-lubricating grinding wheel having GNP with surface area $750 \text{ m}^2/\text{g}$ at 2 wt% concentration (Wheel K) is chosen for grinding in a dry environment. These two wheels have also been considered to test their performance under a nanoMQL environment with the best nano-cutting fluid having GNP with surface area $750 \text{ m}^2/\text{g}$ at 0.3 wt% concentration (MQL CF 11). Grinding experiments are carried out with the combination of grinding wheels and grinding environment as shown in Table 6.1 and performance is evaluated as discussed in Section 3.7.

Table 6.1. Various combinations of grinding

Grinding conditions	Grinding Wheel
Dry	Wheel A
Dry	Wheel K
Nano MQL	Wheel A
Nano MQL	Wheel K

6.2.1 Grinding forces

Grinding forces are measured online by using Kistler 4 - component piezoelectric dynamometer (Model: 9272) and analyzed with Dyno software. Dynamometer placement and specifications are as mentioned in Section 3.5.3.

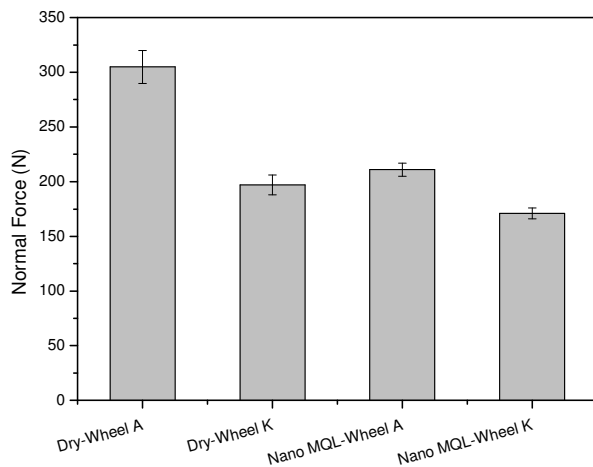


Fig 6.1. Normal force for various combinations of grinding

Fig. 6.1 and 6.2 show the variations in normal and tangential forces that were generated while grinding Inconel 718 with varying combinations of grinding wheels and grinding conditions. Significant reduction in normal force and tangential force is observed with NanoMQL-Wheel K grinding combination as compared to other combinations of grinding. Normal and tangential forces for NanoMQL-Wheel K combination reduced by approximately 44% and 47% respectively as compared to Dry-Wheel A combination and 13% and 17% respectively as compared to Dry-Wheel K combination.

Significant reduction in normal and tangential force may be attributed to the low coefficient of friction at grinding zone because of the dual functionality of GNP, as a solid lubricant with layered structure presenting in the self-lubricating grinding wheel and as a lubricating film on the workpiece surface as a nanoparticle suspension in cutting fluid.

Self-lubricating grinding wheels are effective when compared to the standard grinding wheel, but their performance is comparable to nanoMQL, which may be attributed to the higher coefficient of friction offered by GNP as a nano-particle than a solid lubricant. The lubrication offered by layered structure of GNP when impregnated in the grinding wheel is less than the lubrication offered by the film formed on the workpiece surface in NanoMQL. This also shows the wettability of GNP when dispersed in cutting fluids is very high [101].

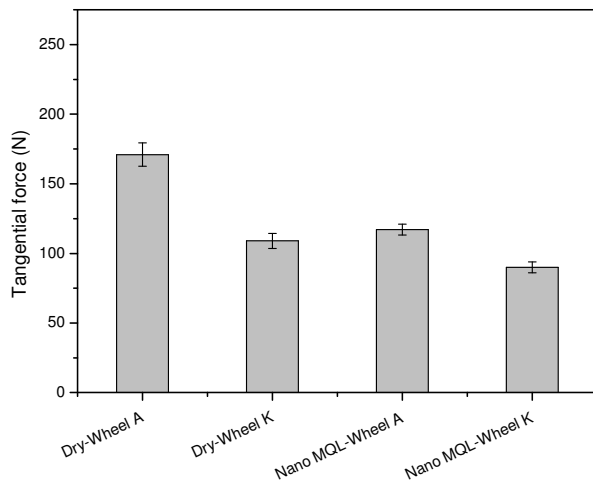


Fig 6.2. Tangential force for various combinations of grinding

6.2.2 Grinding Temperature

Fig 6.3. depicts the variations in grinding temperatures that are generated while grinding Inconel 718 with varying combinations of grinding. Among various grinding combinations considered, NanoMQL-Wheel K combination has resulted in the lowest grinding temperature as compared to other combinations. As compared to Dry-Wheel A combination, the grinding temperature is reduced by approximately 38% for NanoMQL-Wheel K combination. This significant reduction in the grinding temperatures may be attributed to the reduction of the heat from the grinding zone by GNP in the form of solid lubricant having high thermal conductivity

and a nano-cutting fluid having improved thermal conductivity. When compared to NanoMQL-Wheel A combination, NanoMQL-Wheel K combination has led to a reduction in grinding temperature by approximately 26%. Though the cooling effect for both these combinations is same, reduction in grinding temperature for NanoMQL-Wheel K combination might be due to additional lubrication provided by GNP impregnated in the self-lubricating grinding wheel.

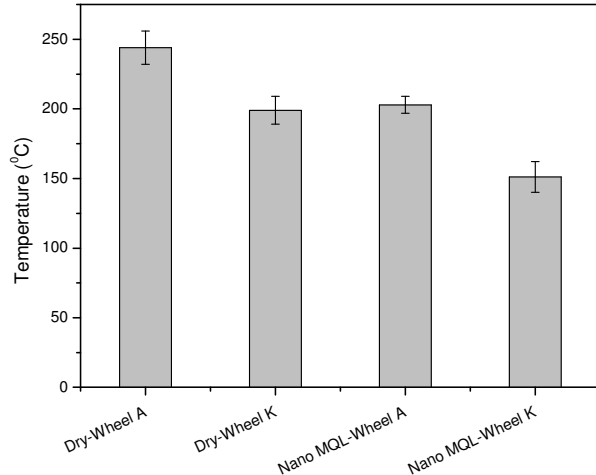


Fig 6.3. Grinding temperatures for various combinations of grinding

No doubt GNP has a good thermal conductivity as a solid lubricant, but its ability to carry heat is much more when it is suspended in cutting fluids. It can be attributed to the Brownian motion of GNP when those are freely suspended. That is, once after absorbing heat from the grinding zone, GNP in nano-cutting fluids can move rapidly and randomly distributing the heat to the atmosphere. Whereas, GNP impregnated in the grinding wheel could transfer heat to the next particle attached to it. But, GNP is very high in number to carry the heat in grinding wheel (2 wt%) compared to GNP available in the nano-cutting fluid (0.3 wt%). This is the reason why, a small amount of high temperature is reported in case of NanoMQL-Wheel A when compared to Dry-Wheel K. It can be observed that there is a drop in the temperature in case of NanoMQL-Wheel K which may be attributed to GNP suspensions absorbing heat from the GNP embedded in the grinding wheels and could be able to dissipate to the surroundings, resulting lower grinding temperature.

6.2.3 Surface roughness

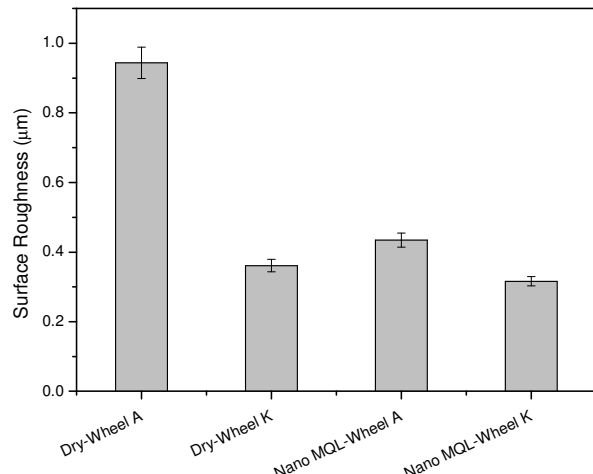


Fig 6.4. Surface roughness for various combinations of grinding

The effect of grinding Inconel 718 with varying combinations of grinding wheels on surface roughness is depicted in Fig. 6.4. From this, it is observed that NanoMQL grinding of Inconel 718 with a self-lubricating grinding wheel (Wheel K) has resulted in lowest surface roughness as compared to other combinations of grinding. As compared to Dry-Wheel A combination, nanoMQL-Wheel K combination has resulted in a significant reduction in surface roughness by approximately 67%. This significant reduction in surface roughness may be attributed to synergetic functioning of GNP, as a lubricant acted through self-lubricating grinding wheels and as a coolant through the nano-cutting fluid. The reduced forces and temperatures led to improved surface quality of ground Inconel 718 component.

Very poor surface finish is reported with Dry-Wheel A, as there is neither a sufficient amount of lubrication nor cooling. Surface finish is improved in all the three other combinations. This also may be attributed to less wheel clogging. Wheel clogging increases normal forces and also affects the wheel geometry negatively making tool blunt. Impregnated GNP in the grinding wheels slides the chips to sideways and pressurized nanofluid makes swarf fall off from the grit, leaving the wheel clean and making abrasives ready for the further grinding. This clean wheel

and sharp abrasives leading better surface quality which is the objective of the current research work.

6.3 Grinding coefficient

Variations in grinding coefficient for varying combinations of grinding is depicted in Fig. 6.5. As grinding coefficient is a measure of frictional effects at the wheel-workpiece interface, lower grinding coefficient for NanoMQL-Wheel K combination as compared to other combinations indicate effective lubrication of the grinding site through efficient application of GNP into the grinding zone, as self-lubricant being present in grinding wheels and providing lubrication at physical contact being injected from externally.

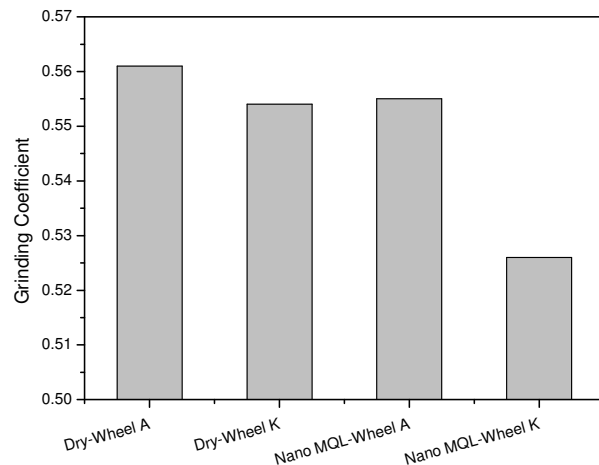


Fig. 6.5 Grinding coefficient for various combinations

6.4 Specific Grinding Energy

Fig. 6.6 shows the specific grinding energy requirement for various combinations of grinding. NanoMQL-Wheel K combination requires lowest grinding energy as compared to other combinations. Specific grinding energy required for this combination is 47% lower than that of the grinding energy requirements for dry grinding of Inconel 718 with a conventional grinding wheel. As specific grinding energy largely depends on the energy required for ploughing and sliding which in turn depends on friction, decreased energy requirements for nanoMQL-Wheel K might be ascribed to reduced friction in pursuant to effective lubrication provided by the GNP

impregnated in Wheel K, GNP inclusions in cutting fluid and soluble oil. Additional lubrication provided by the impregnated GNP resulted in a reduction of grinding energy for NanoMQL-Wheel K combination by approximately 23% as compared to NanoMQL-Wheel A combination.

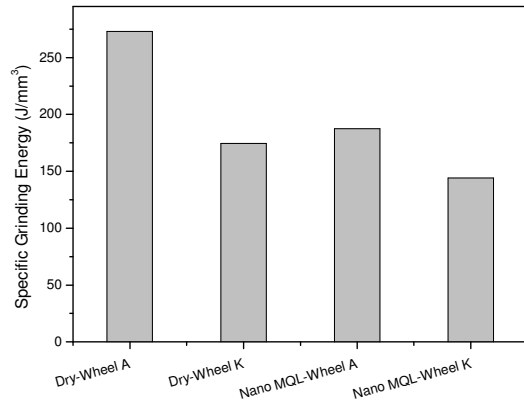


Fig. 6.6 Specific Grinding Energy for various combinations of grinding

6.5 Summary

In the present study, effect of nano MQL grinding of Inconel 718 with self-lubricating grinding wheel on various grinding performance measures is evaluated and compared the results with various other combinations like dry grinding with standard grinding wheel, dry grinding with self-lubricating grinding wheel and nano MQL grinding with standard grinding wheel. Among various combinations, nano MQL grinding of Inconel 718 with self-lubricating grinding wheel resulted in a lower grinding forces, lower grinding temperatures, better surface finish, lower energy requirement, and lower grinding coefficient.

GNP has functioned brilliantly as a solid lubricant and as a nanoparticle in grinding Inconel. This dual functionality reduced coefficient of friction at the grinding zone leading to reduced cutting forces. GNP's thermal conductivity as a solid lubricant and colloidal substance reduced the cutting temperatures effectively. GNP presented in the grinding wheel as well as nano-cutting fluids improved surface fining by lowering cutting forces, grinding temperatures and wheel clogging.

Finally, GNP played a great role as a lubricant when impregnated in the grinding wheel and as a coolant when suspended in cutting fluid resulting in improving the surface quality of ground Inconel 718 component, which is the primary objective of this research.

Chapter VII

Conclusions and future scope of the work

7.1 Conclusions

The present research focuses on improving the surface quality and to reduce the energy requirements for grinding of difficult to machine materials like Inconel 718 with an ultimate objective of enhancing the life of the components. For this purpose, self-lubricating grinding wheels and nano-cutting fluids were developed by varying concentrations and surface area of GNP. Experimental investigations on the effect of grinding Inconel 718 with the developed self-lubricating grinding wheel and nano-cutting fluids on various grinding performance measures were carried out and the conclusions drawn from these studies are summarized below.

7.1.1 Performance evaluation of self-lubricating grinding wheels

- Impregnation of GNP into grinding wheels has resulted in a reduction of surface roughness of Inconel 718, grinding temperature, grinding forces, specific grinding energy and wheel wear as compared to the standard grinding wheel.
- Among the self-lubricating grinding wheel with varying concentration of GNP, grinding wheel with 2wt.% GNP exhibited better performance in terms of surface quality and specific energy requirements.
- Self-lubricating grinding wheels with 1wt.% GNP concentration has a better wheel life as compared to grinding wheels with 0.25, 0.5, 2 and 4wt.% GNP concentration.
- When surface quality and specific energy requirements are the prime concerns, grinding wheel with 2wt.% GNP concentration is recommended. Whereas, when wheel wear is of prime concern, self-lubricating grinding wheel with 1wt.% GNP is recommended.

- Among various surface areas of GNP i.e. 300, 500, 750 m^2/g , self-lubricating grinding wheel with 2wt.% of GNP having 750 m^2/g has exhibited better surface finish and lower specific grinding energy requirements.

7.1.2 Performance evaluation of grinding with nanoMQL

- Incorporation of GNP with varying concentrations and surface areas into soluble-oil has a profound influence on Viscosity.
- Viscosity was found to be increased with an increase in GNP concentration and surface area, while decreased with an increase in temperature.
- The thermal conductivity of the soluble-oil is also significantly increased with the dispersion of GNP.
- The thermal conductivity of soluble-oil was found to be increased with an increase in GNP weight fractions, specific surface area, and temperature.
- As compared to dry grinding and MQL grinding with soluble oil, MQL grinding with nano-cutting fluids has exhibited improved grinding performance due to the diminution of frictional effects at the grinding zone in pursuant to better lubrication and cooling provided by the GNP. This, in turn, can be attributed to the enhanced viscosity and thermal conductivity with the addition of GNP to soluble oil apart from inherent ability of GNP to provide lubrication and effective penetration of GNP into grinding zone with MQL technique.
- Among various concentrations considered, nano-cutting fluid with 0.3 wt% GNP has resulted in a significant decline in grinding force, grinding coefficient, roughness, specific grinding energy, and temperature.
- GNP with higher specific surface area i.e. 750 m^2/g is more effective in enhancing the surface quality of Inconel 718.

7.1.3 Performance evaluation of self-lubricating grinding wheels with nanoMQL

- Grinding of Inconel 718 with a combination of nanoMQL and the self-lubricating grinding wheel has resulted in significant improvement in surface quality and a decrease of specific grinding energy requirements.
- As compared to dry grinding, nanoMQL grinding with self-lubricating grinding wheel exhibited a 67% decrease in surface roughness, a 38% decrease in grinding temperature and a 47% decrease in specific grinding energy.

The research work presented here may be useful for researchers who want to improve machining of difficult machine materials, who are exploring the GNP applications in different fields especially machining and who are working on developing self-lubricating machining tools.

Aerospace, gas turbine, nuclear power plant, military and other applications which are being operated at extreme operating conditions can adopt GNP as a solid lubricant in improving machining of difficult machine materials.

7.2 Future Scope of the work

The present work provides a basis for further research to be carried out for improving surface quality and energy requirements during grinding of difficult to machine materials. The work may be extended to study the effect of various process parameters like feed, infeed, wheel speed etc or out-put parameters like dimensional/geometrical tolerances etc.

Effect of various MQL parameters like flow rate, flow angle, the distance of nozzle, etc. on various grinding performance measures can be studied.

Effect of self-lubricating wheel and nano-cutting fluids on corrosion, residual stresses, phase changes, etc. can be studied.

Other effective methods of applying GNP at the wheel-workpiece interface like coating/spray depositing GNP on the surface of the workpiece, applying in the form of a paste, etc. can be explored.

Future work is proposed in the direction where another type of solid lubricant can be tested for their effectiveness in improving various grinding performance measures.

References

1. Pereira JM, Lerch BA. Effects of heat treatment on the ballistic impact properties of Inconel 718 for jet engine fan containment applications. *International Journal of Impact Engineering*. 2001 Sep 1;25(8):715-33.
2. Dudzinski D, Devillez A, Moufki A, Larrouquere D, Zerrouki V, Vigneau J. A review of developments towards dry and high speed machining of Inconel 718 alloy. *International Journal of Machine Tools and Manufacture*. 2004 Mar 1;44 (4):439-56.
3. Liao YS, Lin HM, Wang JH. Behaviors of end milling Inconel 718 super alloy by cemented carbide tools. *Journal of Materials Processing Technology*. 2008 May 26; 201(1-3):460-5.
4. Chattopadhyay A.B. (2011), *Machining and Machine tools*, New Delhi (India): Wiley India Pvt. Ltd.
5. Brinksmeier E, Heinzel CM, Wittmann Friction cooling and lubrication in grinding. *CIRP Ann Manuf Technol*. 1999; 48(2):581–598
6. Brinksmeier E, Walter A, Janssen R, Diersen P. Aspects of cooling lubrication reduction in machining advanced materials. *Proc Inst Mech Eng B J Eng Manuf*. 1999; 213:769–778
7. Howes T. Assessment of the cooling and lubricative property of grinding fluids. *Ann CIRP*, 1990; 39(1):313–316
8. Cholakov GS, Rowe GW. Lubricating properties of grinding fluids II. Comparison of fluids in four-ball tribometer tests. *Wear*. 1992 Jun 30; 155(2):331-42.
9. Howes TD, Toenshoff HK, HeuerW. Environmental aspects of grinding fluids. *Ann CIRP*, 1991; 40(2):623–629
10. Kopeliovich D (2012/06/02), Boron nitride as solid lubricant, http://www.substech.com/dokuwiki/doku.php?id=boron_nitride_as_solid_lubricant
11. Young RJ, Kinloch IA, Gong L, Novoselov KS. The mechanics of graphene nanocomposites: a review. *Composites Science and Technology*. 2012 Jul 23;72(12):1459-76.

12. Fukushima H, Drzal LT. Graphite nanoplatelets as reinforcements for polymers: structural and electrical properties. InProceedings of the 17th annual conference of the american society for composites, Purdue University, West Lafayette, IN 2002 Oct 21.
13. Kalaitzidou K, Fukushima H, Drzal LT. Mechanical properties and morphological characterization of exfoliated graphite–polypropylene nanocomposites. Composites Part A: Applied Science and Manufacturing. 2007 Jul 1; 38(7):1675-82.
14. Filleter T, McChesney JL, Bostwick A, Rotenberg E, Emtsev KV, Seyller T, Horn K, Bennewitz R. Friction and dissipation in epitaxial graphene films. Physical review letters. 2009 Feb 27; 102(8):086102.
15. Wang DY, Chang CL, Chen ZY, Ho WY. Microstructural and tribological characterization of MoS₂–Ti composite solid lubricating films. Surface and Coatings Technology. 1999 Nov 1; 120: 629-35.
16. Shaji S, Radhakrishnan V. Application of solid lubricants in grinding: investigations on graphite sandwiched grinding wheels. Machining science and technology. 2003 Jan 3;7(1):137-55.
17. Shaji S, Radhakrishnan V. An investigation on solid lubricant moulded grinding wheels. International Journal of Machine Tools and Manufacture. 2003 Jul 1;43(9):965-72.
18. Amrita M, Srikant RR, Sitaramaraju AV. Performance evaluation of nanographite-based cutting fluid in machining process. Materials and Manufacturing Processes. 2014 May 4;29(5):600-5.
19. Srikant RR, Prasad MM, Amrita M, Sitaramaraju AV, Krishna PV. Nanofluids as a potential solution for minimum quantity lubrication: a review. Proceedings of the Institution of Mechanical Engineers, Part B: Journal of Engineering Manufacture. 2014 Jan; 228(1):3-20.
20. Smith WF, Structure and properties of engineering alloys, McGraw-Hill: New York. 1993, 2nd ed.
21. Kuppan P, Rajadurai A, Narayanan S. Influence of EDM process parameters in deep hole drilling of Inconel 718. The International Journal of Advanced Manufacturing Technology. 2008 Jul 1; 38(1-2):74-84.

22. Inconel alloy 718 (Sept 2007) , retrieved from url: http://www.specialmetals.com/assets/smc/documents/inconel_alloy_718.pdf
23. Axinte DA, Dewes RC. Surface integrity of hot work tool steel after high speed milling- experimental data and empirical models. *Journal of Materials Processing Technology*. 2002 Oct 3;127(3):325-35.
24. Field M, Khales JF. Review of surface integrity of machined components. *Ann CIRP*. 1971; 20(2):153–163
25. Arunachalam RM, Mannan MA, Spowage AC. Surface integrity when machining age hardened Inconel 718 with coated carbide cutting tools. *International Journal of Machine Tools and Manufacture*. 2004 Nov 1; 44(14):1481-91.
26. Devillez A, Le Coz G, Dominiak S, Dudzinski D. Dry machining of Inconel 718, workpiece surface integrity. *Journal of Materials Processing Technology*. 2011 Oct 1;211(10):1590-8.
27. Outeiro JC, Pina JC, M'saoubi R, Pusavec F, Jawahir IS. Analysis of residual stresses induced by dry turning of difficult-to-machine materials. *CIRP Annals-Manufacturing Technology*. 2008 Jan 1; 57(1):77-80.
28. Pawade RS, Joshi SS, Brahmankar PK. Effect of machining parameters and cutting edge geometry on surface integrity of high-speed turned Inconel 718. *International Journal of Machine Tools and Manufacture*. 2008 Jan 1; 48(1):15-28.
29. Sharman AR, Hughes JI, Ridgway K. Surface integrity and tool life when turning Inconel 718 using ultra-high pressure and flood coolant systems. *Proceedings of the Institution of Mechanical Engineers, Part B: Journal of Engineering Manufacture*. 2008 Jun 1; 222(6):653-64.
30. Mao C, Zhou Z, Zhang J, Huang X, Gu D. An experimental investigation of affected layers formed in grinding of AISI 52100 steel. *The International Journal of Advanced Manufacturing Technology*. 2011 May 1; 54(5-8):515-23.
31. Tasdelen B, Thordenberg H, Olofsson D. An experimental investigation on contact length during minimum quantity lubrication (MQL) machining. *Journal of materials processing technology*. 2008 Jul 18; 203(1-3):221-31.

32. Nam JS, Lee PH, Lee SW. Experimental characterization of micro-drilling process using nanofluid minimum quantity lubrication. *International Journal of Machine Tools and Manufacture*. 2011 Jul 1; 51(7-8):649-52.
33. Iqbal A, Ning H, Khan I, Liang L, Dar NU. Modeling the effects of cutting parameters in MQL-employed finish hard-milling process using D-optimal method. *Journal of Materials Processing Technology*. 2008 Apr 1; 199(1-3):379-90.
34. Dhar NR, Kamruzzaman M, Ahmed M. Effect of minimum quantity lubrication (MQL) on tool wear and surface roughness in turning AISI-4340 steel. *Journal of materials processing technology*. 2006 Feb 28; 172(2):299-304.
35. Tawakoli T, Hadad MJ, Sadeghi MH, Daneshi A, Stöckert S, Rasifard A. An experimental investigation of the effects of workpiece and grinding parameters on minimum quantity lubrication—MQL grinding. *International Journal of Machine Tools and Manufacture*. 2009 Oct 1; 49(12-13):924-32.
36. Skerlos SJ. Prevention of metalworking fluid pollution: environmentally conscious manufacturing at the machine tool. *Environmentally conscious manufacturing*. Walley, Hoboken, NJ. 2007 Mar 16:95-122.
37. Viktor P. Astakhov. *Machining: Fundamentals and Recent Advances*, Springer, Chap.7., *Ecological Machining: Near-dry Machining*, 2008.
38. McClure TF, Gugger MD. Microlubrication in metal machining operations. *Tribology & Lubrication Technology*. 2002 Dec 1;58(12):15.
39. Dixit US, Sarma DK, Davim JP. *Environmentally friendly machining*. Springer Science & Business Media; 2012 Jan 10.
40. Heisel, U., Lutz, M., Spath, D., Wassmer, R. A., & Walter, U. Application of minimum quantity cooling lubrication technology in cutting processes. *Production Engineering* Vol. II/1. 1994.
41. Yasir A, Che Hassan CH, Jaharah AG, Nagi HE, Yanuar B, Gusri AI. Machinability of Ti-6Al-4V under dry and near dry condition using carbide tools. *The Open Industrial & Manufacturing Engineering Journal*. 2009 Apr 3;2(1).
42. Alves JA, Fernandes UD, Silva Júnior CE, Bianchi EC, Aguiar PR, Silva EJ. Application of the minimum quantity lubrication (MQL) technique in the plunge

cylindrical grinding operation. *Journal of the Brazilian Society of Mechanical Sciences and Engineering*. 2009 Mar;31(1):1-4.

- 43. Tai BL, Dasch JM, Shih AJ. Evaluation and comparison of lubricant properties in minimum quantity lubrication machining. *Machining science and technology*. 2011 Oct 1;15(4):376-91.
- 44. Mao C, Tang X, Zou H, Zhou Z, Yin W. Experimental investigation of surface quality for minimum quantity oil–water lubrication grinding. *The International Journal of Advanced Manufacturing Technology*. 2012 Mar 1;59(1-4):93-100.
- 45. Thakur DG, Ramamoorthy B, Vijayaraghavan L. Investigation and optimization of lubrication parameters in high speed turning of superalloy Inconel 718. *The International Journal of Advanced Manufacturing Technology*. 2010 Sep 1;50(5-8):471-8.
- 46. Sadeghi MH, Hadad MJ, Tawakoli T, Vesali A, Emami M. An investigation on surface grinding of AISI 4140 hardened steel using minimum quantity lubrication-MQL technique. *International Journal of Material Forming*. 2010 Dec 1;3(4):241-51.
- 47. Tawakoli T, Hadad MJ, Sadeghi MH. Investigation on minimum quantity lubricant-MQL grinding of 100Cr6 hardened steel using different abrasive and coolant–lubricant types. *International Journal of Machine Tools and Manufacture*. 2010 Aug 1;50(8):698-708.
- 48. da Silva LR, Bianchi EC, Fusse RY, Catai RE, Franca TV, Aguiar PR. Analysis of surface integrity for minimum quantity lubricant—MQL in grinding. *International Journal of Machine Tools and Manufacture*. 2007 Feb 1;47(2):412-8.
- 49. B. Bhushan, *Modern Tribology Handbook*, CRC Press LLC, New York, 2001.
- 50. G.W. Stachowiak, A.W. Batchelor, *Engineering Tribology*, Butterworth- Heinemann, Woburn, 2001.
- 51. Venu Gopal A, Venkateswara Rao P. Performance improvement of grinding of SiC using graphite as a solid lubricant. *Materials and manufacturing processes*. 2004 Dec 28; 19(2):177-86.
- 52. Tsai MY, Jian SX. Development of a micro-graphite impregnated grinding wheel. *International Journal of Machine Tools and Manufacture*. 2012 May 1; 56:94-101.

53. A.R. Lansdown, High Temperature Lubrication, Mechanical Engineering Publication Ltd, London, 1994.
54. R.I. King, R.S. Hahn, Hand Book of Modern Grinding Technology, Chapman and Hall, New York, 1986.
55. S. Malkin, Grinding Technology: Theory and Applications of Machining with Abrasives, Ellis Horwood Ltd, UK, 1989.
56. S.C. Salmon, Modern Grinding Process Technology, McGraw- Hill, New York, 1992.
57. Eastman JA, Choi SU, Li S, Yu W, Thompson LJ. Anomalously increased effective thermal conductivities of ethylene glycol-based nanofluids containing copper nanoparticles. *Applied physics letters*. 2001 Feb 5; 78(6):718-20.
58. Buongiorno J, Venerus DC, Prabhat N, McKrell T, Townsend J, Christianson R, Tolmachev YV, Kebinski P, Hu LW, Alvarado JL, Bang IC. A benchmark study on the thermal conductivity of nanofluids. *Journal of Applied Physics*. 2009 Nov 1;106(9):094312.
59. Xie H, Yu W, Li Y, Chen L. Discussion on the thermal conductivity enhancement of nanofluids. *Nanoscale research letters*. 2011 Dec 1; 6(1):124.
60. Ding Y, Chen H, Wang L, Yang CY, He Y, Yang W, Lee WP, Zhang L, Huo R. Heat transfer intensification using nanofluids. *KONA Powder and Particle Journal*. 2007;25:23-38.
61. Garg J, Poudel B, Chiesa M, Gordon JB, Ma JJ, Wang JB, Ren ZF, Kang YT, Ohtani H, Nanda J, McKinley GH. Enhanced thermal conductivity and viscosity of copper nanoparticles in ethylene glycol nanofluid. *Journal of Applied Physics*. 2008 Apr 1; 103(7):074301.
62. Tavman I, Turgut A, Chirtoc M, Hadjov K, Fudym O, Tavman S. Experimental study on thermal conductivity and viscosity of water-based nanofluids. *Heat transfer research*. 2010; 41(3).
63. Li X, Zhu D, Wang X. Experimental investigation on viscosity of Cu-H₂O nanofluids. *Journal of Wuhan University of Technology-Mater. Sci. Ed.*. 2009 Feb 1; 24(1):48-52.
64. Mirmohammadi SA, Behi M. Investigation on Thermal Conductivity, Viscosity and Stability of Nanofluids. 2012.

65. Zhang D, Li C, Jia D, Zhang Y, Zhang X. Specific grinding energy and surface roughness of nanoparticle jet minimum quantity lubrication in grinding. *Chinese Journal of Aeronautics*. 2015 Apr 1; 28(2):570-81.
66. Setti D, Sinha MK, Ghosh S, Rao PV. Performance evaluation of Ti-6Al-4V grinding using chip formation and coefficient of friction under the influence of nanofluids. *International Journal of Machine Tools and Manufacture*. 2015 Jan 1; 88:237-48.
67. Zhang Y, Li C, Jia D, Zhang D, Zhang X. Experimental evaluation of MoS₂ nanoparticles in jet MQL grinding with different types of vegetable oil as base oil. *Journal of Cleaner Production*. 2015 Jan 15; 87:930-40.
68. Kalita P, Malshe AP, Rajurkar KP. Study of tribo-chemical lubricant film formation during application of nanolubricants in minimum quantity lubrication (MQL) grinding. *CIRP Annals-Manufacturing Technology*. 2012 Jan 1; 61(1):327-30.
69. Berman D, Erdemir A, Sumant AV. Graphene: a new emerging lubricant. *Materials Today*. 2014 Jan 1; 17(1):31-42.
70. Ho KI, Boutechich M, Su CY, Moredu R, Marianathan ES, Montes L, Lai CS. A Self-Aligned High-Mobility Graphene Transistor: Decoupling the Channel with Fluorographene to Reduce Scattering. *Advanced Materials*. 2015 Nov; 27 (41):6519-25.
71. Novoselov KS, Geim AK, Morozov SV, Jiang DA, Zhang Y, Dubonos SV, Grigorieva IV, Firsov AA. Electric field effect in atomically thin carbon films. *Science*. 2004 Oct 22;306(5696):666-9.
72. Novoselov KS, Jiang D, Schedin F, Booth TJ, Khotkevich VV, Morozov SV, Geim AK. Two-dimensional atomic crystals. *Proceedings of the National Academy of Sciences*. 2005 Jul 26; 102(30):10451-3.
73. Chen D, Tang L, Li J. Graphene-based materials in electrochemistry. *Chemical Society Reviews*. 2010; 39(8):3157-80.
74. Soldano C, Mahmood A, Dujardin E. Production, properties and potential of graphene. *Carbon*. 2010 Jul 1; 48(8):2127-50.
75. Lotya M, King PJ, Khan U, De S, Coleman JN. *ACS Nano* 4, 3155 (2010).

76. Mohammadi S, Kolahdouz Z, Darbari S, Mohajerzadeh S, Masoumi N. Graphene formation by unzipping carbon nanotubes using a sequential plasma assisted processing. *Carbon*. 2013 Feb 1; 52:451-63.
77. Kim KS, Zhao Y, Jang H, Lee SY, Kim JM, Kim KS, Ahn JH, Kim P, Choi JY, Hong BH. Large-scale pattern growth of graphene films for stretchable transparent electrodes. *Nature*. 2009 Feb; 457 (7230):706.
78. Li X, Cai W, Colombo L, Ruoff RS. Evolution of graphene growth on Ni and Cu by carbon isotope labeling. *Nano letters*. 2009 Aug 27;9(12):4268-72.
79. The Nobel Prize in Physics 2010, The Nobel Foundation, www.nobelprize.org
80. Lee C, Li Q, Kalb W, Liu XZ, Berger H, Carpick RW, Hone J. Frictional characteristics of atomically thin sheets. *Science*. 2010 Apr 2; 328(5974):76-80.
81. Bunch JS, Verbridge SS, Alden JS, Van Der Zande AM, Parpia JM, Craighead HG, McEuen PL. Impermeable atomic membranes from graphene sheets. *Nano letters*. 2008 Jul 17;8(8):2458-62.
82. Singh E, Thomas AV, Mukherjee R, Mi X, Houshmand F, Peles Y, Shi Y, Koratkar N. Graphene drape minimizes the pinning and hysteresis of water drops on nanotextured rough surfaces. *ACS nano*. 2013 Mar 19;7(4):3512-21.
83. Balandin AA, Ghosh S, Bao W, Calizo I, Teweldebrhan D, Miao F, Lau CN. Superior thermal conductivity of single-layer graphene. *Nano letters*. 2008 Feb 20;8(3):902-7.
84. Chu B, Singh E, Koratkar N, Samuel J. Graphene-enhanced environmentally-benign cutting fluids for high-performance micro-machining applications. *Journal of nanoscience and nanotechnology*. 2013 Aug 1; 13(8):5500-4.
85. Ranjbarzadeh R, Meghdadi AH, Hojaji M. The analysis of experimental process of production, stabilizing and measurement of the thermal conductivity coefficient of water/graphene oxide as a cooling nanofluid in machining. *Journal of Modern Processes in Manufacturing and Production*. 2016 May 1; 5(2):43-53.
86. Singh RK, Sharma AK, Dixit AR, Tiwari AK, Pramanik A, Mandal A. Performance evaluation of alumina-graphene hybrid nano-cutting fluid in hard turning. *Journal of cleaner production*. 2017 Sep 20; 162:830-45.

87. Uysal A. Investigation of flank wear in MQL milling of ferritic stainless steel by using nano graphene reinforced vegetable cutting fluid. *Industrial Lubrication and Tribology*. 2016 Jun 13; 68(4): 446-51.
88. ASTM Standard D5334-08. Standard Test Method for Determination of Thermal Conductivity of Soil and Soft Rock by Thermal Needle Probe Procedure. *ASTM Book of Standards 04.08*, March 2005
89. ASTM Standard D2983- 03. Standard Test Method for Low-Temperature Viscosity of Lubricants Measured by Brookfield Viscometer, *Book of Standards, 05.01, Petroleum Products and Lubricants*, ASTM International, 2004
90. Shaji S, Radhakrishnan V. An investigation on surface grinding using graphite as lubricant. *International Journal of Machine tools and manufacture*. 2002 May 1; 42(6):733-40.
91. Brinksmeier E, Tönshoff HK, Inasaki I, Peddinghaus J. Basic parameters in grinding—report on a cooperative work in STC «G». *CIRP annals*. 1993; 42(2):795-9.
92. Samuel J, Rafiee J, Dhiman P, Yu ZZ, Koratkar N. Graphene colloidal suspensions as high performance semi-synthetic metal-working fluids. *The Journal of Physical Chemistry C*. 2011 Feb 10;115(8):3410-5.
93. Yuan SM, Yan LT, Liu WD, Liu Q. Effects of cooling air temperature on cryogenic machining of Ti–6Al–4V alloy. *Journal of Materials Processing Technology*. 2011 Mar 1;211(3):356-62.
94. Prasher R, Song D, Wang J, Phelan P. Measurements of nanofluid viscosity and its implications for thermal applications. *Applied physics letters*. 2006 Sep 25; 89(13):133108.
95. Das SK, Putra N and Wilfried R. Pool boiling characteristics of nano-fluids. *Int J Heat Mass Tran* 2003; 46(5): 851–862.
96. Putra N, Wilfried R and Das SK. Natural convection of nano-fluids. *Heat Mass Transfer* 2003; 39(8–9): 775–784.
97. Hussein AM, Sharma KV, Bakar RA, Kadirgama K. The effect of nanofluid volume concentration on heat transfer and friction factor inside a horizontal tube. *Journal of Nanomaterials*. 2013 Jan 1; 2013:1.

98. Tenne R and Redlich M. Recent progress in the research of inorganic fullerene like nanoparticles and inorganic nano tubes. *Chem Soc Rev* 2010; 39: 1423–1434.
99. Rabiei FA, Rahimi AR, Hadad MJ. Performance improvement of eco-friendly MQL technique by using hybrid nanofluid and ultrasonic-assisted grinding. *The International Journal of Advanced Manufacturing Technology*. 2017 Oct 1;93(1-4):1001-15.
100. Jia D, Li C, Zhang Y, et al. Specific energy and surface roughness of minimum quantity lubrication grinding Nibased alloy with mixed vegetable oil-based nanofluids. *Precis Eng*, 2017; 50: 248–262.
101. Zhang Y, Li C, Jia D, Li B, Wang Y, Yang M, Hou Y, Zhang X. Experimental study on the effect of nanoparticle concentration on the lubricating property of nanofluids for MQL grinding of Ni-based alloy. *Journal of Materials Processing Technology*. 2016 Jun 1; 232:100-15.
102. Chu B, Singh E, Koratkar N, Samuel J. Graphene-enhanced environmentally-benign cutting fluids for high-performance micro-machining applications. *Journal of nanoscience and nanotechnology*. 2013 Aug 1; 13(8):5500-4.
103. Mehrali M, Sadeghinezhad E, Latibari ST, Kazi SN, Mehrali M, Zubir MN, Metselaar HS. Investigation of thermal conductivity and rheological properties of nanofluids containing graphene nanoplatelets. *Nanoscale research letters*. 2014 Dec 1;9(1):15.

List of publications from this research work

International Conference:

- **Pavan RB**, Srikanth RR, Gopal AV, Kiran GB. Investigations on grinding of Inconel 718 using newly developed graphene nanoplatelets impregnated grinding wheels. In Proced 5th Int. & 26th All India Manufacturing technology, design and research conference (AIMTDR-2014) 2014.

International Publications:

- **Ravuri BP**, Revuru RS, Anne VG, Goriparthi BK. Performance evaluation of grinding wheels impregnated with graphene nanoplatelets. *The International Journal of Advanced Manufacturing Technology*. 2016 Aug 1;85(9-12):2235-45.
- **Pavan RB**, Venu Gopal A, Amrita M, Goriparthi BK. Experimental investigation of graphene nanoplatelets-based minimum quantity lubrication in grinding Inconel 718. *Proceedings of the Institution of Mechanical Engineers, Part B: Journal of Engineering Manufacture*. 2017 Sep 3:0954405417728311.

Bio-Data

Name	Ravuri Bhanu Pavan
Date of Birth	26-08-1981
Marital status	Married
Present Position	Assistant Professor, Department of Mechanical Engineering GITAM Institute of Technology GITAM (Deemed to be university) Visakhapatnam - 530045 Andhra Pradesh, India
Qualification	M.E. (CAD/CAM)
Permanent Address	S/o R. Nageswara Rao, Flat No D1, Hamsadwani Apartment, Mithilapur VUDA colony, Visakhapatnam - 530041 Andhra Pradesh, India. E-mail: bhanuinresearch@gmail.com bhanupavan.ravuri@gitam.edu